12-2010

UNCERTAINTY OF DIMENSIONAL MEASURMENTS OBTAINED FROM SELF-INITIALIZED INSTRUMENTS

Vincent Lee
Clemson University, vinny_lee@msn.com

UNCERTAINTY OF DIMENSIONAL MEASURMENTS OBTAINED FROM SELF-INITIALIZED INSTRUMENTS

A Dissertation
Presented to
the Graduate School of
Clemson University

In Partial Fulfillment
of the Requirements for the Degree
Doctor of Philosophy
Mechanical Engineering

---

by
Vincent Lee
December 2010

Accepted by:
John C. Ziegert, Committee Chair
Gregory M. Mocko
Laine M. Mears
Todd H. Hubing

ABSTRACT

Precision dimensional measurement instruments often contain sensors that can only measure displacement of a moving body from some reference position. In order to measure the length of an object they often require a calibrated artifact to initialize their measurement sensors so that they may provide an absolute measurement instead of displacement. Instruments which can realize a null value, i.e. zero length, don't require one; however instruments which can't need to reference an object of known size. These calibration artifacts also serve as part of the chain of metrological traceability.

The group of instruments presented in this dissertation can self-initialize by deriving their own calibrated artifact. These instruments rely on a unique artifact geometry, which is un-calibrated, to determine a length value via a series of displacement measurements provided by the self-initializing instrument. All of the self-initializing instruments described in this dissertation rely on a precision sphere coupling with a three point kinematic seat (TPKS) as the mechanical interface between the instrument and un-calibrated artifact. The combination of the TPKS and sphere are deterministic in nature in defining a point in space, e.g. the location of the center of the sphere relative to the body of the TPKS. In practice, high precision spheres are inexpensively available, and testing has shown that the locational repeatability of the sphere/TPKS coupling to be in the range of the surface roughness of the spheres, thus allowing nanometer-level repeatability. The combination of this feature and the displacement measurement sensors in these instruments allow the instrument to directly measure length without resorting to a measure of extension.

The Laser Ball Bar instrument, an instrument which pioneered the self-initialization method for length measurement instruments, and can't realize a null value measurement for initialization, is functionally decomposed to better understand the requirements for self-initialization. Two instruments that fulfill these requirements will be presented as case studies of how a self-initialized instrument may be designed, and constructed. Measurement uncertainty with these instruments, using self-initialization, and initialization with an independently calibrated

artifact will be explored. A complete uncertainty analyses are provided for both instruments using both the self-initialization mode and the calibrated artifact mastering mode of operation; and the predicted results are compared to experimental measurement data.

This dissertation:

- Derives and/or explains the geometric conditions which enable self-initialization in an instrument
- Describes two novel instruments that are capable of self-initialization
- Provides an uncertainty analyses for these instruments when they are self-initialized and when they are initialized using a master artifact
- Compares and contrasts the achievable uncertainty for each mode of use, and
- Provides conditions under which lower uncertainty is achievable using self-initialization.

DEDICATION

To Mom and Dad,

for their personal sacrifices.

ACKNOWLEDGEMENTS

First and foremost I would like to thank Dr. John Ziegert for giving me the guidance to become the engineer and researcher that I am today. With his support, I was able to finish my PhD, and begin a career in a field of study that I truly enjoy. I would also like to thank my committee members Dr. Greg Mocko, Dr. Laine Mears, and Dr. Todd Hubing for their advice. And of course my friends and fellow office mates Dr. James Gibert, Robert M. Clippard, Chan Wong, Dr. Balajee Ananthasayanam, Robert Fogle, Carlos Montes, Evan Lowe, and the entire CEDAR group at Clemson.

I would like to acknowledge those at National Institute of Science and Technology's (NIST) Large Scale metrology group and the Timken Company for funding the projects which made the research presented in this dissertation possible, especially Dr. Stephen Phillips (NIST), Tyler Estler (NIST) Daniel Sawyer (NIST), Bruce Borchardt (NIST), Michael Thompson (Timken), Joseph Pack (Timken), and Bob Hiltbrand (Timken).

And last but not least, all of the support staff at Clemson University Mechanical Engineering and ICAR departments, that keep the wheels turning especially Gary Mathis, David Mann, Frank Web, Tameka Boyce, Gwen Dockins, Kaye Golden, and Kathryn Poole.

TABLE OF CONTENTS

Page

TABLE OF TABLES

TABLE OF FIGURES

CHAPTER ONE

OVERVIEW OF RESEARCH

This section provides an introduction to this dissertation's topic by providing relevant background material, outlining the scope of the research, and its relationship to practical applications.

Introduction

All length measurement instruments in some fashion, relate the physical boundaries of objects which they measure to the fundamental unit of measure, the meter. Many of these instruments provide a measurement result by making physical contact with objects. These points of contact are linked to a graduated scaled, via mechanical framework, to define their position relative to other points or boundaries on the object. The graduations on the scales are calibrated to ensure that each measurement accurately represents the correct proportion of the meter. Swyt [1, 2] outlined four dimensional measurement types, they are:

'*position – location of an object in space*

displacement – the change in location of an object over a time interval

distance – the difference in location of two objects at the same time

extension – the distance between points on opposing-face boundaries of an object"

Objects subjected to be measured can be a simple geometry such as a sphere, or may be an object which contains other features, such as a rectangular block that contain multiple features such as holes, pockets, and slots. A measurement instrument is used to assign a dimension to the object and its features by utilizing at least one of the four dimensional measurement types [3]. Referring to the following figure (Figure 1-1) as an example, extension is used to define the dimensions of the block, the slot, and the hole by measuring the extents of their boundaries. Distance is used to define the relative location of each "object", and their boundaries, to each other. The position of the center of the hole and slot, relative to a coordinate system defined by reference surfaces on the body are derived from measures of extension and distance. The results from these measurement types assign an absolute dimension, in units of length, to each feature.

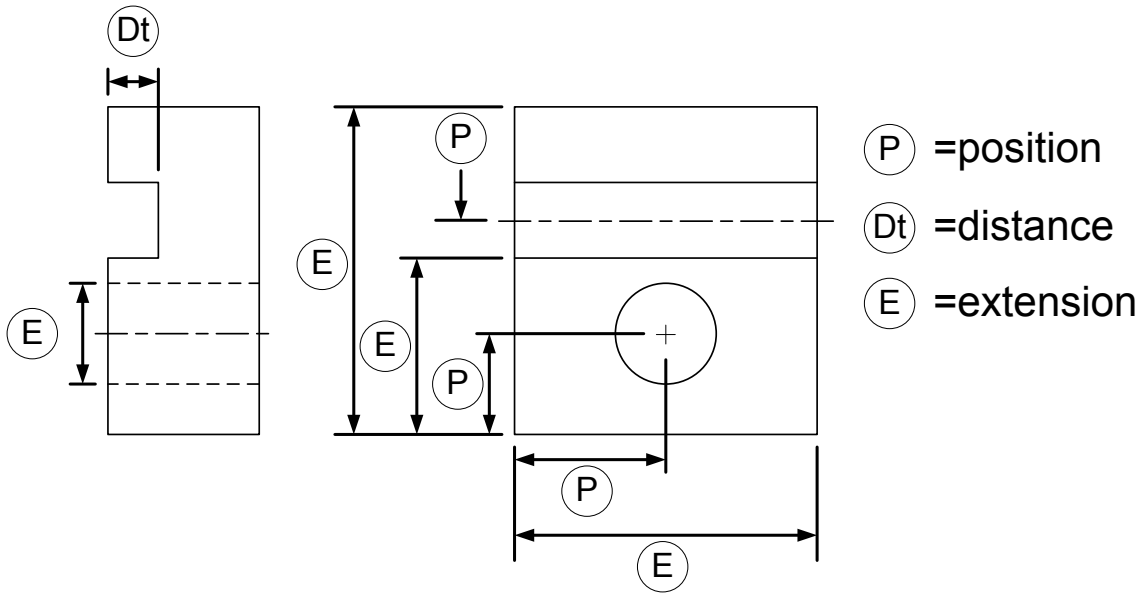

Figure 1-1: Position, distance, and extension are used to quantify the dimensions of a machine part.

To perform absolute dimensional measurements, for instruments with sensors that can only measure displacement, a means to initialize an instrument's measurement system to a known value is required. The term initialization means to "set to a value" [4]. For a dimensional measurement instrument, initialization "sets" the instrument to a known reference value, which displacement is measured from. Initialization essentially performs what is defined under definition 3.11 in the International Vocabulary of Basic General Terms in Metrology (VIM), as "a adjustment of a measurement system", which reads [3]:

> "*set of operations carried out on a measuring system so that it provides prescribed indications corresponding to given values of a quantity to be measured*."

This definition is followed by three important notes:

> "*NOTE 1: Types of adjustment of a measuring system included zero adjustment of a measuring system (*definition 3.12 in the VIM*), offset adjustment, and span adjustment (sometimes called gain adjustment).*
>
> *NOTE 2: Adjustment of a measuring system should not be confused with calibration, which is a prerequisite for adjustment.*

NOTE 3: After an adjustment of a measuring system, the measuring system must usually be recalibrated."

"*Note 1*" defines the type of 'measurement system adjustments' and reflects the adjustment (offset adjustment) that initialization accomplishes. "Note 2" specifically outlines that the actions outlined in "*Note 1*" are not calibration. For instruments which are subject to initialization or adjustment of its measurement system, the displacement sensor(s) contained by the instrument are considered to be calibrated such that each graduation is a known proportional representation of a fundamental unit of measure. The process of initialization or scale offset adjustment is often confused by even the most technically experienced individuals as calibration, which has its own definition in the VIM under definition 2.39, which is:

"*operation that, under specified conditions, in a first step, establishes a relation between the quantity values with measurement uncertainties provided by measurement standards and corresponding indications with associated measurement uncertainties provided by measurement standards and corresponding indications with associated measurement uncertainties and, in a second step, uses this information to establish a relation for obtaining a measurement result from an indication*"

As for "*Note 3*" indicating that an instrument "*must usually be recalibrated*" after an adjustment to its measurement system, I believe this to be true for gain adjustments, since a gain adjustment may alter the calibration of the measurement system. In the case of an offset or zero adjustment, recalibration shouldn't be necessary since the scaling of the measurement system is preserved.

There are two possible initialization techniques self-initialization, and initialization with an independently calibrated artifact. A measurement instrument such as a dial caliper can butt their measurement surfaces together to provide a zero-length value, and thus can self-initialize or "*zero*" its displacement measurement sensor, since it can realize a null measurement value. Others type of instruments, such as a gauge block comparator, which can't perform such a feat will require a calibrated artifact of known dimensions to serve as a reference standard to set its displacement sensor to a known initial value [5]. More recently developed instruments which

contain measurement points that aren't able to touch each other, or otherwise realize a zero-length condition, are still able self-initialize [6-9]. However these instruments utilize an initialization method, via an un-calibrated artifact that has no metrological traceability to a fundamental unit of measure. Without metrological traceability, a measurement uncertainty can't be confidently assigned to a measured value, thus compromising any assurance one would have in the results provided by the instrument. In order to maintain traceability these instruments must rely on alternate methods such as external calibration of their displacement sensors.

Background of Research

Traditional Measurement Instruments

Instruments which are unable to self-initialize reference a calibrated artifact prior to measuring a part of unknown size. For example, consider a comparator type instrument which comprises of a rigid frame, an anvil, and a calibrated displacement sensor; the sensor's sensitive direction is normal to the surface of the anvil (Figure 1-2).

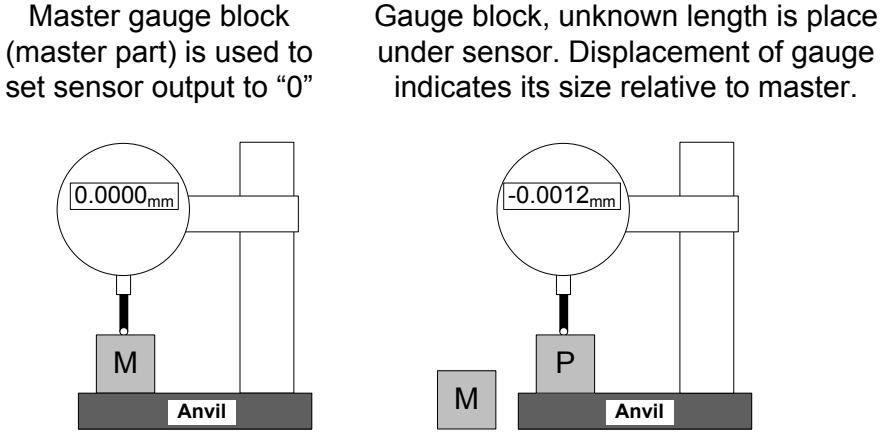

Figure 1-2: Initializing a length comparator, and measuring a part of unknown size

One way to initialize the comparator is to bring the anvil and the tip of the sensor into physical contact so that a null measurement value can be realized. However since the sensor has a limited range of travel and is unable to bring its tip into contact with the anvil, it would be unable to perform a zero adjustment of the measurement system onto itself. Therefore a part of known

size (the master part) is used to initialize the instrument by setting a known offset from the anvil's surface to the sensor's tip. This procedure is often referred to as "mastering" an instrument. When the master part is placed in between the anvil and the sensor's tip, the output value of the displacement sensor is "zeroed"; analogous to accounting for a tare weight for weight measurements. Other parts of unknown size may now be measured by placing them in between the anvil and the sensor's tip, as long as the displacement limits of the sensor aren't exceeded (Figure 1-2). By measuring a calibrated master part of known size and dimensional uncertainty, the size of the new parts and the uncertainty of that size can be estimated.

Another example of a measurement system which requires a calibrated artifact for initialization of its measurement sensor is the coordinate measuring machine (CMM). A CMM measures a part by physically touching various points along its surface(s), typically using a touch probe which carries a spherically tipped stylus. The points which the stylus contacts are transferred to a measurement scale via a mechanical link to a reference coordinate system. The most common modern CMM embodies a 3-D Cartesian coordinate system to provide the coordinates of the stylus center at each of the points which are probed. However, in order to accurately determine the location of the contact points on the part, the dimensions of the stylus need to be known (typically its tip radius). This is important since a CMM actually tracks the position of the probe holder assembly; which is set by its manufacturer. The relative position of the stylus's tip to the probe assembly is set by the end user since there are a seemingly infinite number of stylus geometries available. Qualification of a stylus is typically performed by touching a precision sphere of known size and form error, at specific locations, which afterwards the tip radius of the stylus may be determined. During this qualification process the CMM measures the sphere without compensating for the stylus radius or offset. The coordinates of the probed points are best fit to spherical geometry and the relative coordinates of the best-fit sphere center and the known location of the physical sphere center are used to determine the relative position of the stylus tip center and the probe holder. The radius of the best fit sphere will be larger than the

actual radius of the physical sphere since it passes through the stylus center, not the contact points (Figure 1-3).

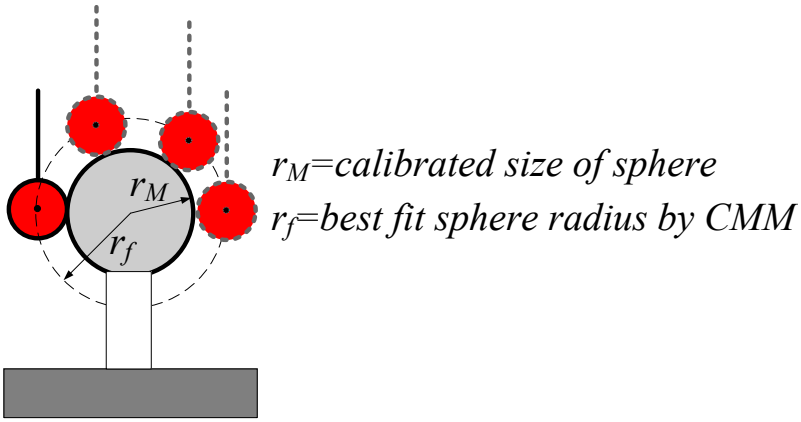

Figure 1-3 : Qualifying a CMM stylus with a sphere of knonw size

However, if the physical sphere's size is known, the radius of the stylus tip can be resolved by calculating the difference between measured sphere size and the actual size. With the styli's radius known, the location of the point of contact at a given part may be resolved to the probe assembly, by accounting for the stylus's offset and tip radius, and then to the reference coordinate system (Figure 1-4).

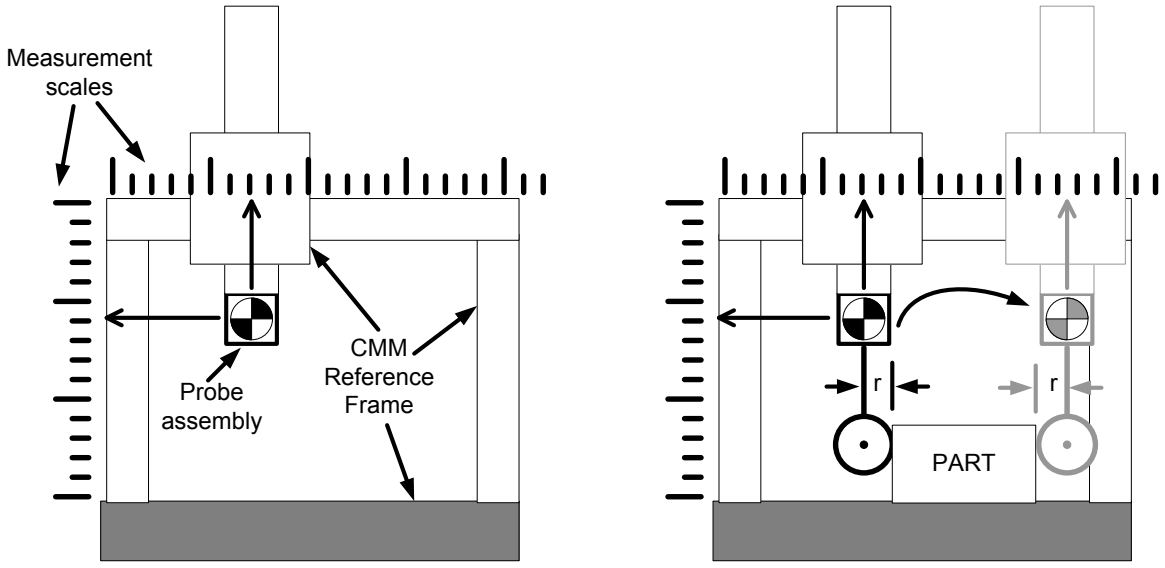

Figure 1-4: Simple CMM assembly showing a 2D coordinate system (*left*), two points probed at opposing ends determine part's lateral dimension, after probe radius is compensated (*right*)

From a conceptual standpoint, to avoid the stylus qualification process, the most ideal stylus radius is zero, so that a calibrated artifact needs not be referenced. With a stylus of zero radii (a null value) any point measured on a part can be directly related to the scale without any intermediary length to transfer that point. Sine a stylus of zero radiuses isn't physical possible, one must rely on a calibrated artifact to qualify the stylus.

For these two examples, a calibrated artifact was necessary to initialize each instrument to some known value to enable an absolute dimensional measurement. This is due to the nature of their sensors inability to self-initialize to a null value or null point. Instruments which are able to self-initialize to a null value by bringing their measurement points of contact together, have been limited to "C-frame" shaped instruments such as a dial caliper, and short range micrometers. By butting the measurement points of these instruments together and "zeroing" the sensor's output indicator, initialization has been completed.

Self-Initialized Instruments

Novel instruments which do not rely on master artifacts for measurement scale initialization have been developed in recent years. However, these instruments don't self-initialize by realizing a null measurement value, like the dial caliper or micrometer. They rely on an artifact or fixture to capture a displacement measurement from the instrument, directly convert it to a length, which may then be reused to initialize the same instrument. A physical embodiment of such an instrument is the Laser Ball Bar (LBB) system, by Ziegert et al.; illustrated in the following figure (Figure 1-5) [7, 10].

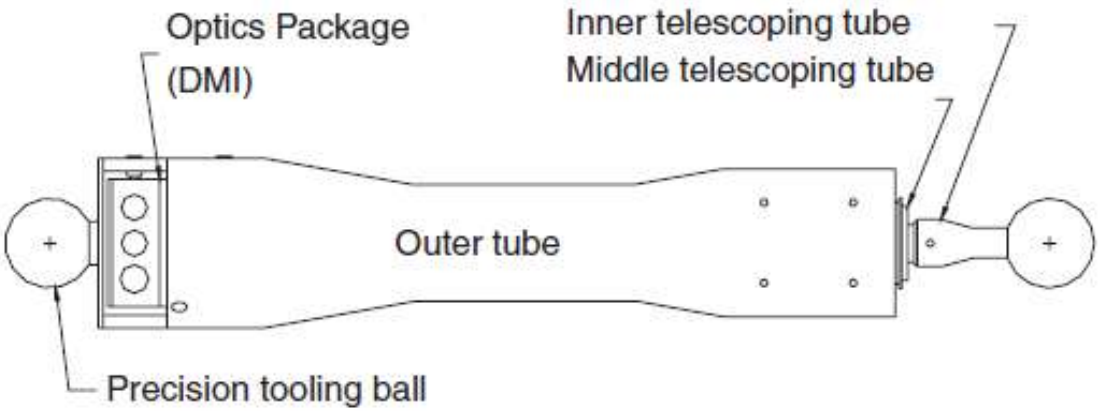

Figure 1-5: Laser Ball Bar (LBB) concept and component layout [7, 10]

The LBB is an instrument consisting of three concentric precision telescopic tube assemblies which houses a set of interferometer optics, and two precision spheres, on each end of the instrument. As the tube extends, the laser interferometer system measures the relative displacement of the optics, i.e. the change in distance between the sphere centers. The spherical ball ends on this instrument permit precision interface to a specially designed three-point kinematic seat (TPKS) [11]. Each of these TPKS's has three precision points which make contact with the ball (Figure 1-6). These three contacts constrain all translation motion of the center of the sphere, but do not restrict any rotation of the sphere.

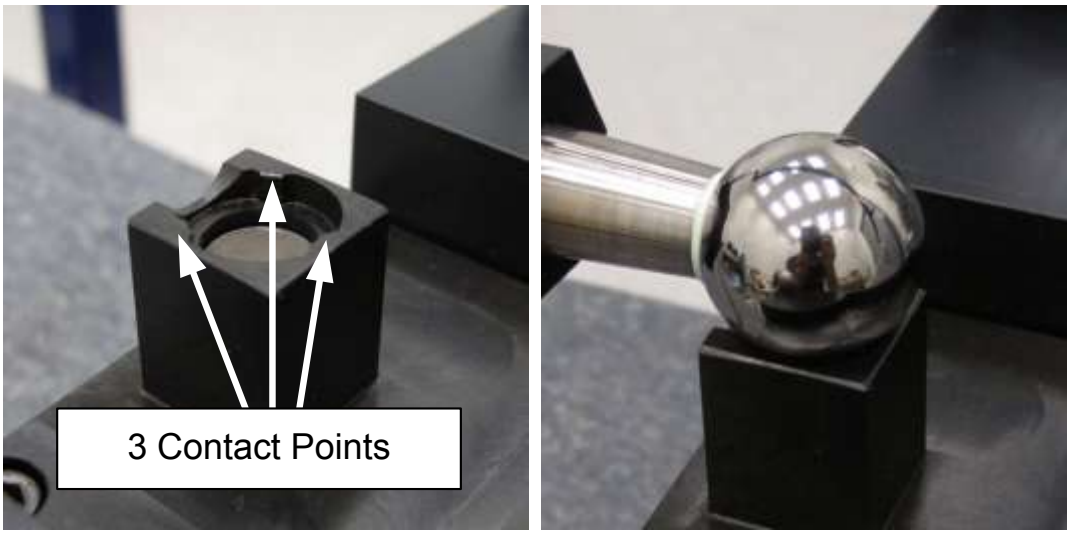

Figure 1-6: Quasi Kinematic seat detail; points of contact exposed, and ball mounted

This feature allows the LBB to interface with measurement points with excellent repeatability. To initialize the laser interferometer to measure an absolute distance between the sphere centers, an un-calibrated artifact, with three TPKS's, is used in combination with the following procedure (Figure 1-7).

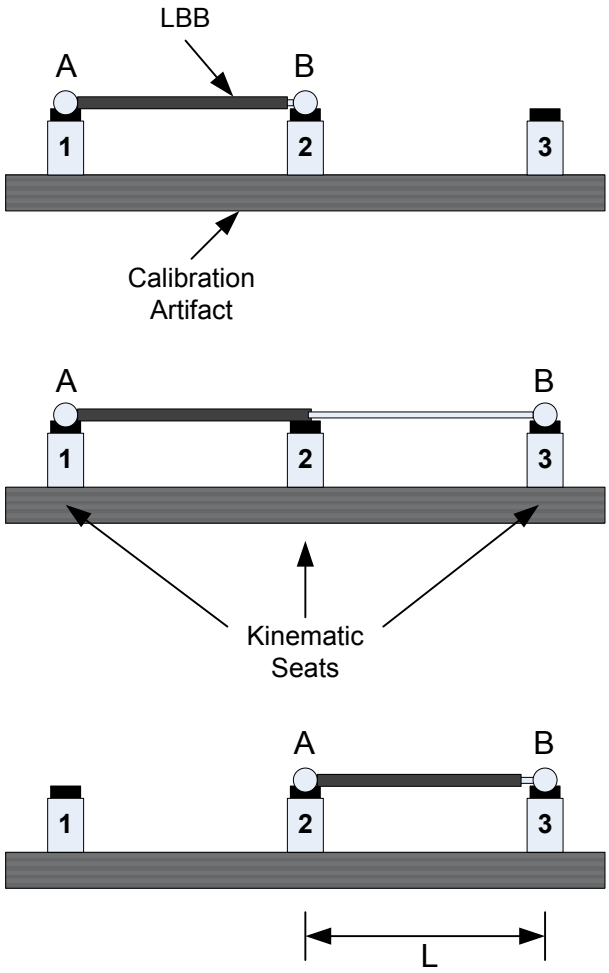

STEP 1
Set ball A and B of laser ball bar into seats 1 and 2; "zero" the instrument

STEP 2
Unseat ball B from seat 2 and place onto seat 3 while extending LBB. Record the distance displaced during movement; this measured length will be used to initialize the laser encoder.

STEP 3
Unseat ball A from seat 1 and seat ball A onto seat 2. Enter the value recorded from STEP 2 to initialize the instrument.

Figure 1-7: Self-initialization procedure of LBB [12]

In the procedure outlined in Figure 1-7, the first measurement of displacement, when Ball B is moved from seat 2 to seat 3, also was a measurement of the previously unknown distance between points 2 and 3 on the artifact. This distance, measured from the center of seat 2 to the center of seat 3, is in turn used to initialize the displacement measurement sensors of the LBB in

step 3, so that now the instrument always provides absolute distance between the ball centers of the instrument.

The calibration artifact used in the LBB measurement system doesn't require any independent calibration. That is, the distance between seats 1, 2 and 3, of the calibration artifact in is unknown and may change over time. To self initialize the LBB all that is required is the following:

- The measurement instrument measures the artifact in more than one position
- The artifact remains dimensionally stable during the short time that is needed to manipulate the instrument on the calibration artifact.
- The laser interferometer displacement measurement is accurate and repeatable
- Interface with the balls of the LBB and the kinematic seats are repeatable.

While it would be possible to initialize the LBB using an externally calibrated master artifact, such as a bar with two sockets a known distance apart, utilizing self-initialization has some key advantages. As already mentioned, a calibrated artifact is not necessary, by doing so the expense of acquiring and periodically recertifying a precision artifact is eliminated. Calibration of precision artifacts will always include a set of defined conditions, where the calibration is valid; usually 20°C for simple parts [13]. In the case of the LBB, it is not unusual for it to be used in environments of varying temperature. Using an artifact which has a calibration that is only valid at a single temperature to initialize an instrument, such as the LBB, would yield an erroneous adjustment of its measurement system; unless the length of the artifact is corrected for thermal expansion. By utilizing a self-initialization method, the initialization of the LBB may be performed under the same operating conditions where the measurement is taking place. A properly designed artifact for self-initialization only needs to remain dimensionally stable during the amount of time that it takes to perform the self-initialization procedure.

Another example of a self-initialized instrument is the One Dimensional Measuring Machine (1-DMM) used for measuring fixed length ball bars, by Ziegert et al [7]. As the name

would suggest, a ball bar is comprised of a fixed-length bar or rod with two or more balls attached along its length, the simplest of these is made of a rod with a precision ball attached to each end. The following figure illustrates the 1-DMM (Figure 1-8) [8].

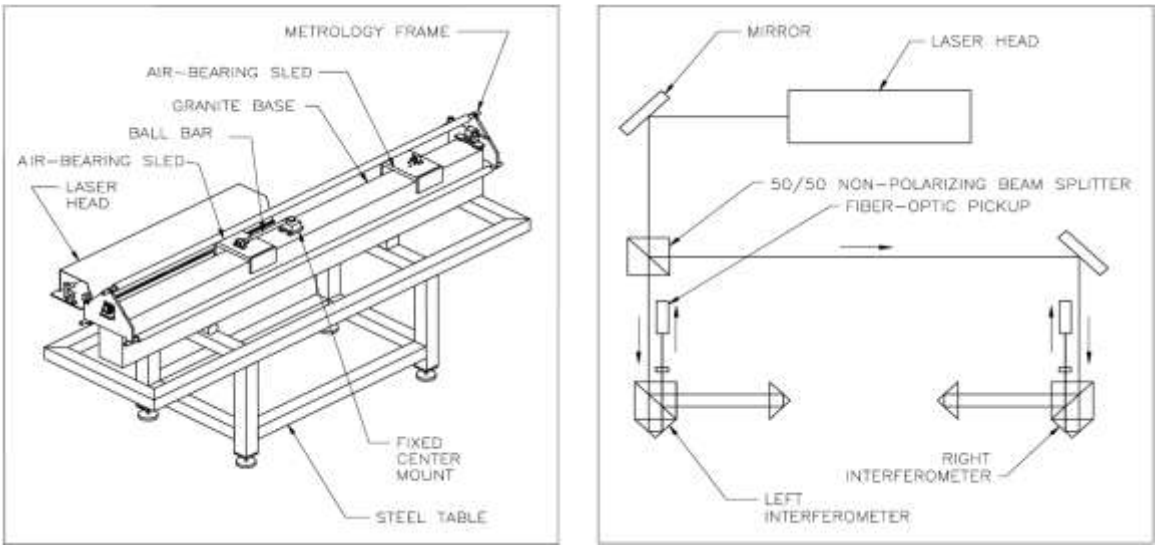

Figure 1-8: One Dimension Measuring Machine (1-DMM) [8]

This instrument is constructed by using a granite straight edge, with two air bearing supported sleds straddling it. Each sled contains a kinematic seat and retro-reflector, with another kinematic seat fixed to the center mount; these seats serve as the measurement points for the ball bar. Laser interferometers are used to track the displacement of each sled as it glides across the granite; travel is limited by the fixed center mount and the metrology frame. When the 1-DMM is initially powered on, the machine has no knowledge of the relative position of the sleds to each other, or to the fixed center mount. In order to utilize the 1-DMM as a measurement machine, a precise datum needs to be set. Initialization of the 1-DMM's displacement measuring system could be accomplished by using a ball bar of known length, as a reference or master-part, or self-initialization may be used. The unique design of the 1-DMM was created with self-initialization ability in mind. The three kinematic seats and their arrangement allows for simultaneous initialization of the 1-DMM, and measurement of the ball bar. This procedure is outlined following figure (Figure 1-9).

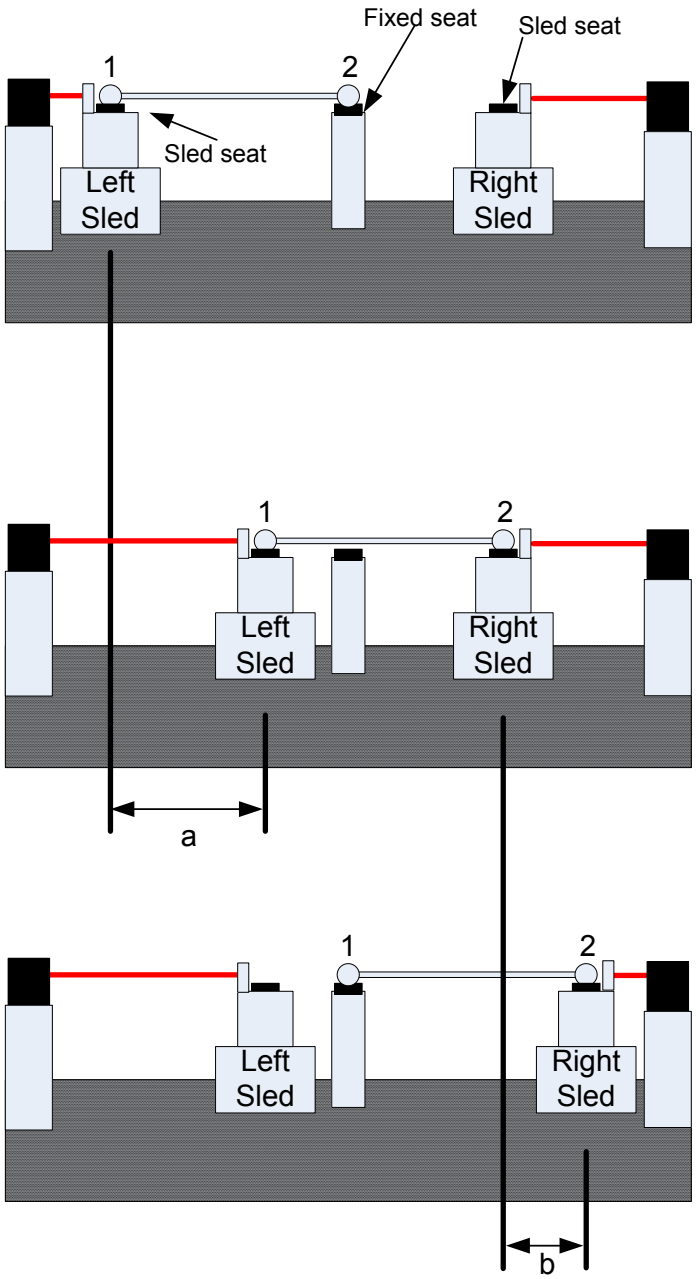

STEP 1
Set left end of ball bar onto kinematic seat of left sled and right end onto the fixed seat; “zero” the left side interferometer

STEP 2
Unseat right end of ball bar and place onto kinematic seat of right sled, simultaneously record the distance traveled by left sled (distance “a”), and “zero” the right interferometer

STEP 3
Unseat left end of ball bar, and place onto fixed seat, record the distance traveled, distance “b”, of right interferometer

Length of ball bar: $L=a+b$

Figure 1-9: Initialization and ball bar measurement sequence for 1-DMM currently installed at NIST

The length of the ball bar is calculated by adding the distances "*a*" and "*b*" [8]. If desired, each interferometer can be initialized to an absolute distance between its TPKS and the fixed TPKS in the center by placing the just measured ball bar onto these seats and setting the output of the corresponding interferometer to the ball bar length, L. This method of self-initialization used a ball bar of unknown length and the displacement measuring sensors of the machine to determine the length of the ball bar and also to initialize the machine. With the machine initialized, ball bars up to two meters in length may be measured simply by placing the ball bar onto the left and right sleds. Of course any subsequent measurement of ball bars after initialization will effectively be a comparative measurement, as these following measurements will rely on the quality of the initial initialization. In effect, the subsequent measurement will have to include the measurement uncertainty of the first ball bar (used to initialize the 1-DMM). One concern with self-initialized instruments is maintaining evaluating their measurement uncertainty and metrological traceability.

Metrological Traceability and Measurement Uncertainty

Regardless of the method used to initialize the instrument, calibration of the instrument to an accepted standard is necessary. For measurements of length, among the countries of the world which have agreed to the Mutual Recognition Agreement [14], the standard unit of measure is the meter. In simple terms, the meter is defined as "the length of path traveled by light in vacuum during the interval of 1/299,792,458 seconds", assuming that the speed of light is 299,792,458 meter per second. [1, 15-17]. Since a meter long light beam can't be physically captured and handled, it is transferred to physical calibration artifacts, by way of fringe counting interferometery;[1, 17]; the following figure displays the traceability of length measurements (Figure 1-10).

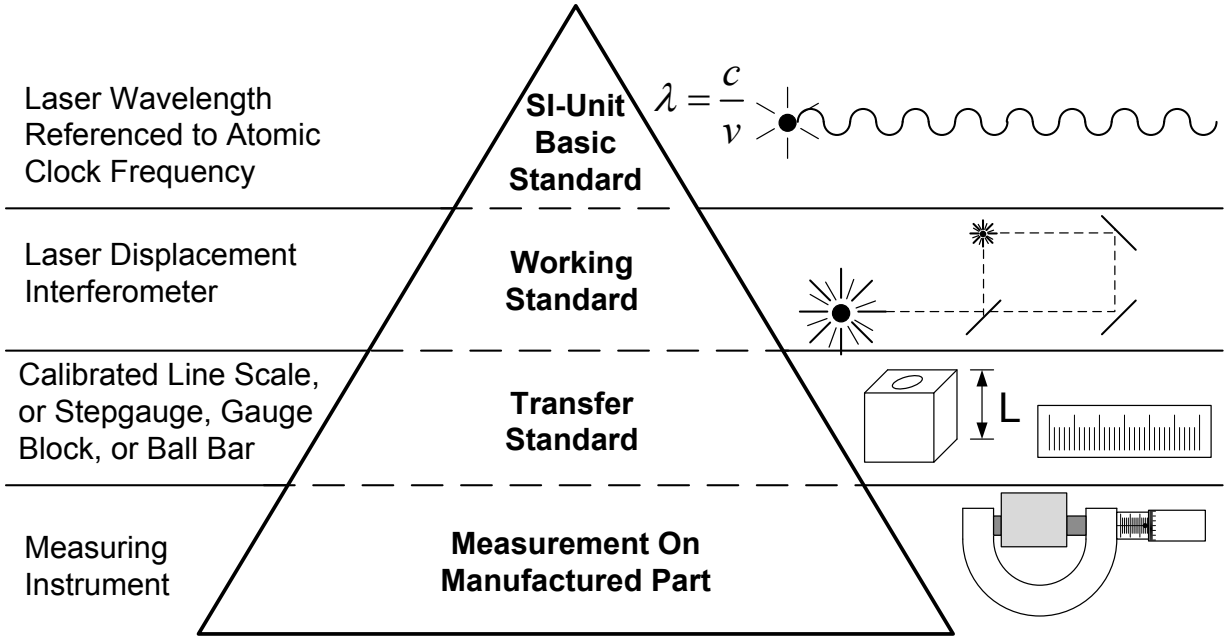

Figure 1-10: Traceability chain for a measurement value to the fundamental SI Unit of measure for length [18]

Calibration of the measurement scale in an instrument or the initialization artifact provides metrological traceability to the standard unit of measure. Metrological traceability is defined in the International Vocabulary of Basic General Terms in Metrology, under definition 2.42 as [3]:

> "*property of a measurement result whereby the result can be related to a reference through a documented unbroken chain of calibrations, each contributing to the measurement uncertainty.*"

As the fundamental unit of length transfers from the top down, each subordinate artifact or instrument is able to realize that unit of measure, but with reduced accuracy and/or higher uncertainty. At the very top of the traceability chain for length measurement lays the definition for the meter. Realization of the meter in a laboratory is through interferometry using an iodine stabilized helium-neon laser light source which generates a wavelength of 632.99139822mm with an uncertainty of $2.5X10^{-11}$ [2]. The act of calibration of an object requires reference to another of higher accuracy and lower measurement uncertainty. As this standard is propagates down the chain of traceability to other length scales and artifacts, measurement uncertainties increase [16].

The uncertainties which are introduced to subsequent calibrations can be due to the inability to exactly replicate the validity conditions which the calibration values are defined. For example the laser interferometer's wavelength defined above is valid when the laser beam is operated in an environment that is controlled to a specified pressure, temperature, humidity, and CO_2 content. Since these values can't be exactly replicated, corrections are made through measuring them, and adjusting the lasers wavelength. However, since the measurement of the validity conditions have their own measurement uncertainties; these will propagate into the measurement uncertainty.

Evaluating Measurement Uncertainty

Because of imperfections in calibration, no measured value can be known with exact absolute certainty; hence measurement uncertainty is used to quantify any doubt one would have on its precision. According to definition 2.26 in the VIM, measurement uncertainty is defined as [3]:

> "*non-negative parameter characterizing the dispersion of the quantity values being attributed to a measurand, based on the information used*"

Evaluating the uncertainty of a measurement is well covered in various literatures [19-22]. Though there is no standard in evaluating measurement uncertainty, some widely accepted methods are outlined in the "*Guide to The Expression of Uncertainty in Measurement*", often referred to as "*The GUM*". The GUM is not a standard, but a guideline of how one is able to estimate the uncertainty of a measurement. A measurement uncertainty is estimated by taking into consideration all of the influencing quantities which affect the measurement, in the form of a standard uncertainty for each of them, and combining them in quadrature to form a combined standard uncertainty for the measured value. There are two basic approaches for estimating the standard uncertainty for each influencing quantity, a Type A, and a Type B approach.

The Type A approach is defined as a "*method of evaluation of uncertainty by the statistical analysis of series of observations*". For a length measuring instrument, a Type A measurement uncertainty evaluation is achieved through a series of repeated measurement on a

artifact of known dimensions. These samplings of measurements are evaluated using descriptive statistics to calculate a measurement mean, and a standard deviation, which is taken as the standard measurement uncertainty.

The Type B approach is defined as a "*method of evaluation of uncertainty by means other than the statistical analysis of series of observations*". When a series of observations of an influencing input quantity is not possible, the Type B approach is used for evaluating its standard uncertainty. Using the information available on the input quantity, if any, an estimate of its standard uncertainty is made. To estimate the standard uncertainty of an input quantity, the first step is to determine the magnitudes of the upper and lower bounds of the input quantity, this information may be provided beforehand or determined based on prior experience or an educated guess. Next, the standard deviation (standard uncertainty) of this interval is estimated. To obtain this estimate, a standard statistical distribution is assigned to the interval. A typical statistical distribution assigned for an uncertainty interval when knowledge is limited is a rectangular distribution. From this assumed probability distribution, a standard deviation is estimated; for a rectangular distribution the standard uncertainty is calculated by dividing the half-width of the uncertainty interval by $\sqrt{3}$.

Each of these individual uncertainties combines to form a combined standard measurement uncertainty. However, the relative influence of each of these individual input uncertainties may be different due to differing sensitivities of the output to the various inputs; thus one will have a greater influence on the output than another. To better understand an estimation of a measurement uncertainty an example is provided in the Appendix using Type B evaluations of standard uncertainty for each influencing quantity.

Motivation and Scope of Research

Calibrated artifacts serve as reference standards used to establish a datum for which accurate units of measure may be realized. In the realm of dimensional metrology, a calibrated

artifact with known metrological traceability is traditionally used to calibrate or initialize a measurement instrument. Maintaining these certified calibration artifacts are time, labor, and cost intensive. The inherent nature of traditional calibration, where the fundamental unit of measure is passed down through the traceability hierarchy, introduces additional measurement uncertainty at each progression down the traceability chain (Figure 1-10). Reducing reliance upon these artifacts may help ameliorate these costs, and stack up of measurement uncertainties.

NIST initiated a program in 2001 to assist manufacturers and laboratories to perform measurements as well as a national measurement institution [23]. With the advanced development of measurement technology, the accuracy and precision of shop floor instruments have improved drastically, reducing the reliance on certified calibration artifacts. Instruments which rely on self initialization, instead of a calibrated artifact, were developed and constructed as part of this effort. However, elimination of these artifacts now presents a new challenge on establishing traceability to a fundamental unit of measure of known measurement uncertainty. Utilizing an instrument initialized/mastered with an uncertified calibration artifact of unknown measurement uncertainty will result in measurement quantities of unknown measurement biases. Maintaining metrological traceability is a concern with the self-initialized instruments previously mentioned.

This dissertation investigates how measurement uncertainties are quantified for measurement results obtained from such self-initialized instruments. Two instruments which utilize self-initialization to obtain the ability to perform an absolute dimensional measurement will be constructed as part of this study. These two instruments will be used as case studies to demonstrate how metrological traceability can be maintained.

Goals of Research

1. *Derive and/or explain the geometric conditions which enable self-initialization in an instrument* – Self-initialization of a measurement instrument can occur under two scenarios, measuring a null value, or relying on a unique artifact that allows the

instrument to derive their own initialization artifact. For the LBB and 1-DMM, a sphere and three point kinematic seat is used as the mechanical interface between the interface and the object to be measured. The geometric conditions which permit this are explained in detail.

2. *Describe two novel instruments that are capable of self-initialization* - Two instruments, one for measuring ball bars up to 3 meters in length, and another used for measuring circular rings will be constructed and used as case studies on developing instruments which are able to self-initialize their displacement measurement sensors.
3. *Provide a Type-B uncertainty analyses for these instruments when they are self-initialized and when they are initialized using a master artifact* – Measurement uncertainty analysis is well covered in literature, such as the "Guide to the Expression of Uncertainty In Measurement", often simply referred to as "The GUM" [19-21]. The measurement uncertainty of the two instruments described above will be evaluated, using Type B approach, when they are operated under two modes, when they're initialized using an externally/independently calibrated artifact, and initialized using self initialization.
4. *Compare and contrast the two modes of use* – what are the advantages and disadvantages of using self-initialization over conventional modes of initialization
5. *Provide Conditions under which lower uncertainty is achieved using self-initialization* – under what conditions and situations where self-initialization may be a preferred method over traditional.

Outline of Dissertation

Chapter Two describes in detail the geometric conditions where instruments can self-initialize through a functional decomposition of the Laser Ball Bar, and how uncertainty is modeled for such instruments

Chapter Three describes the design of a machine used to measure ball bars measuring up to 3 meters in length utilizing a self-initialization method which is similar to the LBB.

Measurement results provided by the instrument are presented, with future work to be completed on the instrument to expand its capabilities

Chapter Four discusses a new discovery on measurement uncertainties of machines which utilize the extended Abbe principle to correct for Abbe offset errors

Chapter Five describe the design of an instrument used to perform absolute measurements of diameters on large circular objects in the shapes of cup, cones, and rings. Measurement results provided by the instrument are presented, with future recommendations on further development of the instrument

Chapter Six provides concluding remarks, and suggestions for future research.

CHAPTER TWO

SELF-INITIALIZED ONE DIMENSIONAL MEASUREMENT INSTRUMENTS

This section discusses in detail the geometric conditions which allow an instrument to self-initialize. The Laser Ball Bar (LBB) is functionally decomposed to better understand what allows it to self-initialize. A uncertainty analysis using Type B evaluation for standard uncertainties is used to compare and contrast measurement uncertainty of length measurements provided by the LBB when it is initialized with a independently calibrated artifact, and when it's self-initialized.

Introduction

Instruments which are able to self-initialize don't require a calibrated artifact to set their measurement sensors to a known reference value in order to perform an absolute measurement. The dial caliper and micrometer for example, butt their measurement anvils together to realize a zero length measurement, and are then initialized by "zeroing" the measurement sensor. Other types of length measuring instruments which are unable to realize a null length measurement require a calibrated artifact of a known dimension and form to initialize their measurement sensors, such as a the styli of coordinate measuring machines (CMM), or a gauge block comparator [5]. Initialization effectively establishes a known point on the scale, enabling further displacement measurements by the scale to be converted to an absolute distance between the measurement points on the instrument.

The measurement sensors on a CMM and a gauge block comparator are capable of performing accurate measures of displacement, assuming they have been calibrated. However a calibrated artifact of known length needs to be introduced to each of these instruments to serve as a reference to a known dimension, before other objects may be measured. A CMM will require a high precision sphere of known size, and form error to qualify their styli, while the gauge block comparator requires gauge blocks of known size to serve as a reference standard. These artifacts which are used to initialize each instrument need to be traceable to a standard unit of measure, the meter, to ensure that their measurement values can be attributed to a fundamental

unit of measure with a known uncertainty [24-26]. However, there is a class of instruments which are able to self-initialize their measurement sensors because the nature of their design allows a displacement measurement, made by the instrument, to be captured by a fixture or artifact as a length measurement. This length embodied by another object can immediately be reused by the instrument to initialize itself.

The Self-Initialized Instrument System

Self-initialization is where an externally calibrated artifact isn't used to perform an offset adjustment of an instrument's displacement measuring system to a known initial value. The instrument which pioneered the use of the self-initialization method is the Laser Ball Bar (LBB) [7]. A short time later, another instrument used to measure ball bars, called the 1-Dimensional Measuring Machine (1-DMM) utilize a similar method for self-initialization [8, 27]. Not having to rely on an independently calibrated artifact provides several key advantages, they are:

- No need to maintain a calibrated artifact which needs to be periodically re-calibrated
- Measurement uncertainty which accompanies an artifact from a previous calibration isn't passed on to other measurements
- The end user of the instrument isn't reliant on calibration laboratories, and can realize absolute measurements on their own.

Self-initialization, in concept is similar to self-calibration [28], "*where an un-calibrated artifact, that may measured by the instrument in more than one position, can be used to improve both the calibration of the artifact and the instrument*". However, self-initialization is not calibration, but rather a offset adjustment of the measurement sensor [3]. A self-initialized measurement system consists of the instrument, which contains the calibrated displacement sensor, and a specially designed artifact that isn't calibrated.

Unlike the instruments mentioned earlier (CMM and gauge block comparator), these instruments perform measurements of position, displacement, and distance, without relying on measures of extension. These instruments accomplished this by utilizing a design which limits

them to making purely measurements of position, displacement, and distance. The mechanical interface which permits this is a coupling between a sphere and a three-point kinematic seat (TPKS) [11, 29]. The natural arrangement between the TPKS and the spheres they cradle allows a singular point in space, the center of the sphere, to be resolved by their geometrical relationship with each other (Figure 2-1).

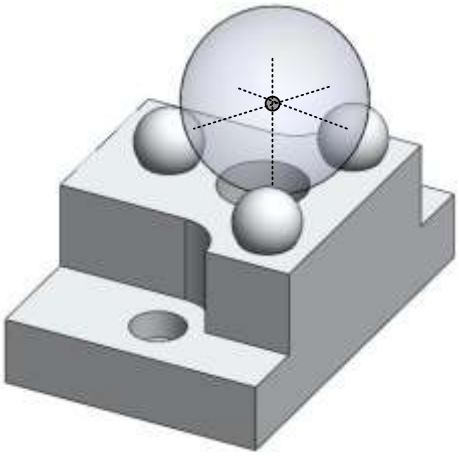

Figure 2-1: Sphere and three point kinematic seat coupling

In practice, precision spheres with sphericity errors less than a few millions of an inch are inexpensively available. Testing has shown that the positioning repeatability of the sphere in the TPKS is on the order of magnitude of the surface roughness of the contact surfaces, thus enabling nanometer level realization of repeatability in locating of the sphere center. These characteristics enable practical realization of self-initialization.

There are numerous embodiments of a TPKS, some are assembled with pre-fabricated components such as spheres, spherical buttons, rods, half-rounds, and quarter rounds[30], while some can be manufactured in a monolithic fashion with three mechanically burnished arc shaped surfaces, serving as the TKPS [11]. A sphere, which by mathematical definition is a solid bounded by a surface which has all its points' equal distance from the center, is an ideal geometric shape because it is the only object that can approach from any direction above the plane of the TPKS, to make contact with it, and deterministically resolve a point in space, which is the geometric center.

One method of constructing a TPKS may be accomplished by placing three spheres in close proximity to each other. These three spheres form a hollow in the middle which is able to cradle another sphere. By placing a larger sphere on top of the hollow of the TPKS, three points of contact are formed, generating three tangent sphere intersections. This coupling geometrically forms a tetrahedron between the three points of contact, and the center of the larger sphere. One may imagine this by drawing three lines normal to the tangent points of contact, the point which they intersect is through the center of the larger sphere (Figure 2-2).

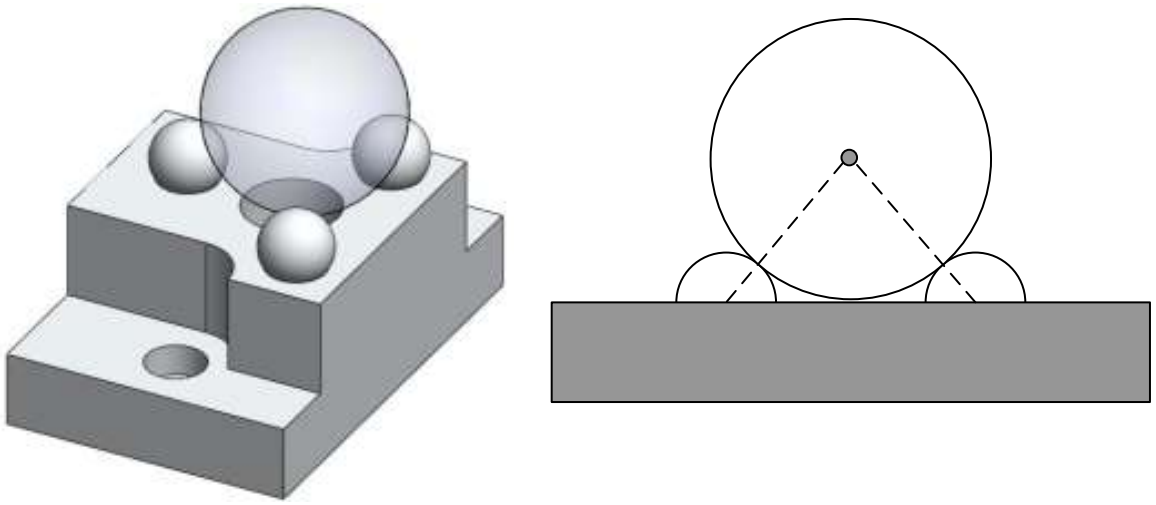

Figure 2-2: Three-ball kinematic seat [29]

Self-initialized instruments utilize at least two of these couplings at different locations, along with a linear displacement sensor, such as a linear encoders, laser interferometers, or angle encoder to produce a measure of distance. A physical embodiment of such an instrument is the Laser Ball Bar (LBB) system, by Ziegert et al.; illustrated in the following figure (Figure 2-3) [7, 10].

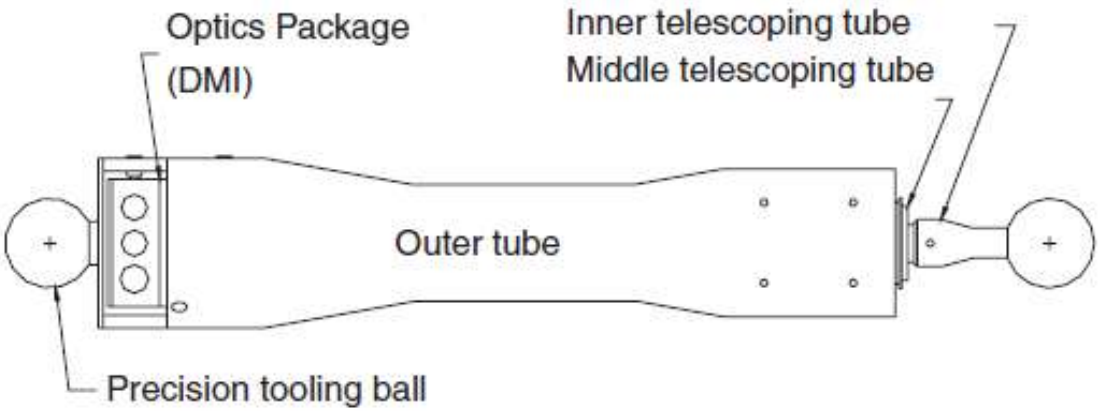

Figure 2-3: Laser Ball Bar (LBB) concept and component layout [7, 10]

The LBB is an instrument consisting of three concentric precision telescopic tube assemblies which houses a set of interferometer optics, and two precision spheres, on each end of the instrument. As the tube extends, the laser interferometer system measures the relative displacement of the optics, i.e. the change in distance between the sphere centers. The spherical ball ends on this instrument permit precision interface to a TPKS [11]. Each of these kinematic seats has three precision points which make contact with a sphere (Figure 2-4). These three contacts constrain all translation motion of the center of the sphere, but do not restrict any rotation of the sphere.

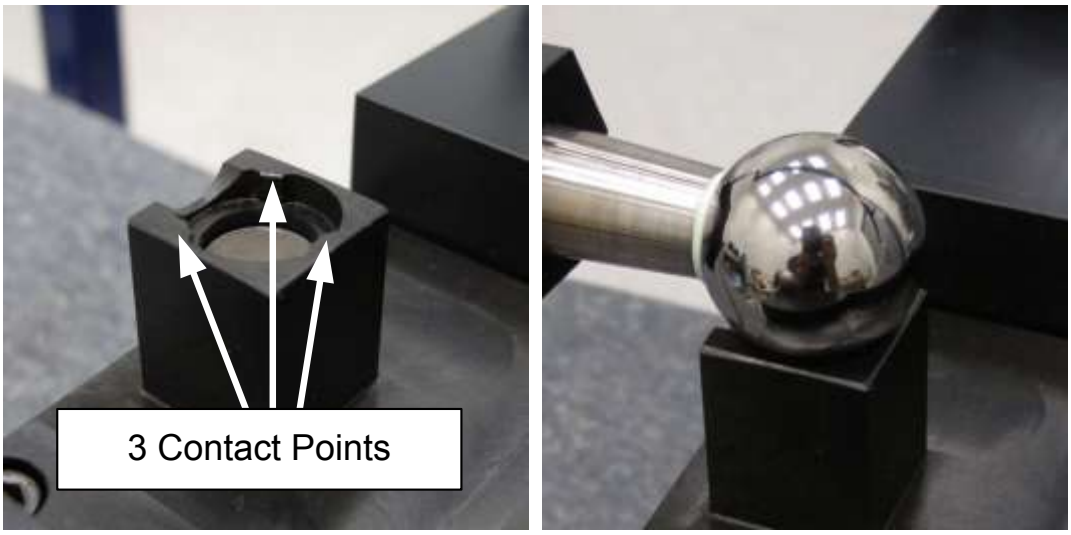

Figure 2-4: Quasi Kinematic seat detail; points of contact exposed, and ball mounted

This feature allows the LBB to interface with measurement points with excellent repeatability. To initialize the laser interferometer to measure the distance between the sphere centers, an un-calibrated artifact with three TPKS is used in combination with the following procedure is used (Figure 1-7).

The LBB is able to self initialize because it can resolve position, displacement, and distance, in one dimension, without needing to resort to measures of extension. This instrument is able to accomplish this because it is able to directly and simultaneously locate two discrete fixed points. The unique mechanical interface between the instruments and the objects which they measure are fashioned by two three point kinematic couplings. Each of these couplings are formed by matting spheres with a three-point kinematic seat (TPKS), which deterministically define discrete points in space (Figure 2-1), the sphere center [10, 29]. To more thoroughly understand self-initialization, let's take a closer look at the procedure for the LBB.

The measurement quantity, or measurand, that this instrument provides is defined by a length, the center to center distance between the two spheres. (Figure 2-5).

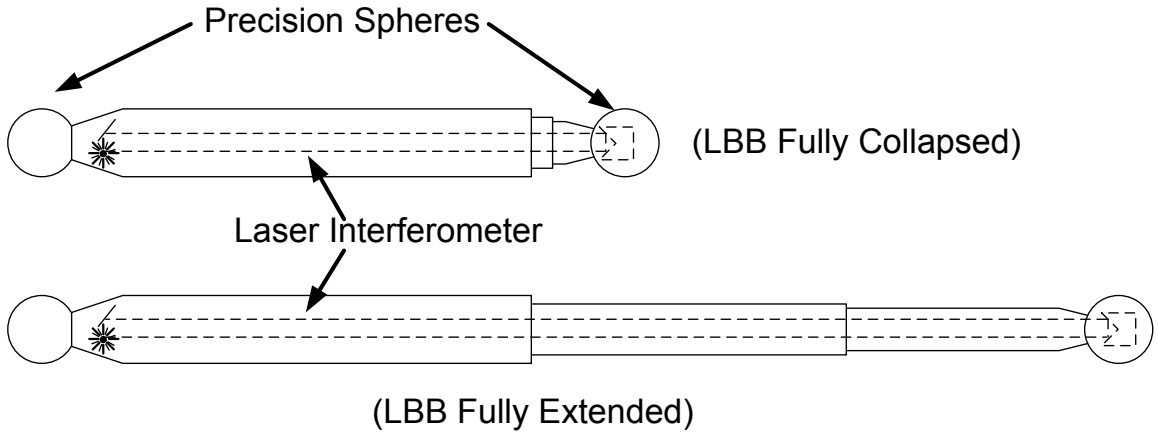

Figure 2-5: Laser ball bar (LBB), critical components displayed

The laser interferometer in the LBB is unable to natively provide an absolute distance value between the two spheres. Since these tubes are unable to collapse together to make the spheres concentric, and thus realize a null length measurement (so the interferometer may be "*zeroed*"), an external artifact consisting of two TPKS's mounted on a rigid structure and a known distance

apart may be introduced to the LBB for initializing its displacement sensors. Rather than relying on an externally calibrated artifact to initialize the LBB, a fixture which contains three collinear TPKS's is used. If an imaginary sphere is placed on top of each TPKS on the fixture, there will be three distinct points defined which all lie along a line; the distances between these points on the artifact are unknown.

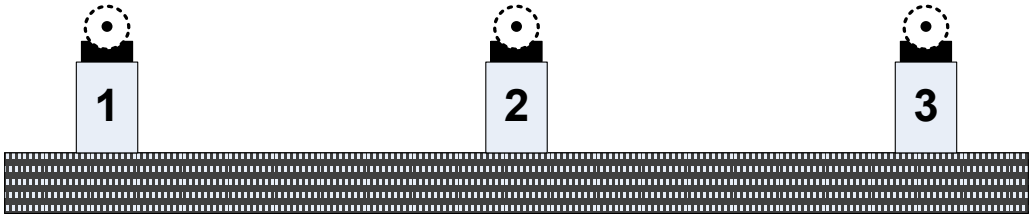

Figure 2-6: Calibration artifact for LBB; distance between seats 1, 2, & 3 are unknown

By placing the spheres of the LBB on these seats, two points may be determined along a line at any given moment. Since the change in length of the LBB is continuously monitored, the distances between points on the fixture can be measured using only displacement information from the LBB sensor by following the three-step procedure outlined as follows [12].

The self-initialization sequence begins by placing the two spheres of the LBB onto two of the three TPKS's. While the instrument is supported by the two TPKS, the displacement measurement sensor is reset to read a zero value (Figure 2-7).

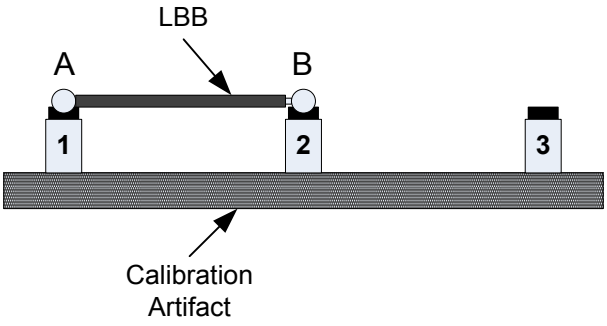

STEP 1
Set ball A and B of laser ball bar into seats 1 and 2; "zero" the instrument

Figure 2-7: First step constrains LBB, followed by "zeroing" the displacement sensor

In this step a zero datum point has been established at point "*2*" along the line. In the next step, the sphere on the LBB that is closest to a vacant TPKS is lifted off its current seat, and placed

onto the vacant seat; the other sphere remains coupled with the first TPKS. During this motion, the distance between TPKS 2 and 3 is measured by the LBB's displacement sensor (Figure 2-8).

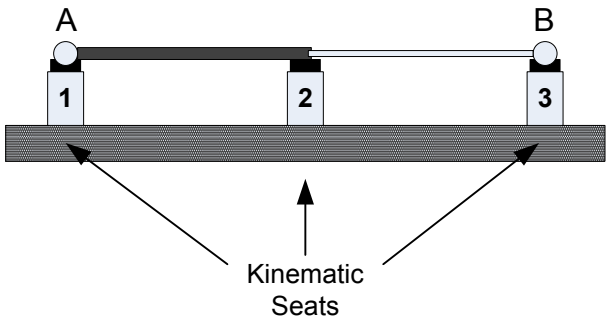

STEP 2
Unseat ball B from seat 2 and place onto seat 3 while extending LBB. Record the distance displaced during movement; this measured length will be used to initialize the laser encoder.

Figure 2-8: The distance between two TPKS is measured during step 2

In this step a line segment, $\overline{23}$, between TPKS 2 and TPKS 3 has been measured. This was possible because ball "B" on the LBB was able to resolve distance between two discrete points along a line. With this known distance, it may be used to initialize the LBB by placing spheres A and B on top of TPKS's 2 and 3 and initializing the displacement measuring system to the length of line segment $\overline{23}$ (Figure 2-9).

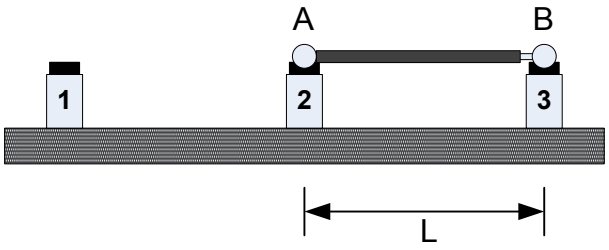

STEP 3
Unseat ball A from seat 1 and seat ball A onto seat 2. Enter the value recorded from STEP 2 to initialize the instrument.

Figure 2-9: Initialize using the distance recorded in step 2

As demonstrated by the previous three figures, self-initialization is possible with an artifact of unknown length and an instrument which measured with an unknown bias. Because of the unique nature of the TPKS to deterministically resolve a singular point in space when coupled with a sphere, a displacement measurement from "Point 2" to "Point 3" using the LBB, directly transforms to a length measurement between TPKS 2 and 3 (Figure 2-8) [7, 10]. Being able to

directly assign a length measurement onto the artifact is possible because three singular points in space and their relative distance from each other can be evaluated directly from displacement measurements produced by the instrument.

Functional Requirements Necessary for Self-Initialization in One Dimension

For an instrument to self-initialize its displacement measuring sensor, four necessary functional requirements can be drawn from the preceding example:

1 The calibration artifact needs to have a length measurand that is definable by at least two distinct point locations

2 The displacement sensor on the instrument needs to be able to resolve the location and distance between each point deterministically

3 The artifact needs to be able to receive/capture a displacement value recorded by the instrument, and transform it to an absolute dimensional value

4 The instrument needs to be able to interface with the points on the artifact in at least two different positions along a line.

There may be other methods to deterministically define a point in space through the coupling of two separate objects. The TPKS and sphere coupling is one practical method to define a point in space, or in this case along a line. By arranging a series of TPKS that are collinear with each other, and at fixed locations along a line, this creates an artifact that has a length measurand that is defined by distinct points. In the case of the LBB, by affixing spheres to an extensible, one degree of freedom measuring instrument, relative distances between the fix seats can be evaluated. Once evaluated, the measured values contained by the artifact can be used to initialize the same instrument that determined them.

This concept of a sphere and TPKS coupling has been successfully used to invent several other self-initialized instruments, two ball-bar measuring machines, and an instrument to measure diameters of large circular parts [6, 8, 27]. These instruments use variations of the self-initialization procedure that is employed by the LBB, but still adhere to the four functions outlined

in the previous paragraph. While these instruments have been shown to be repeatable in performing measurement tasks they were designed for, the question of measurement uncertainty when used in the self-initialization mode as opposed to the master-part initialization mode needs to be addressed.

Measurement Uncertainty of Self-initialization

Quantification of a measurement uncertainty is important to deem if the measurement instrument is appropriate for a specific application. For example, manufacturing and assembly type applications often require part tolerances to be controlled within a certain interval. These tolerances defined on a part not only take into account variations and errors due to the manufacturing process, but the metrology which is involved in measuring them. In a part's metrology process, the expanded uncertainty of the measurement typically should take up no more than 15%-25% of the tolerance band; often referred to as gauge R&R. This provides an allowance for variability due to a part‘s manufacturing process.

In the case of the LBB it's used to evaluate the volumetric positioning accuracy of machine tools. If the positioning accuracy for a given machine tool is better than what the LBB can measure, the instrument wouldn't be able to provide any useful feedback on the machine's performance. The uncertainty of measurements provided by the LBB has been well evaluated when it is self-initialized [7, 10]. An alternative to self-initializing would be to initialize with an externally calibrated artifact. To see how this can change the uncertainty of measurements provided by the LBB a simple Type B uncertainty analysis is performed.

To initiate a Type B uncertainty analysis, we'll begin with establishing the mathematical model for a self-initialized measurement; for the LBB, a simplified model is:

$$L = L_0 + x$$

where: L is the resultant length between ball A and B of the LBB
L_0 is the initialization length (2.1)
x is the displacement measurement from the LBB following initialization

This model is no different than that of a gauge block comparator, where a calibrated master reference gauge block is the initialization length (L_0), and the displacement (x) is measured by a calibrated sensor, when a gauge block of unknown length is measured. The uncertainty of each component for equation 2.1 is assigned as a result of calibration which relates to the fundamental unit of measure, the meter. If each input into the model is traceable, in the case of a comparator instrument, we can logically deduce that the measurement from a self-initialized instrument is traceable and its uncertainty is quantifiable [24].

In the case of a self-initialized instrument, the initialization length is assigned by a displacement senor attached to the instrument itself, which is traceable via calibration. Since the initialization length was obtained from a traceable displacement sensor or calibrated scale; measurements performed by a self-initialized instrument are inherently traceable. Traditional traceability chains dictate that an artifact or instrument used to initialize or calibrate another needs to be more accurate and have a lower measured uncertainty. This traditional use of higher accuracy artifacts and systems to propagate the traceability cannot be realized in self-initializing instruments. What effect does this have on the overall achievable measurement uncertainty of such devices?

With the self-initialized instrument providing the length measurement to the initialization artifact, it stands to reason that the uncertainty in establishing this initialization length value will be on the same order of magnitude as subsequent measurements performed by that instrument post initialization. Because of this, subsequent measurements will have an uncertainty that is no better than the uncertainty of establishing the initialization length which is closely related to the

displacement measuring uncertainty of the displacement measurement sensor. Therefore it is critical to quantify the uncertainty of the initialization length for a self-initialized instrument.

Evaluating the uncertainty of a measurement is well covered in various literatures [19-22]. The most widely use methods for evaluating measurement uncertainty is the "*Guide to the expression of measurement uncertainty*"; often referred to as the "GUM"[20]. The GUM defines two basic approaches for estimating the uncertainty of a measurement, a Type A, and a Type B approach. The Type A approach is defined as a "*method of evaluation of uncertainty by the statistical analysis of series of observations*". For a length measuring instrument, a Type A measurement uncertainty evaluation is achieved through a series of repeated measurement on a artifact of known dimensions. These samplings of measurements are evaluated using descriptive statistics to calculate a measurement mean, and a standard deviation, which is taken as the standard measurement uncertainty.

The Type B approach is defined as a "*method of evaluation of uncertainty by means other than the statistical analysis of series of observations*". This method relies on a mathematical model of the measurement, and knowledge of the individual measurement uncertainties of each input into the model. Each of these individual uncertainties combines to form a standard measurement uncertainty. However, the relative influence of each of these individual input uncertainties may be different due to differing sensitivities of the output to the various inputs; thus, one will have a greater influence on the output than another. To better understand a Type B measurement uncertainty, an example is provided in the Appendix.

In the case of the LBB, a simple Type B uncertainty analysis is performed using equation 2.1. to shed some light on how the LBB's length measuring uncertainty is evaluated when self-initialization is used. The uncertainty of each input to this mathematical model for length measurements can arise from many sources, but to simplify this analysis only two are considered, the laser interferometer, and the TPKS couplings. The laser interferometer will mostly likely be furnished with a calibration certificate, stating its measurement uncertainty in reference to the fundamental unit of measure [7, 17, 23, 31, 32], we'll call this uncertainty U_L. A length scale

manufacturer will mostly likely calibrate their products against a more accurate interferometer system.

Shifting our focus on to the TKPS, the self-initialization procedure requires decoupling and re-coupling of the spheres, and TPKSs. Serving as the measurement points for the instrument, the TPKS and sphere coupling have an uncertainty in defining a singular point in space. Their uncertainty is a result of their non-repeatability in its mechanical connection, which is due to elastic deformation, imperfections in their surface finishes, and form errors between the two components [11, 33]. Along one dimension, this non-repeatability can be expressed as an uncertainty U_k.

Recalling equation 2.1, there are two inputs into this equation, the initialization length, L_0, and displacement measurements relative to the initialization length, x. Each of these inputs will have an uncertainty associated with them. Assuming that there are only two sources for uncertainty in establishing the initialization length, U_L and U_k, the combined standard uncertainty for the initialization length is calculated by adding these two in quadrature; the square root of the sum of the squares, (assuming that U_L isn't dependent on the magnitude of displacement):

$$u_{L_0} = \sqrt{u_L^2 + u_k^2} \qquad (2.2)$$

Once the initialization length L_0 has been used to initialize the instrument, any additional displacement of the instrument adds to the initialization length to produce a total measurement value, equation 2.1. However, since the initialization sequence was treated as a separate measurement, this next stage of measurement needs to be evaluated. Since this displacement measurement also relies on the same laser interferometer and similar kinematic seats to define its measurand, the uncertainties that were present during the self-initialization sequence reappear for measuring values of x in the measurement model, equation 2.1. The uncertainty of measuring displacement x is:

$$u_x = \sqrt{u_L^2 + u_k^2} \qquad (2.3)$$

In this case the total combined measurement uncertainty for a measured value provided by the ball bar, according to the highly simplified model provided by equation 2.1 is:

$$u_L = \sqrt{u_{L_0}^2 + u_x^2} = \sqrt{2\left(u_L^2 + u_k^2\right)} \qquad (2.4)$$

In this simplified uncertainty analysis example for the LBB, the result in equation 2.4 shows that the displacement measurement uncertainty in the instrument contributes twice to the absolute length measurement uncertainty when self-initialization is used. If the initialization length L_0 was provided by an externally calibrated artifact, the length measurement uncertainty becomes the following:

$$u_L = \sqrt{u_{L_0}^2 + u_x^2} = \sqrt{u_{L_0}^2 + u_L^2 + u_k^2} \qquad (2.5)$$

Under this mode of initialization the uncertainty term of the instrument's displacement sensor appears once, however there is an additional uncertainty term is introduced by the externally calibrated artifact. Of these two analyses, the initialization mode which provides the lowest length measurement uncertainty will depend on the uncertainty of initialization lengths provided by each initialization mode respectively. For initialization using an externally calibrated artifact to have a lower length measurement uncertainty than self-initialization, the uncertainty in the initialization length value needs to be lower than that provided by self-initialization.

In this analysis, there are many more variables that can contribute to the total combined measurement uncertainty. Other factors such as environmental influences (vibration, electronic noise, temperature fluctuations, etc.), human error, and instrument instabilities, are often contributors in evaluating a measurement uncertainty. In particular with an initialization artifact, non-co-linearity of the points defined by the TPKS couplings can affect the initialization length.

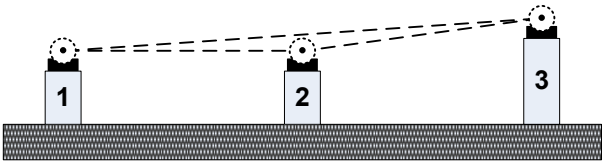

Figure 2-10: LBB initialization fixture, non-co-linearity of TPKS exaggerated

This effect will induce a cosine error in establishing the initialization length. There are more uncertainties that can influence measurements with a self-initialized instrument, as with any instrument. The challenge is identifying those that contribute the most to the overall measurement uncertainty.

Concluding Remarks

Despite the inability to realize a null measurement value, the laser ball bar is able to provided an absolute length measurement though self-initialization [12]. Through a functional decomposition of the Laser Ball Bar length measuring instrument, four functions are necessary for an instrument to achieve self-initialization are defined. The functions outlined for self initialization are not definite, but provide a starting point to design other instruments that can utilize a self-initialization procedure to perform a zero adjustment for their measurement system. The measurement uncertainty of a length quantity provide by these type of self-initialized measurement instruments will always be at least two times its displacement measurement uncertainty. Using an independently calibrated initialization artifact to initialize a length measurement instrument will provide a lower measurement uncertainty, if uncertainty of the initialization value provided by the artifact is lower than that provided by self-initialization. The following chapters of this dissertation detail two novel instruments which utilize self-initialization to initialize their displacement measurement sensors. These chapters will cover their application, design, construction, measurement uncertainty analysis, and provide experimental results.

CHAPTER THREE

A MACHINE FOR MEASURING BALL BARS UPTO 3 METERS IN LENGTH

This chapter discusses the design of an instrument that is used to measure ball bars up to 3 meters in length. The design of this machine demonstrates how self-initialization can be utilized to facilitate the ability to perform an absolute measurement. Alternatively an independently calibrated artifact may be used to initialize its measurement sensors to achieve the same tasks. Experimental results comparing and contrasting the two methods are provided.

Introduction

Ball bars are typically used to evaluate the volumetric performance of coordinate measuring machines (CMM). As their name suggests, a ball bar is an artifact which is constructed by affixing two precision spheres on the end of a nominally rigid bar. These ball bars are used in CMM test standards such as ASME B89.4.1 & B89.4.22 as a reference length artifact. The measurand of a typical ball bar is defined as the distance between the centers of its spheres. A 1-dimensional measuring machine (1-DMM) has been in use at the National Institute of Standards and Technology for measuring and calibrating the length of ball bars. The original 1-DMM is capable of measuring ball bars up to one meter in length with expanded (k=2) uncertainty of U = 0.2 + 0.2L, where L is in meters, and U is in microns. With the ever increasing sizes of CMMs and with wide spread application of larger articulated arm CMMs, longer ball bars are needed. In addition, laser tracker systems also require long reference length artifacts (i.e. optical ball bars which are at least 2.3 meters long), for evaluating their performance in accordance with standards similar to ASME's B89.4.19. As these ball bars grow in size and evolve, new capabilities and techniques are necessary to calibrate them. During the 2001 ASPE Annual conference the one dimensional measuring machine (1-DMM), a machine specifically designed to calibrate ball bars up to one meter in length, was introduced [8]. While this design concept was suitable for short ball bars (≤1m), it was impractical for longer ball bars as it would require the machine to be about 6 meters long to measure a 3 meter long ball bar. To overcome this difficulty an alternate design

which also utilizes a self-initialization method was commissioned. The new 1-DMM discussed in this chapter has the capability of measuring ball bars up to 3 meters in length, incorporates interferometer displacement measurement, and utilizes a dedicated un-calibrated artifact to self-initialize the instrument's displacement measurement system. The following figure provides a conceptual design view of the 1-DMM.

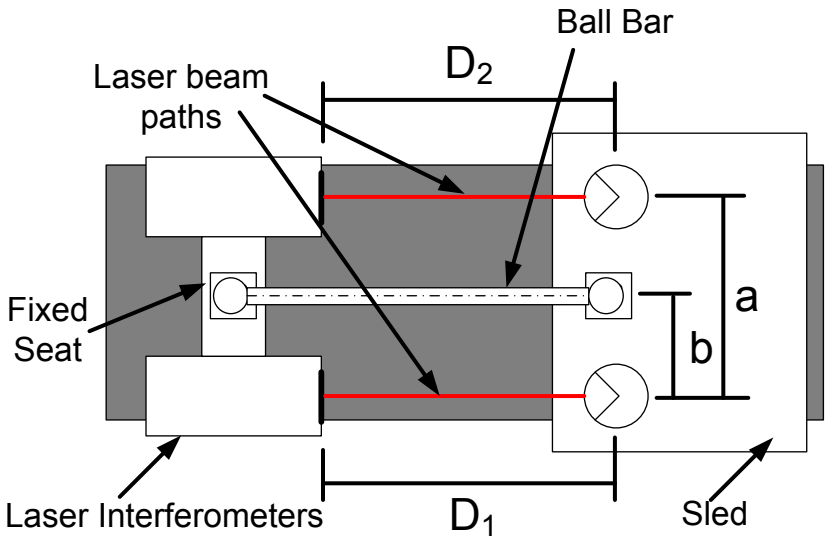

Figure 3-1: Top view of new 1-DMM

Instrument Design

This new instrument is a variant design of a similar 1-DMM currently in service at NIST. This new version of the 1-DMM uses a precision granite straight edge beam, with a steel sled supported by air bearings straddling it. The ball bar being measured is supported at one end by a three point kinematic seat (TPKS) rigidly affixed to the granite beam, and at the other end by a TPKS affixed to the sled. Movement of the sled allows ball bars ranging from 100mm to 3,000mm in length to be measured. The TPKSs are nominally centered along the longitudinal centerline of the granite beam. A pair of laser interferometers is symmetrically arranged on the machine such that their measurement axes are parallel to the sensitive direction of motion, and co-planar to the axis of a ball bar when it is supported by the kinematic seats. These laser interferometers are

used to track the linear displacement of the two sides of the sled. Since the measurement line is between the measurement axes, this allows for correction of any Abbe errors due to yaw motions of the sled [34] (Figure 3-2).

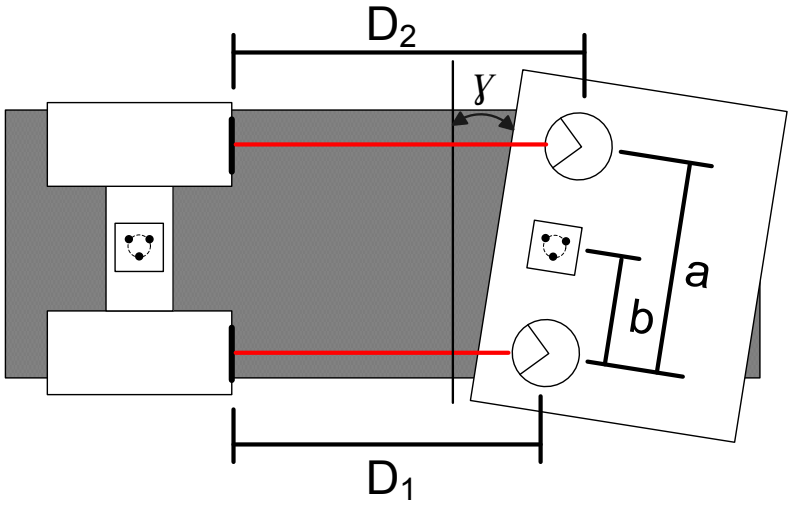

Figure 3-2: Yaw of sled

Referring to Figure 3-1, if just a single laser interferometer, D_1, was used to measure the displacement of the TPKS mounted on the sled, any yaw motion of the sled will results in motion additional motion of the sled that isn't measured. The addition of a second laser interferometer, D_2, is used to measure the yaw motion of the sled. If the lateral separation between the lasers beam paths, the distance from one of the laser beams to the TPKS, and the relative displacement between the lasers is also known, the yaw motion of the sled may be accounted for in the displacement measurement of the TPKS; the amount of yaw, γ, is estimated using the following equation (Eq. 3.1)

$$\gamma = \sin^{-1}\left(\frac{D_2 - D_1}{a}\right) \approx \left(\frac{D_2 - D_1}{a}\right) \tag{3.1}$$

where: D_1 is the displacement measured by sensor 1

D_2 is the displacement measured by sensor 2

a is the separation between sensor 1 and 2

Direct measurement of a ball bar is performed by placing the ball bar onto the TPKSs. The distance between these two TPKSs are used to define the length of a ball bar. However, before the 1-DMM can perform measurements it needs to be initialized to provide an absolute distance between the kinematic seats rather than displacements of the sled. The final design of the instrument is shown in Figure 3-3.

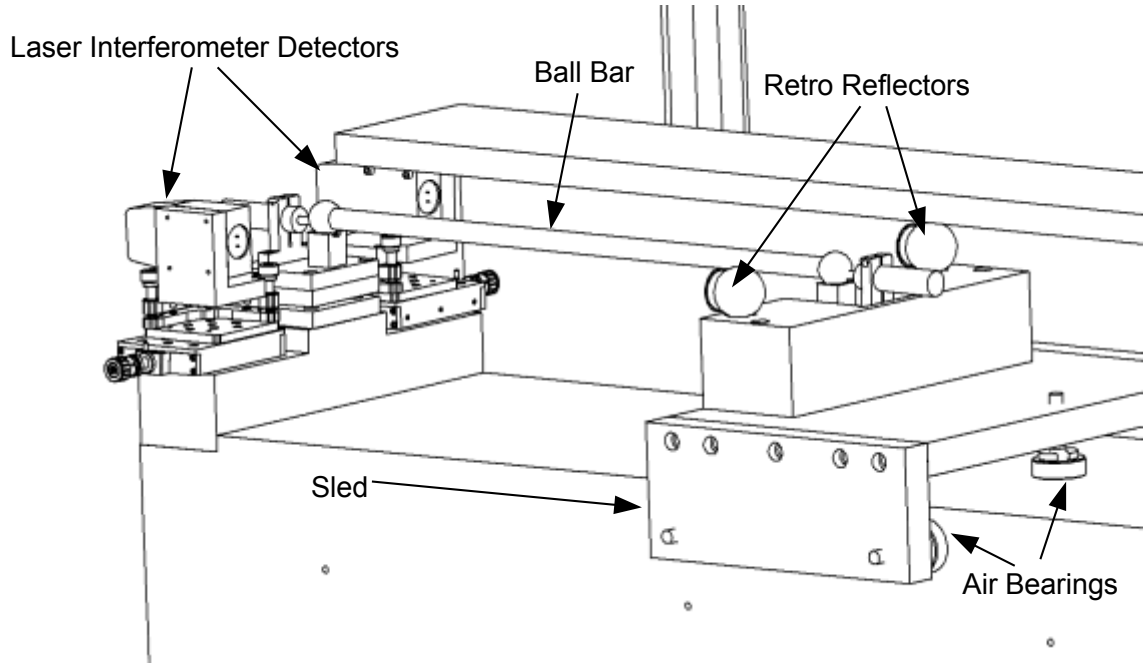

Figure 3-3: Final design and layout of 1-DMM instrument

The main difference between the 1-DMM currently installed at NIST and this new design is the arrangement of the laser interferometer beams. This new arrangement allows for a more compact design to fit inside the metrology labs located at NIST's metrology facility. Since the laser beams of the interferometer are not co-linear with the axis of the ball bar, the second laser interferometer is used to correct for any yaw error motions of the sled as it traverses along its axis of travel.

Initializing the 1-DMM

The 1-DMM's primary function is to provide an absolute distance between the centers of its two TPKS. When these TPKS cradle a ball bar, the absolute distance between these TPKS also define the measurand of the ball bar. However, in order for it make absolute measurement of ball bars, the 1-DMM needs to be initialized with a known distance. Just like a comparator type instrument, the 1-DMM defines a measurement as some initial distance, L_0, plus a displacement, D.

$$L = L_0 + D$$
$$\text{where: } L_0 \text{ is the initialization length} \qquad (3.2)$$
$$D \text{ is the displacement of TPKS on sled}$$

There are two methods which may be used to initialize the 1-DMM, using an independently calibrated ball bar, or a self initialization method. Using a three step self-initialization similar to the one used for the laser ball bar (mentioned in chapter 2), an artifact which may be measured by the instrument in more than one position can be used to initialize the 1-DMM. In this case the initialization artifact is a 3-ball ball bar (3-BBB), which is constructed by assembling two lengths of circular rod to three equal diameter spheres. Once assembled, the balls are nominally arranged co-linear with each other. By placing these spheres onto the TPKS's of the 1-DMM, three unique points in space can be defined along the sled's center line of travel. By measuring the displacement between two of these points, the length of one section of the 3-BBB can be resolved. This length, which is embodied by a section of the 3-BBB can then, be used to initialize the 1-DMM by placing the sphere's which bound the measured section onto the TPKS's. The following figure illustrates this initialization procedure (Figure 3-4).

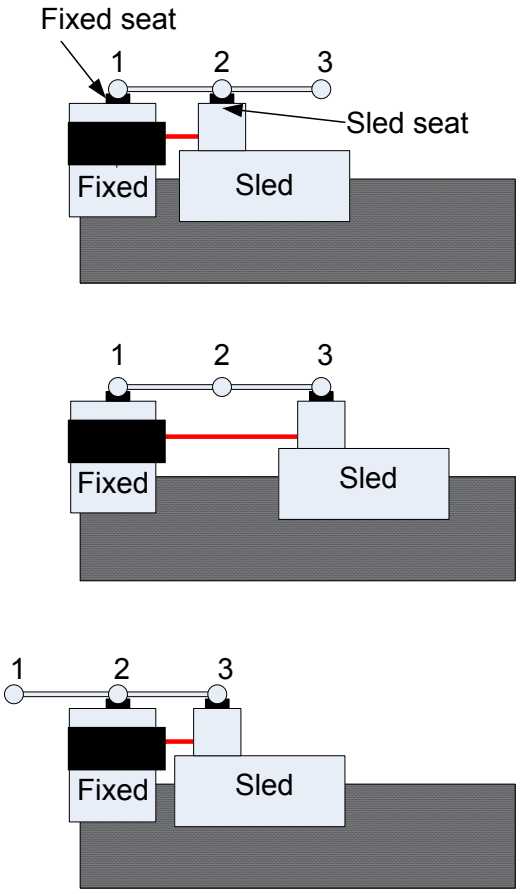

STEP 1

Set calibration artifact with ball 1 in fixed seat and ball 2 onto sled seat. Reset laser interferometers to read "zero"

STEP 2

Unseat ball 2 from sled seat and seat ball 3 onto sled seat. Record the distance displaced during movement; this measured distance between ball 2 &3 will be used to initialize the laser interferometer.

STEP 3

Unseat ball 1 from fixed seat and seat ball 2 onto fixed seat. Enter the value recorded from STEP 3 to initialize 1-DMM's laser interferometer.

Figure 3-4: Self-initialization procedure for the 1-DMM

Initialization of the1-DMM and measurement of a ball bar are independent operations, with each one contributing to the measurement uncertainty of a ball bar. Measurement uncertainty of a ball bar can be generalized from the standard uncertainty of these two inputs. From earlier, the equation for measuring the length of a ball bar is:

$$L_{BB} = L_0 + D \qquad (3.3)$$

Where L_0 is the initialization length and D is the displacement from that length. To calculate the uncertainty of LBB, the law of propagation of uncertainty is applied to equation 3.3, from which the uncertainty in measuring the length of the ball bar becomes:

$$u_{L_{BB}} = \sqrt{u_{L_0}^2 + u_D^2} \qquad (3.4)$$

Each uncertainty component of equation 3.4 is determined by a displacement measurement. Since laser interferometers are used as the displacement sensors for the 1-DMM, the uncertainty of measurement increases as a function of displacement. Therefore, the uncertainty of each term in equation 3.4 increases with displacement (e.g. uncertainty is a function of displacement, L_0 and D). The uncertainty of displacement measured for initialization length and displacement is:

$$\begin{aligned} u_{L_0} &= a + bL_0 \\ u_D &= a + b\left(L - L_0\right) \end{aligned} \qquad (3.5)$$

where: a and b are constants describing the uncertainty of the interferometer sensor

Substituting equation 3.5 into 3.4, the following expression is obtained:

$$u_{L_{BB}} = \sqrt{\left[\left(a + bL_0\right)^2 + \left(a + b\left(L - L_0\right)\right)^2\right]} \qquad (3.6)$$

Evaluating the partial derivative of equation 3.6 with respect to L_0, the following expression is obtained.

$$\frac{\partial u_{L_{bb}}}{\partial L_0} = \frac{b^2\left(L - 2L_0\right)}{\sqrt{2a^2 + 2abL + b^2L^2 - 2b^2LL_0 + 2b^2L_0^2}} \qquad (3.7)$$

By equating this equation to zero, and solving for L_0 we'll find that the uncertainty of a ball bar measurement is minimized when L_0=L/2. Now the question is when to use self-initialization versus, initialization using a pre-calibrated artifact.

Recalling equation 3.4, the combined standard uncertainty of a ball bar measurement is a quadrature summation of the standard uncertainty of the initialization artifact, and displacement measurement. If there is a target uncertainty to be met, equation 3.4 constrains the magnitude of each of these uncertainty contributors. To better visualize this, equation 3.4 is used to generate a chart displaying lines which represent a target uncertainties, the vertical and horizontal axes of

the chart show the allowable uncertainty which displacement, and initialization may contribute to the measurement to achieve the target, respectively.

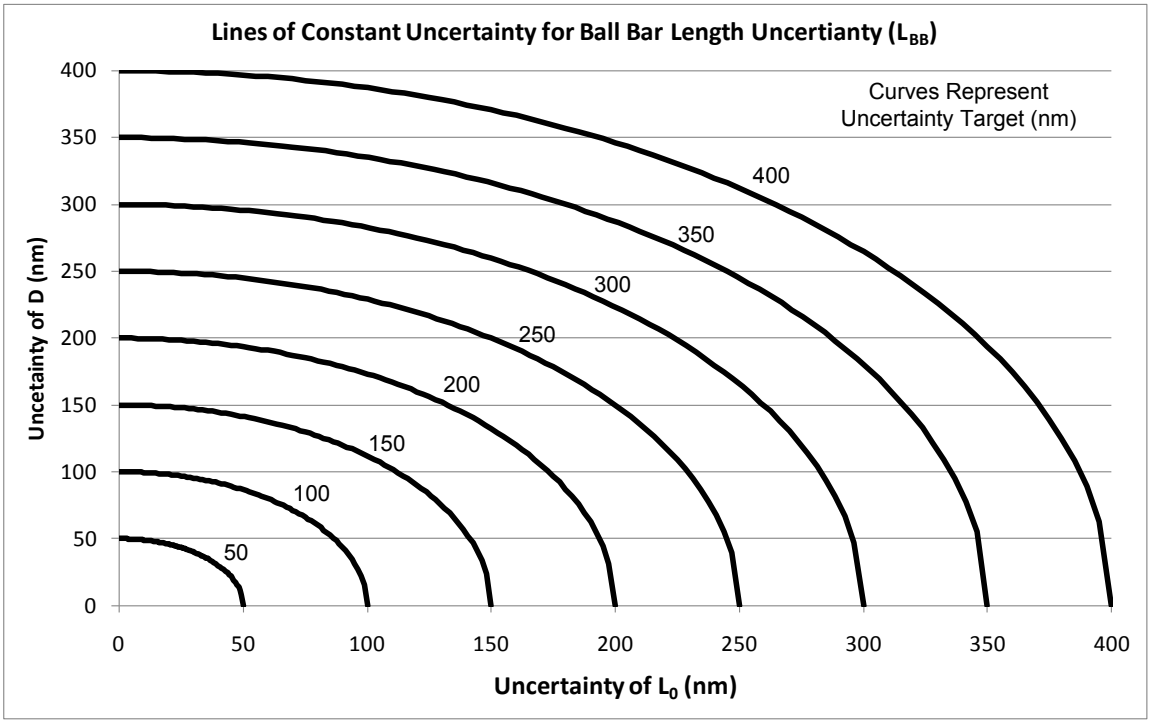

Figure 3-5: Chart displaying lines of constant/target uncertainty

Whether initialization is performed with self-initialization or a pre-calibrated artifact, for a given targeted measurement uncertainty, the amount of uncertainty which initialization contributes will determine the remainder which displacement measurement can contribute to the combined measurement uncertainty; a budget. Measurements of a ball bar are made as a displacement relative to the initialization length. Since the uncertainty of displacement measurement increases with length, an initialization artifact with a large measurement uncertainty may limit the ball bar size (relative to the initialization length L_0) that can be measured, depending on the uncertainty target. A decision to use one method of initialization over another will be determined by factors which include:

- Uncertainty of the initialization length
- The uncertainty of the displacement measurement

- The relative (nominal) displacement from the initialization length to measure a ball bar of unknown length.

To obtain a ball bar measurement with the lowest amount of uncertainty, one might initially believe that an initialization length which contains the lowest uncertainty is needed, but that may not always be the case. For example, a ball bar of 0.5m needs to be measured. The operator of the 1-DMM has the option of using a pre-calibrated artifact to initialize the machine or self-initialization. The pre-calibrated artifact has a length of 0.9m with an expanded uncertainty (k=2) of 0.24μm. To measure the 0.5m ball bar, the machine has to displace and additional 0.4m (backwards) with an expanded measurement uncertainty of 0.28μm, assuming the expanded displacement measurement uncertainty of the 1-DMM is 0.2+0.2D[μm] (where D is in units of meters). The expanded uncertainty of a ball bar measurement is 0.369μm.

Using self-initialization, an initialization length of 0.25m can be realized with an expanded uncertainty of 0.25μm. A displacement of 0.25m relative to the initialization artifact is made, with an expanded uncertainty of 0.25μm, to measure the 0.5m ball bar. The expanded uncertainty of this measurement is 0.353μm.

Although the pre-calibrated artifact has a lower measurement uncertainty than the self-initialized artifact, and lower measurement uncertainty was obtained since the 1-DMM had to displace a shorter distance relative to this artifact to measure the 0.5m ball bar.

Measuring Ball Bars

After initialization of the machine, the length of any other ball bar (up to 3 meters) is determined by supporting it in the two kinematic seats (Figure 3-4), and is the distance between the kinematic seats. From equation 3.4, the length of a ball bar is composed of a displacement measurement relative to an initial length, L_0. Displacement measured by the 1-DMM is composed of inputs from two displacement sensors. From the measurement sensor inputs, the length of the ball bar (L) is calculated from the following equation:

$$L = L_0 + d_1 + \frac{b(d_2 - d_1)}{a}$$

where: L_0 is the initialization length

d_1 is the displacement of laser path 1 (3.8)

d_2 is the displacement of laser path 2

a is the lateral distance between the two laser beams

b is the distance from laser beam 1 to the axis of the ball bar.

Ideally, a single laser interferometer, arranged coaxially with the axis of the ball bar, should be used to measure its length, this is to fulfill the Abbe Principle [34, 35]. Since this new design does not allow for a laser beam to be collinear with the ball bar axis, it does not adhere to the Abbe principle, and therefore the extended Abbe principle is employed to correct for yaw motions of the moving stage by using two parallel displacement sensors [36]. By knowing the values of "a" and "b", (Figure 3-1) and the two readings for the laser interferometers, D_1 and D_2, (Figure 3-2) the length of the ball bar can be precisely estimated using equation 3.2. The yaw of the sled is implicit in equation 3.2 and its value can be calculated.

The initialization length can be introduced using a pre-calibrated artifact or self initialization. If self initialization is chosen, the initialization length is determined from a displacement measurement, Step 2 shown in Figure 3-4. The following equation is used to evaluate the initialization length derived from the self-initialization procedure.

$$L_0 = d_1 + b\frac{(d_2 - d_1)}{a} \qquad (3.9)$$

Uncertainty of Ball Bar Measurements

The uncertainty of measurements provided by this new 1-DMM was analyzed in accordance to the GUM [20]. This uncertainty analysis gathers information on the standard uncertainties of each influencing input quantity which is used to determine the length of a ball bar, modeled using (equation 3.3), and provides an estimate on the resultant measurement's uncertainly. A Type B evaluation of standard uncertainty for each influencing quantity is derived

from information provided by manufacturers, previous experiments, or ones' general knowledge. For this instrument an uncertainty analysis will be performed for the self-initialization sequence of the instrument, and the measurement of ball bars. These two uncertainties add in quadrature to produce the standard uncertainty for a ball bar measurement. To begin the uncertainty analysis, the law of propagation of uncertainties is applied to equation 3.8, this law is expressed by the following equation [19, 20]:

$$u_c = \sqrt{\sum_{i=1}^{N}\left(\frac{\partial f}{\partial x_i}\right)^2 u^2\left(x_i\right) + 2\sum_{i=1}^{N-1}\sum_{j=i+1}^{N}\frac{\partial f}{\partial x_i}\frac{\partial f}{\partial x_j}u\left(x_i, x_j\right)} \quad (3.10)$$

The second term of equation 3.10 is to account for input quantities that may be correlated. For the purposes of this analysis we believe that dual measurement axes may have a correlation between them large enough to influence the measurement uncertainty. Applying this to equation 3.4 we obtain the following expression for uncertainty of a ball bar measurement;

$$u_c = \sqrt{\left(\frac{\partial D}{\partial L_0}\right)^2 u_{L_0}^2 + \left(\frac{\partial D}{\partial d_1}\right)^2 u_{d_1}^2 + \left(\frac{\partial D}{\partial d_2}\right)^2 u_{d_2}^2 + \left(\frac{\partial D}{\partial a}\right)^2 u_a^2 + \left(\frac{\partial D}{\partial b}\right)^2 u_b^2 + \left(2r\frac{\partial D}{\partial d_1}\frac{\partial D}{\partial d_2}\right)u_{d_1}u_{d_2}} \quad (3.11)$$

The terms $\frac{dL}{dL_0}, \frac{dL}{dD_1}, \frac{dL}{dD_2}, \frac{dL}{da}, \text{and } \frac{dL}{db}$ are the sensitivity coefficients, which are the partial derivatives of the mathematical model (equation 3.4), evaluated as follows:

$$\frac{\partial D}{\partial L_0} = 1 \quad (3.12)$$

$$\frac{\partial D}{\partial d_1} = 1 - \frac{b}{a} \quad (3.13)$$

$$\frac{\partial D}{\partial d_2} = \frac{b}{a} \quad (3.14)$$

$$\frac{\partial D}{\partial a} = -b\frac{\left(d_2 - d_1\right)}{a^2} \quad (3.15)$$

$$\frac{\partial D}{\partial b} = \frac{\left(d_2 - d_1\right)}{a} \quad (3.16)$$

An additional sensitivity coefficient, the last term in equation 3.11, is to account for correlations between the two laser interferometers, which is as follows:.

$$2r\frac{\partial D}{\partial d_1}\frac{\partial D}{\partial d_2} = 2rb\frac{\left(1-\frac{b}{a}\right)}{a} \qquad (3.16)$$

where: r is the correlation coefficient

Substituting all these sensitivity coefficients into equation 3.11, the following expression for uncertainty of a ball bar measurement is obtained:

$$u_c = \sqrt{u_{L_0}^2 + \left(1-\frac{b}{a}\right)^2 u_{d_1}^2 + \frac{b^2}{a^2}u_{d_2}^2 + \frac{b^2(d_2-d_1)^2}{a^4}u_a^2 + \frac{(d_2-d_1)^2}{a^2}u_b^2 + \left(2r\frac{b}{a}\left(1-\frac{b}{a}\right)\right)u_{d_1}u_{d_2}} \qquad (3.17)$$

The terms $u_{L_o}, u_{d_1}, u_{d_2}, u_a,$ and u_b are the standard uncertainties for initialization length, the displacement measured by laser interferometer one and two, the lateral separation between the laser beams, and the lateral distance between laser one and the axis of the ball bar respectively. The values for u_a and u_b are evaluated based on the “Uncertainties of the hardware location”. There are other uncertainties which need to be accounted for such as, non-repeatability of the kinematic seats, misalignment between the ball bar and the axis of the laser interferometers, correction of the ball bar temperature, etc, these are added to equation 3.17 in quadrature; i.e. square root of the sum of the squares of each uncertainty contributor.

Determining the uncertainty of an initialization length derived via self-initialization is performed by evaluating equation 3.9 in a similar manner.

The targeted expanded measurement uncertainty for this instrument with (k=2) is one part per million. Possible contributors to this measurement uncertainty include items such as the laser interferometer system, guide way straightness and flatness, ball bar misalignment, etc. Several possible uncertainty contributors have been identified that may have a significant impact on the measurement uncertainty of the 1-DMM. Each of them is detailed in the following sub-

sections, with standard uncertainties estimated for 3,000mm long ball bar under the following assumed conditions.

Table 3-1: Assumed conditions for Type B uncertainty analysis

Property	Value
Room temperature	(20±0.01) °C
Room Relative Humidity	50 %±4 %
Room Air Pressure	(101.3±0.3) kPa.
Ball Bar Temperature	(20±0.01)°C
Component misalignment	± 0.25 mm
Correlation Coefficient	0.4

Environmental Error

Once this instrument is fully constructed it will reside in an environmentally controlled metrology lab at NIST's Advanced Measurement Lab for its entire service life. Although the temperature and relative humidity content of the air is controlled to tight tolerances, there are still fluctuations in these air properties [32]. These changes in the air properties affect its refractive index which in turn affects the wavelength of the laser light as it travels from the emitter, to the retro-reflector and back to the laser detector. Since the laser interferometer system relies on knowledge of the laser's wavelength and the stability of that wavelength to make a measurement, any deviations from its nominal expected value will cause a measurement error [32].

To estimate the changes in refractive index of air, a modified version of Edlen's equation [37] is used, based on measures of temperature, pressure and relative humidity content in the lab's air. The modified version of Edlen's equation is:

$$n_{air} = 1 + \frac{7.86(10)^{-4} p}{273 + t} - 1.5(10)^{-11} RH\left(t^2 + 160\right) \tag{3.18}$$

where: p is air pressure, absolute, kPa

t is temperature, °C

RH is relative humidity, %

Evaluating the uncertainty of each input to Edlen's equation will influence the uncertainty of calculating the index of refraction of air, which in turn affects the uncertainty of displacement measurements. Calculating the wave length of a laser is performed using the following equation:

$$\lambda_{air} = \frac{\lambda_{vac}}{\eta_{air}}$$

where: λ_{air} is the interferometer's wavelength in air (3.19)

λ_{vac} is the interferometer's wavelength in vacuum

η_{air} is the index of refraction of air (calculated using Edlen's Eq.)

The pressure, temperature and relative humidity characteristics in the laboratory were outlined in Table 3-1. Since little information is known about the probability distribution of these values, a rectangular distribution is assumed. A rectangular distribution is assumed because it essentially means that these errors, and others like it, have a zero probability of lying outside the error band. Usage of a rectangular (uniform) distribution to describe an error band is useful when only their extreme values are known, in this case +/- *a* (Figure 3-6).

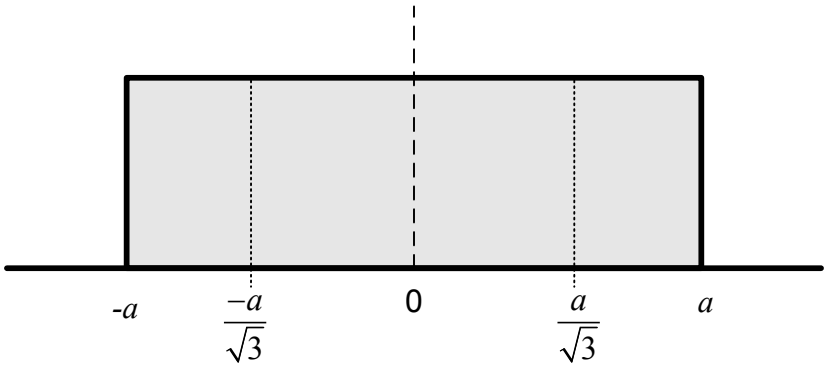

Figure 3-6: Rectangular distribution for expected error

Under this assumed probability distribution, the standard uncertainty due to environmental influences, is calculated by dividing the error by $\sqrt{3}$. For the pressure, temperature, and humidity errors listed in Table 3-1, the standard uncertainties are 0.173kPa, 0.006°C, and 2.7% respectively. Using these values and evaluating equation 3.17 using the law of propagation of

uncertainties, equation 3.10, and assuming that none of the inputs are correlated, the combined standard uncertainty of calculating the index of refraction of air is +/-0.54ppm.

Absolute Wavelength

The absolute wavelength accuracy of the interferometer system per the manufacturer's specifications is +/-0.1ppm. Again assuming a rectangular probability distribution for this error, the standard uncertainty for absolute wavelength error is 0.06ppm.

Wavelength Stability

The wavelength stability as quoted by the manufacturer is +/- 0.05ppm over one hour. Assuming a rectangular probability distribution for this error, the standard uncertainty is: $0.05/\sqrt{3} = 0.03 ppm$.

Interferometer Resolution

The interferometer system has a resolution of 20 nanometers, achieved through interpolation of the quadrature signal. An uncertainty is contributed if the actual displacement is "in between graduations" on the interferometer scale. The estimated standard uncertainty, again assuming a rectangular probability distribution, is 12nm.

Dead-path Error

The dead-path of a laser interferometer system is the portion of the laser beam that is not compensated for any environmental changes. Changes in air temperature, pressure and humidity will alter the refractive index of air. Since the laser interferometer operates in this air environment, it will experience a change in wavelength. The measurement system responds to this change in what would appear to be a displacement measurement, when in fact none of components have actually moved.

A dead-path distance is the length between the laser emitter and the retro-reflector, when the system is initially powered on or reset [32]. Since this distance is unknown, the environmental corrections to wavelength obtained from Edlen's equation are not applied to this distance,

resulting in a “dead path error”. To minimize the dead path error, the axial separation distance between the retro-reflector and the laser emitters are minimized before being turned on; approximately 150mm for this 1-DMM. Under the assumed variations in measurement conditions outlined in Table 3-3, the dead-path error is expected to contribute a 340nm to a measurement’s standard uncertainty.

Laser Alignment

Due to manufacturing tolerances inherent in this machine, there will be a slight misalignment of laser beams relative to the machine’s axis of travel, and the ball bar axis. It is assumed that the main source of this misalignment will be from the flatness and straightness variations inherent in the granite straightedge that serves as the guide way for the sled. From the granite straight edge manufacturer, a flatness and parallelism of 0.0127mm is guaranteed over the entire length (Figure 3-7).

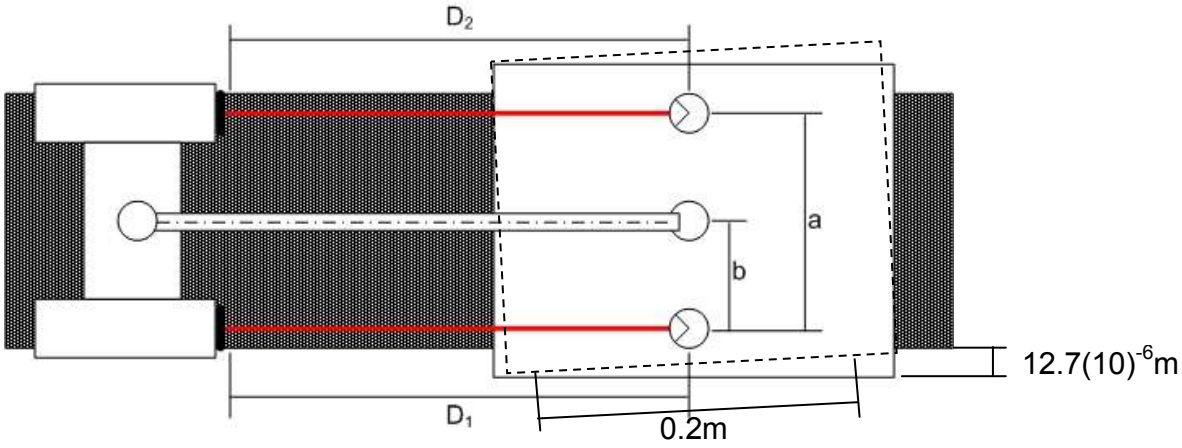

Figure 3-7: Yaw motion of sled as it travels along the guide way.

From these specifications we have estimated the following cosine error and Abbe offsets.

- Cosine Errors

Alignment of the laser will be performed according the manufacturer’s method by monitoring the signal strength. As the sled, which contains the retro reflectors, travels along the granite surface the interferometer system will provide a signal strength feedback that may be

viewed by the user. Once the signal strength stays constant along the entire length of the travel, the lasers are nominally aligned with the motion of travel within at least +/-0.5 mm according to the manufacturer. The approximate cosine error angle is estimated as the following:

$$\varphi = \tan^{-1}\left(\frac{0.5}{3000}\right) = 1.7\left(10^{-4}\right) radians \quad (3.20)$$

For a three meter ball bar, the cosine error is approximately 0.043μm, which is modeled as the half width rectangular probability distribution, and yields a standard uncertainty of 0.025 μm.

- Pitch component of Abbe offset error

The pitch component of the Abbe offset error of the is not corrected. If the centers of the retro-reflectors don't lie on the same plane as the centers of the balls of the ball bar (e.g. they are at different heights), when the sled pitches they will displace by different amounts, causing a measurement error. To minimize this error and to achieve our targeted uncertainty, the centers of the ball bar and the retro-reflectors need to be within +/- 0.5 mm of each other. As specified by the manufacturer, the flatness of the top surface of the granite straight edge is 0.0127mm. From this specification, it is expected that the sled would pitch no more than $62.5(10)^{-6}$ rad. With a height difference of +/-0.5mm, a length measurement error of 31nm is estimated. This gives a standard uncertainty of about 18 nm assuming a uniform distribution.

Glass path thermal error

The laser that passes through the glass optics and prism are uncompensated for temperature gradients, much like the deadpath error. Any thermal expansions of the glass optics changes the optical path length and thus will contribute to the measurement uncertainty. We expect this error to contribute 1 ppm/°C of the measurement based on expected temperature fluctuations and the CTE of the glass. For a glass path of approximately 30mm, we estimate an error of 30 nm. Assuming this error has a rectangular probability distribution, we expect a standard uncertainty of 17.3 nm.

Kinematic Seat Repeatability

Because of continued mounting and dismounting of various ball bars, two three point kinematic seats will be used to interface the 1-DMM with the balls of the ball bars. TPKSs when properly designed will have a very high degree of repeatability. These seats are constructed by bonding three spheres onto a substrate surface, and produced so that they're nominally identical to each other. The non-repeatability of these seats are due to surface finish of the components, form error, and elastic deformation at the points of contact between the intersecting spheres [11, 29, 33]. The seats which we are using are expected to have a positional repeatability of +/-0.1 μm. which will produce a measurement standard uncertainty of 58 nm.

Ball bar misalignment

Aligning the ball bar parallel to the two laser beams is crucial in achieving an accurate measurement. Parallelism of the ball bar to the laser beams will rely on the relative alignment of the ball bar kinematic seat fixed on the granite straight edge, and the one fixed on the sled. We are confident that a misalignment between the two seats is, no greater than +/-0.25mm laterally and vertically can be achieved. For example, measuring a 3 meter ball bar, a +/-0.25mm misalignment will induce a small cosine error which will produce a standard uncertainty of 6nm. Of course this uncertainty will increase as the ball bar being measured becomes shorter.

Correction of Ball bar length to 20°C

Since there is no guarantee that the ball bar's temperature will be at 20°C when it's measured by the 1-DMM, its temperature will be measured and its length will be corrected to what it would be at 20°C. The equation for determining the length of a ball bar l_f at 20°C is:

$$l_{20} = \frac{l_m}{\left(1+\alpha\left(T-20°C\right)\right)}$$

where: l_{20} is the length of the ball bar at 20°C

l_m is the measured length of the ball bar (3.20)

α is the coefficient of thermal exansion for ball bar

T is the measured temperature of the ball bar

Determining the uncertainty of correcting the length of a ball bar to 20°C will require knowing the inputs to equation 3.20 as well as their standard uncertainties. The ball bars which the 1-DMM will measure will vary in length, and material. For the purposes of this analysis, some reasonable assumption for length, coefficient of thermal expansion, ball bar temperature, and their standard uncertainties are outlined if the following table (Table 3-2).

Table 3-2: Properties and standard uncertainties for ball bar

Property	Value	Std. Uncertainty
Length	Varies	1 ppm
CTE	10.6 ppm/C	1 ppm/C
Temperature	20.1	0.1C

From these values, and applying the law of propagation of uncertainty to equation 3.20, the combined standard uncertainty for correcting the length of a ball bar measurement to 20°C is about 1ppm.

Uncertainty of hardware position

The design of the 1-DMM requires that the ball bar axis be located on the same plane as the interferometer's laser beams, and be located half way in between the laser beams, dimensions "*a*", and "*b*" referring to Figure 3-1. In order to achieve our targeted uncertainty budget, the relative location of the kinematics seats, laser detectors, and retro-reflectors will need to be within +/-0.25 mm of the designed dimensions. Assuming a rectangular probability distribution for this error, the standard uncertainty for hardware position is 0.144mm.

Utilizing these estimates for standard uncertainty, an expanded combined uncertainty (k=2) for measuring a 3,000 mm ball bar was estimated (Table 3-3); the self-initialization length used was 250mm.

Table 3-3: Uncertainty of 1-DMM initialization

Uncertainty Analysis	**Value**
Measuring a 3 meter ball bar	Std.Uncr.
Uncertainty in Initializing to L_0(250mm)	**0.1890**
Uncertainty of measuring distance "D"	
Absolute wavelength	0.3175
Wavelength Stability	0.2540
Resolution	0.0200
Environmental error	1.5877
Deadpath error	0.0866
Laser alignment (cosine)	0.0229
Laser alignment (Abbe)	0.0180
Glass path thermal	0.0173
Combined Uncertainty of D	**1.6417**
Other Error Sources	
Ball bar misalignment - u(BBM)	0.0060
Kinematic seat repeatability - u(KSR)	0.0577
Thermal errors - ball bar - u(BBT)	0.9180
Combined Std. Uncertainty (k=1) u (L)	***1.7055***
Expanded Uncertainty (k=2)	**3.4110**
Target Expanded Uncertainty (k=2)	***0.8000***

All units in micrometers

The targeted expanded measurement uncertainty (*k*=*2*) for short ball bar measurements (<1m) is:

$$U_L = (0.2 + 0.2L)[\mu m] \qquad L \text{ is ball bar length, given in meters} \tag{3.21}$$

From this preliminary uncertainty analysis, this instrument didn't meet the target measurement uncertainty. The largest measurement uncertainty contributors are due to environmental influences. However, it is anticipated that the actual operating environment for the new 1-DMM may be better than what was assumed for this analysis. Therefore it was decided to proceed with construction.

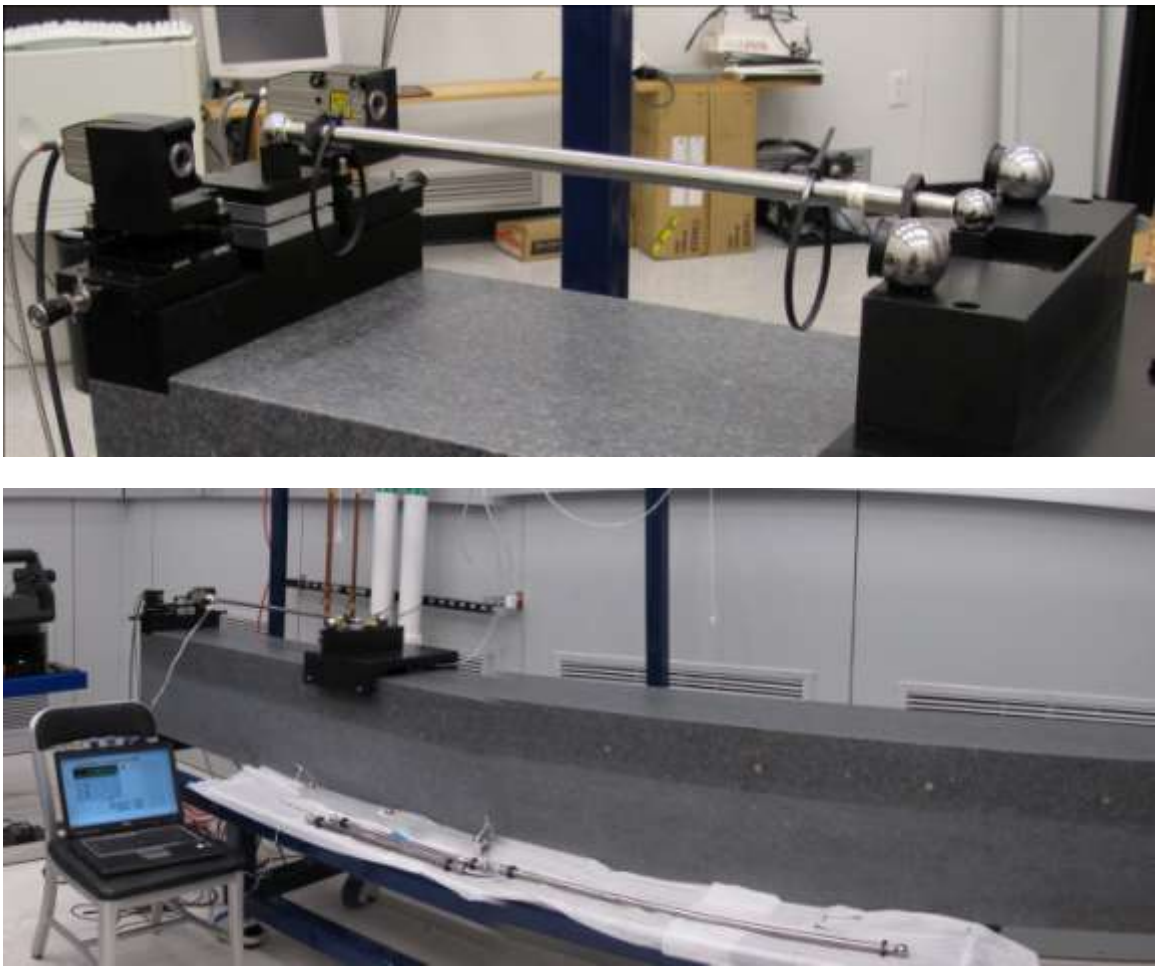

Figure 3-8: New 1-DMM fully constructed

Ball bar Measurement Results

Once construction of the 1-DMM was completed ball bars of different lengths were measured in the NIST laboratory using two methods. One method uses a *master ball bar*, whose length is pre-calibrated on an independent measuring machine, to initialize the separation between the two kinematic seats; we'll call this "mastered gauging". In this method the 1-DMM serves as a comparator type instrument, where each subsequent ball bar measured is compared to the length of the initial ball bar. The second method uses self-initialization, described in Figure 3-4. We'll refer to this as "*masterless gauging*", since a pre-calibrated master artifact isn't used to set the initial distance between the kinematic seats. A series of experiments was performed to

evaluate the accuracy and repeatability of ball bar measurements using each method. Two precision ball bars were calibrated by NIST's Moore M-48 CMM, the machine traditionally used to calibrate ball bars [38], will be used as reference length artifacts. These ball bars were measured by the NIST M48, which is capable of performing 1-D measurements with an expanded uncertainty (k=2) expressed by the following equation [39]:

$$U_L = (0.11 + 0.2L)[\mu m] \qquad L \text{ is length given in meters} \tag{3.22}$$

Using this equation, the length of short and long ball bar, one which measures 499.723358mm and the other 898.766634mm, will have an expanded uncertainty 0.3μm and 0.38μm respectively when measured by the NIST M48 CMM. Environmental compensations are applied to the laser interferometer system, as well as correction for thermal deformations of the ball bar.

As a reminder, the Type B uncertainty analysis performed earlier was under the assumption that the 1-DMM was self-initialized. Under the same assumptions as before, but using the 499mm and 898mm ball bar as the initialization artifact along with their uncertainties, a new Type B uncertainty analysis was performed. With The expected expanded uncertainties (k=2) for measurements of the 499mm and 898mm ball bars by the 1-DMM under this mode of operations, is 0.638μm and 0.984μm respectively. The following table displays the expected expanded measurement uncertainties (Type-B) for the two initialization modes when measuring the short and long ball bar Table 3-4.

Table 3-4: Expected ball bar measurement uncertainties (k=2)

Initialization Mode	Initialization Length (mm)	Ball Bar Length Measured (mm)	Type-B Expanded Uncertainty (k=2) (μm)
Mastered	898	499	0.638
Mastered	499	898	0.985
Self-initialization	250	499	0.659
Self-initialization	250	898	1.023

Mastered Gauging

Using mastered gauging, one of the pre-calibrated ball bars was used to initialize the machine, following which the other was measured as an unknown. These ball bars are constructed out of super invar, with a 1" Grade 2.5 ball attached to each end. To measure the short ball bar with the 1-DMM, the long ball bar would be used to initialize the machine, and vice versa. This measurement procedure was performed ten times for each ball bar to obtain an estimate of the 1-DMM's repeatability. The reported length is the mean of these measurements. The results of the measurements are outlined in the following table (Table 3-5).

Table 3-5: Measurements obtained using mastered gauging method.

Mastered Gauging			
1-DMM	2*Std. Dev	M48 Length	Diff.
499.723358	0.000123	499.723344	0.000014
898.766634	0.000148	898.766586	0.000048

All units in mm

Masterless Gauging

In the second set of experiments the masterless method (self-initialization) was used to initialize the 1-DMM. To perform this test, the instrument is initialized using the initialization procedure outlined in Figure 3-4, followed by a measurement of the 499mm and 898mm ball bar. The instrument is then reset, self-initialized again, and another measurement is taken on the ball bars. This was performed ten times to estimate the measurement repeatability and bias of the machine, when compared to the values assigned by the NIST M48. Three different 3-ball ball bars are used as initialization artifacts to self-initialize the 1-DMM; short, medium and long. These are constructed by bonding two sections of circular rod, and 3 precision balls together. Each of these artifacts are constructed using super invar with grade 2.5 balls bonded to the ends, and the center. The following figure and table describes these 3-ball ball bars (3-BBB) (Figure 3-9 & Table 3-6). (The 3-BBB shown here are symmetric about the middle ball, but they don't necessarily have to be)

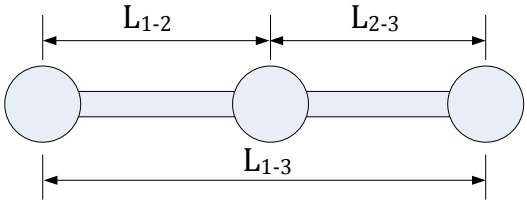

Figure 3-9. 3-ball ball bar used for initializing 1-DMM

Table 3-6.Nominal dimensions of 3-BBBs used for initializing 1-DMM

Nominal Dimensions of 3-BBBs			
Size	L_{1-2}	L_{2-3}	L_{1-3}
Short	100	100	200
Medium	250	250	500
Long	500	500	1000

All values in mm

Ball bar measurement results acquired using the masterless method is outlined in the following table, and figure (Table 3-7).

Table 3-7. Measurements obtained using masterless gauging.

Masterless Gauging Using Short 3-BBB			
1-DMM	2*Std. Dev	M48 Length	Diff.
499.723711	0.000255	499.723344	0.000367
898.766809	0.000862	898.766586	0.000223

Masterless Gauging Using Medium 3-BBB			
1-DMM	2*Std. Dev	M48 Length	Diff.
499.723673	0.000133	499.723344	0.000329
898.766745	0.000166	898.766586	0.000159

Masterless Gauging Using Long 3-BBB			
1-DMM	2*Std. Dev	M48 Length	Diff.
499.722227	0.000172	499.723344	-0.001117
898.765458	0.000185	898.766586	-0.001128

All units in mm

Recall that the initialization length for each sample grouping was derived for one of the 3-BBB. In ten self-initialization trials, the average length for each ball bar and the standard deviation for those lengths are shown in the following table (Table 3-8).

Table 3-8: Initialization lengths derived for each 3-ball ball bar using self-initialization

3-BBB Length	Length (mm)	Std. Dev. (mm)
Short	101.5711	0.000024
Medium	251.4299	0.000034
Long	501.4082	0.000050

Discussion of Results

Utilizing equation 3.21, the target expanded uncertainties for measurements of the 400mm and 900mm ball bar are 0.30μm and 0.38 μm respectively. The mastered method, where a ball bar of known length was used to initialize the machine, provided results which showed a standard deviation of 61.5nm and 74nm for the short and long ball bar respectively. Measurement biases for an average of 10 measurements are 14nm and 48nm for the short and long ball bar respectively, when compared to the measurement value assigned by NIST's M48.

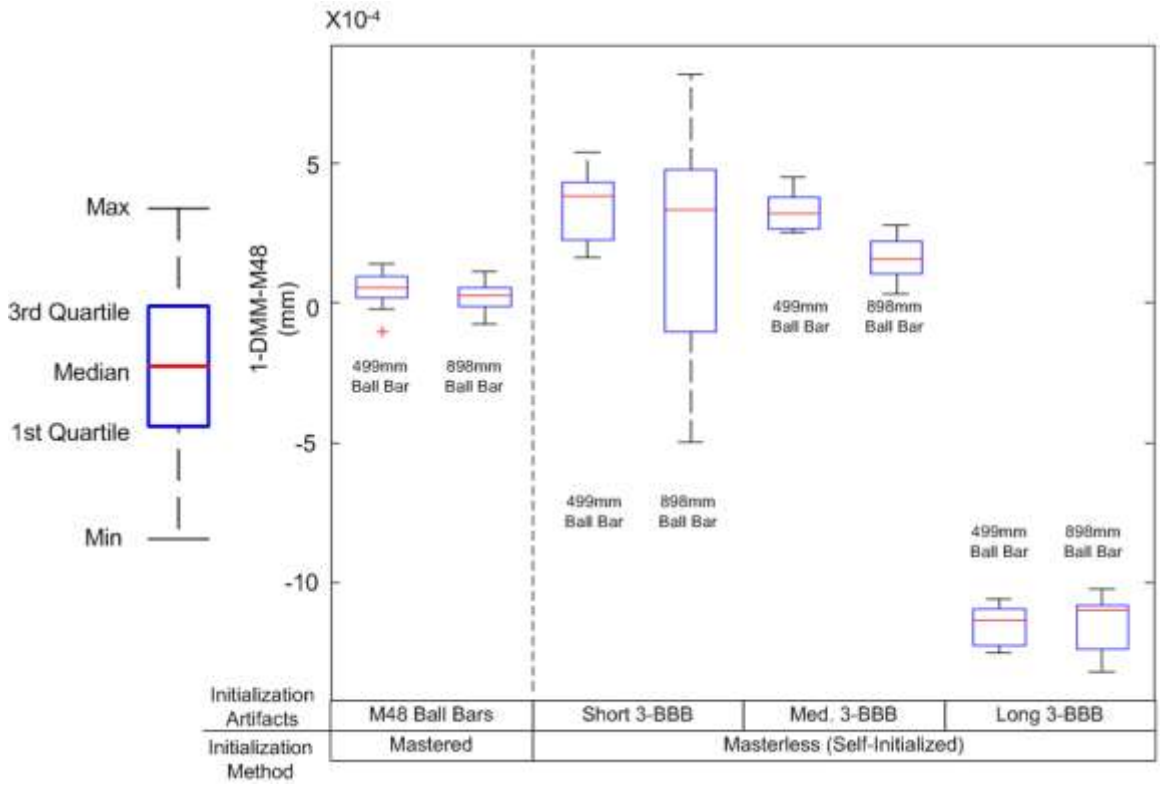

Figure 3-10: Measurement results, mastered, and self-initialized (masterless)

However, utilizing the self-initialization method to initialize the 1-DMM yielded mixed results in measurement repeatability and bias. To investigate the effects of initialization artifacts of varying lengths, 3-ball ball bars of varying sizes were tested. Of the 3-ball ball bars, the medium length ball bar, with a nominal initialization length of 250mm, provided the best results out of all when using self-initialization. The measurement biases that are present in the measurement results are likely due to non-colinearity between the balls on the 3-ball ball bars. Their non-co-linearity can be due to imperfection in manufacturing, and/or gravitationally induced sagging. These effects are believed to be present in all three sets of measurements performed with the 3 different lengths of 3-ball ball bars, but have different influencing effects to the results due to their different lengths. In the first two sets of data obtained with the short and medium 3-BBB, the self-initialization artifact cause a ball bar measurement to have a bias that is positive, relative to results obtained by the M48. If dimensional non-co-linearity is the only influencing

factor, then these ball bar measurements should have a negative bias, not positive. Since these ball bars are supported bellow the neutral axis by the kinematic seats, it could be possible that there is a small amount of sagging in the short and medium ball bar to cause the seats to spread apart, as shown in Figure 3-11.

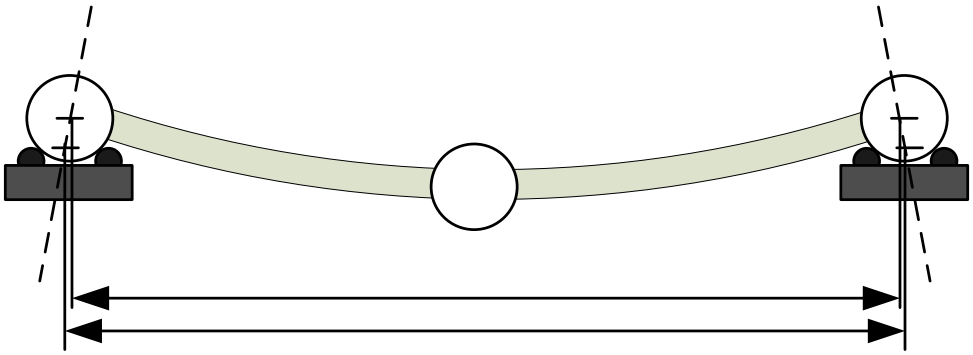

Figure 3-11: Sagging of 3-BBB when supported below neutral axis

Even though the centers of the balls move closer together, the amount that the seats spread apart can overcome this effect; hence there is a positive measurement bias.

However with the long 3-BBB, its sag during initialization has a greater influence in shifting the measurement bias to be negative relative the M48 measurement results. The relatively large measurement difference observed when the long 3-ball ball bar is used is likely due to its higher flexibility. Gravitationally induced sagging of the ball bar may have caused an error in the measurement of the initialization length. It is believed that if a 3-BBB with a initialization length somewhere in between the length of the medium and long 3-BBB will provided measurement results with minimal shift in measurement bias.

Contrasting the two different methods, “mastered” and “masterless” (*self-initialized*) the results show that the “mastered” method provided the lowest measurement bias. The standard deviations in ten measurement trials between the two methods are fairly close to each other (Figure 3-10).

Concluding Remarks

The ball bars which this instrument is designed to calibrate will be used to evaluate the measuring performance of a CMM in accordance to standardized tests [40, 41]. Their length needs to be traceable to the fundamental unit of measure within a given uncertainty to provide an accurate assessment of a CMM's performance. For this 1-DMM, metrological traceability is maintained through the accuracy of the instrument's interferometer system, its ability to transfer a displacement measurement to distance measurement using the self-initialization artifact, and its ability to reassign that distance measurement as the correct initialization distance. If the uncertainty of each stage of the self-initialization procedure can be quantified, metrological traceability is maintained.

One of the main advantages of this new 1-DMM is the ability to self-initialize with an uncalibrated artifact. Pre-calibrated artifacts need to be calibrated on a separate machine, which is time consuming and costly. By shifting to a self-initialization method to initialize the 1-DMM, these costs can be negated. The 3-ball ball bars constructed for the experiments in comparison, can be produced relatively inexpensively. To accommodate the various lengths of ball bars, a new 3-ball ball bar can be produce quickly and easily.

Initial measurements of ball bars less than one meter long demonstrate that the 1-DMM can achieve measurement uncertainty to meet the target value when using the mastered method. The masterless method was highly repeatable, but measured with noticeable biases when compared to the mastered method. One possible reason for this bias could be due to the flexibility of the 3-ball ball bars. When the 3-ball ball bars are on the kinematic seats, they are supported below their neutral axis. Under this condition, because of their flexibility, any bending of these initialization artifacts under gravity will cause the 1-DMM to measure them longer than the true values of their center to center distances. Nonetheless an attempt should be made to address the systematic bias that is present for self-initialized measurements. At the moment using the mastered method provides ball bar measurement results which closely agree with those

produced by NIST's M48. For applications where a ball bar with a higher measurement uncertainty is sufficient, a measurement produced with a self-initialization method may be used. Future experiments will involve investigating optimal geometry and construction techniques for a 3-ball ball bar (self-initialization artifact), and evaluating the measurement performance of this machine when ball bars up to 3 meters in length are measured.

CHAPTER FOUR

UNCERTAINTY OF ABBE OFFSET ERROR CORRECTIONS IN ONE DIMENSION

Application of the Extended Abbe Principle is not without uncertainty in its own respect, since it involves a measurement. This chapter explains how Abbe offset uncertainties are calculated, minimized, and uses the 1-DMM as a case study.

Introduction

Ernst Abbe states in his Abbe Principle that "*If errors in parallax are to be avoided, the measuring system must be placed coaxially with the axis along which the displacement is to be measured on the workpiece*." This principle, known as the Abbe Principle, is an important aspect in machine design that should be followed if one is to avoid amplification of errors due to offsets of the measurement scale axis from the measurement point of interest (POI) [34, 36]. A common example which displays the Abbe principle in action can be found by comparing the construction of a handheld micrometer to a dial caliper (Figure 4-1) [35, 42].

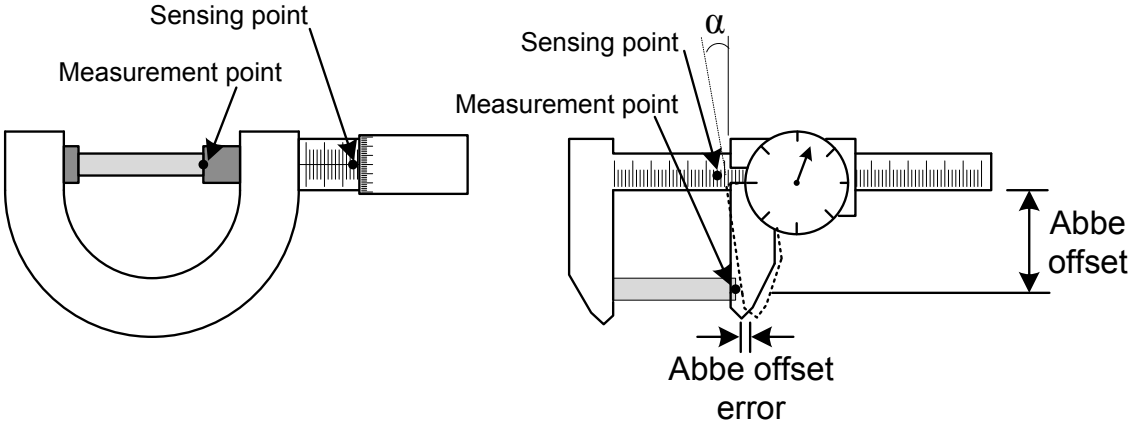

Figure 4-1: Abbe offset error with hand held measurement instruments (micrometer vs. dial caliper)

With the micrometer, the instrument is constructed such that the measurement scale's axis is directly in-line with the workpiece being measured. Because of this, the line formed by the measurement point and the sensing point is co-linear with the measurement axis; hence the Abbe

principle is preserved. In the case of the dial caliper, the line formed by the measurement point and the sensing point is not co- linear with the measurement scale's axis, therefore in this case the Abbe principle has been violated. By design, the dial caliper's slider has a small amount of running clearance between it and the slide bar. This small running clearance is what allows the slider to move freely along the slide bar, but it also allows it to pivot about the slide bar. By not adhering to the Abbe principle, the combination of the angular deflection of the sliding jaw and the Abbe offset from the measurement scale results in an erroneous measurement of the workpiece's length. By designing an instrument in this manner, the offset of the sensing point from the instrument's measurement axis forms a lever arm, the length of which is commonly known as the *Abbe offset* [35, 42].

Due to space limitations and the kinematic layout for a given machine it may not always be possible or feasible to design and construct machines which adhere to the Abbe principle, nor is it always necessary. Accuracy requirements of the machines may not require Abbe offset induced errors to be compensated. Careful construction of machines using precisely fitted components can help ameliorate significant Abbe offset errors. Error mapping of machines and using the machine's control algorithm to compensate for these errors is also a solution, so long as they are repeatable [43]. In situations where design requirements require precise knowledge of a machine's position, reliance on an error mapped machine may not be adequate. In this case in-situ estimation and compensation of Abbe offset errors may be required [36]. This was the case during the design of an instrument which will be used to measure ball bars; more detailed information about the design of this instrument is provided in the previous chapter.

In Situ Abbe Offset Error Estimation

Consider a machine with one axis of motion and a carriage guided by a guide way. Due to imperfections in the manufacture of the guide way, the carriage may pitch, roll, and yaw about the axis of travel, as it traverses along the guide ways. If it is only the gross linear displacement of

the carriage that is of interest, then these small angular displacements are of no concern (Figure 4-2).

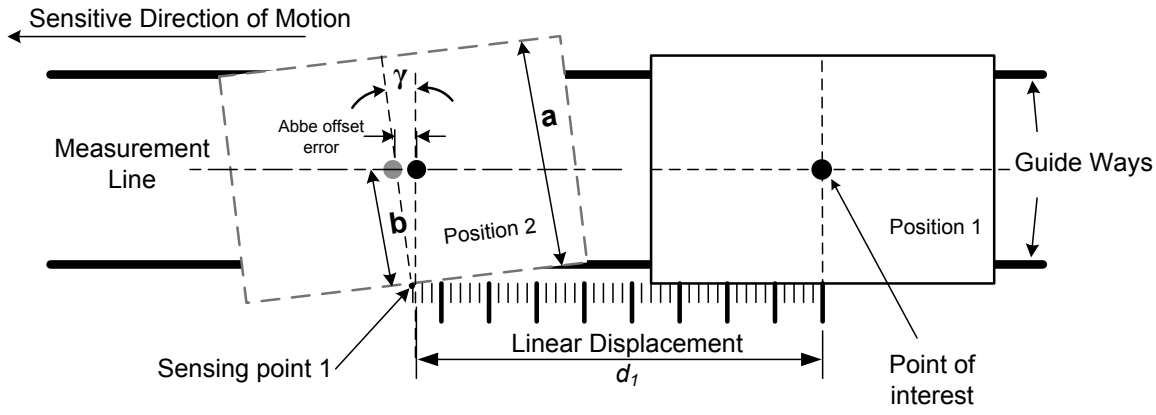

Figure 4-2: An example of how angular displacements induce error motions during translational displacement of guide way

However, in precision applications, the surface of the carriage will contain points of interest (POI) which need to be tracked with great precision. Focusing on just one POI, located at the center of the carriage, angular displacements inherent in the motion of the carriages will introduce unwanted error motions in the sensitive direction of motion as it traverses along the guide ways. For small changes in angular displacements, the amount of error in the motion is approximately proportional to the angular displacement multiplied by the amount of lateral offset from the measurement scale. On a typical machine, where only one linear displacement measurement system is utilized to measure the motions of each axis; angular displacements are usually not measured. To account for these error motions, in lieu of error mapping, Abbe offset error compensation or correction can be accomplished in situ by following the Extended Abbe Principle[34, 35].

The Extended Abbe principle utilizes multiple, parallel displacement measurements a known distance apart, at known distances from the target POI to correct for the effects of the angular motion. With the additional information provided by the extra sensor, the displacement of any point on the carriage, including the POI can be tracked with much greater accuracy. The

extended Abbe Principle is useful in situations where the measurement axis/scales can't be coaxially aligned with the measurement. One method of applying this principle to account for machine motion error is to use two (or more) displacement measurement sensors for each axis of motion. Knowing the distance between the two measurement axes, and the relative linear displacement that they measure, the angular displacement of the machine's table or carriage may be measured. Using this information and the lateral distance from either of the scales to the POI, the error motions induced on the POI can be more accurately estimated. Additionally actuators may be used to correct any angular errors of the machine's carriage, or for a multi axis machine, existing actuators may be used to actively compensate for error motions, given the continuous knowledge of machine position provided by the multiple measurement sensors [34, 36].

Expanding on the previous example displayed in Figure 4-2, to measure the displacement of a single POI located on the carriage, and to account for the Abbe offset error, which is in the sensitive direction of motion, two measurement axes are utilized to measure the amount of angular displacement of the carriage as it traverses along the guide ways (Figure 4-3).

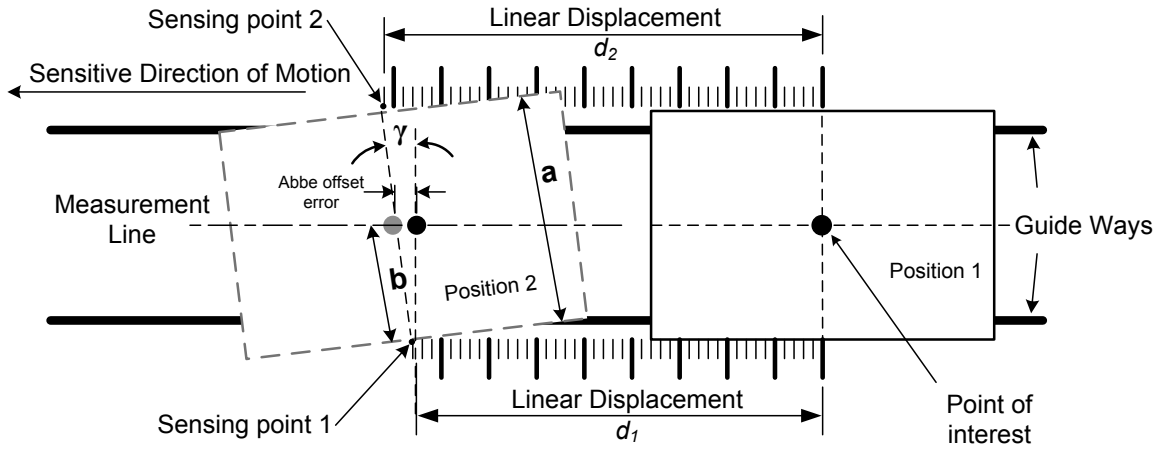

Figure 4-3: Angular displacement of carriage induces error motions to the functional point of interest

Knowing the position of the POI, in relation to the two measurement scales, allows for estimation of the Abbe offset error in the sensitive direction of motion, and allows for a more accurate

estimation of the actual displacement of the POI in the direction of motion. To do so, the amount of angular displacement γ is estimated using the following equation (Eq. 4.1)

$$\gamma = \sin^{-1}\left(\frac{d_2 - d_1}{a}\right) \approx \left(\frac{d_2 - d_1}{a}\right)$$

where: d_1 is the displacement measured by sensor 1 (4.1)
d_2 is the displacement measured by sensor 2
a is the separation between sensor 1 and 2

Next the amount of Abbe offset error is estimated by the following equation (Eq. 4.2).

$$\Delta d \approx b\gamma \approx b\frac{\left(d_2 - d_1\right)}{a}$$

where: b is the perpendicular distance from the (4.2)
POI to displacement measurement axis 1

Now the total displacement of the POI in the sensitive direction of motion may be estimated by adding the error motion calculated using equations 4.1 and 4.2, to the displacement d_1.

$$D = d_1 + \Delta d \qquad (4.3)$$

This application of the Extended Abbe Principle is well known and widely practiced in the design of precision machines. However, the correction, Δd, is only an estimate. At the highest levels it is necessary to know the uncertainty of that estimate. Referring to the preceding figure the uncertainty of measuring the displacement of the carriage, while using the extended Abbe principle, will depend on many influences, such as:

- Uncertainty of the distance between the two measurement axes
- Uncertainty of the location of the POI relative to the measurement axes
- Arrangement of the measurement axes relative to the POI
- Uncertainty of the displacement measurement system

Uncertainty of Abbe Offset Error Estimations in 1-Dimension

Determination of measurement uncertainties is well covered in the literature [19, 20]. Considering planar motion in one dimension, as displayed in Figure 4-3, the mathematical model for Abbe error correction using the extended Abbe offset principle is given by equations 4.1 to 4.3. Pitch and roll motions of the axis are not considered; although they may also induce an Abbe offset error in an orthogonal direction, depending on the location of the displacement sensors for those directions. The measurement equation for estimating the displacement of the POI is given by:

$$D = d_1 + b\frac{\left(d_2 - d_1\right)}{a} \qquad (4.4)$$

Determination of displacement measurement uncertainty may be obtained by applying the law of propagation of uncertainties; this is expressed by the following equation:

$$u_c = \sqrt{\sum_{i=1}^{N}\left(\frac{\partial f}{\partial x_i}\right)^2 u^2\left(x_i\right) + 2\sum_{i=1}^{N-1}\sum_{j=i+1}^{N}\frac{\partial f}{\partial x_i}\frac{\partial f}{\partial x_j}u\left(x_i, x_j\right)} \qquad (4.5)$$

Evaluating equation 4.4 with equation 4.5 the following expression is obtained for the uncertainty of displacement measurements.

$$u_c = \sqrt{\left(\frac{\partial D}{\partial d_1}\right)^2 u_{d_1}^2 + \left(\frac{\partial D}{\partial d_2}\right)^2 u_{d_2}^2 + \left(\frac{\partial D}{\partial a}\right)^2 u_a^2 + \left(\frac{\partial D}{\partial b}\right)^2 u_b^2 + \left(2r\frac{\partial D}{\partial d_1}\frac{\partial D}{\partial d_2}\right)u_{d_1}u_{d_2}} \qquad (4.6)$$

Sensitivity coefficients are calculated as follows:

$$\frac{\partial D}{\partial d_1} = 1 - \frac{b}{a} \qquad (4.7)$$

$$\frac{\partial D}{\partial d_2} = \frac{b}{a} \qquad (4.8)$$

$$\frac{\partial D}{\partial a} = -b\frac{\left(d_2 - d_1\right)}{a^2} \qquad (4.9)$$

$$\frac{\partial D}{\partial b} = \frac{\left(d_2 - d_1\right)}{a} \qquad (4.10)$$

The last term in equation 4.6 accounts for uncertainties between correlated input quantities. For this analysis, only correlations between the two displacement measurements sensor are taken into account. If laser interferometers are considered for use as displacement sensors, the environment in which these sensors operate will influence their measurement uncertainty. Uncertainties which arise due to the level of correlation between these two measurement axes are expected to have a greater impact on the magnitude of displacement measurement uncertainty than the other input quantities. The additional sensitivity coefficient for correlations between these two uncertainty contributors is:

$$2r\frac{\partial D}{\partial d_1}\frac{\partial D}{\partial d_2} = 2rb\frac{\left(1-\frac{b}{a}\right)}{a} \qquad (4.11)$$

where: r is the correlation coefficient

The combined standard measurement uncertainty for determining the displacement of the POI in Figure 4-3 is as follows:

$$u_c = \sqrt{\left(1-\frac{b}{a}\right)^2 u_{d_1}^2 + \frac{b^2}{a^2}u_{d_2}^2 + \frac{b^2(d_2-d_1)^2}{a^4}u_a^2 + \frac{\left(d_2-d_1\right)^2}{a^2}u_b^2 + \left(2r\frac{b}{a}\left(1-\frac{b}{a}\right)\right)u_{d_1}u_{d_2}} \qquad (4.12)$$

Equation 4.12 may be simplified by applying the following simplifications:

- Express ratio $\frac{b}{a}$ as α;
- Since $\left(d_1 \approx d_2\right)$, and the laser interferometers used are identical and operate in a common environment we expect $u_{d_1}^2 = u_{d_2}^2 = u_d^2$;
- Also, since $\left(d_1 \approx d_2\right)$, $(d_2 - d_1)^2$ will be at least an order of magnitude smaller than $(d_2 - d_1)$ so $(d_2 - d_1)^2$ will be ignored.

The resultant combined standard uncertainty after these simplifications is:

$$\frac{u_c}{u_d} = \sqrt{(1-\alpha)^2 + \alpha^2 + \left[2r\alpha(1-\alpha)\right]} \qquad (4.13)$$

What remains is a function that is dependent on "α" and "*r*". For various correlation coefficients the normalized uncertainty for estimating the displacement of the POI is plotted in the following figure (Figure 4-4).

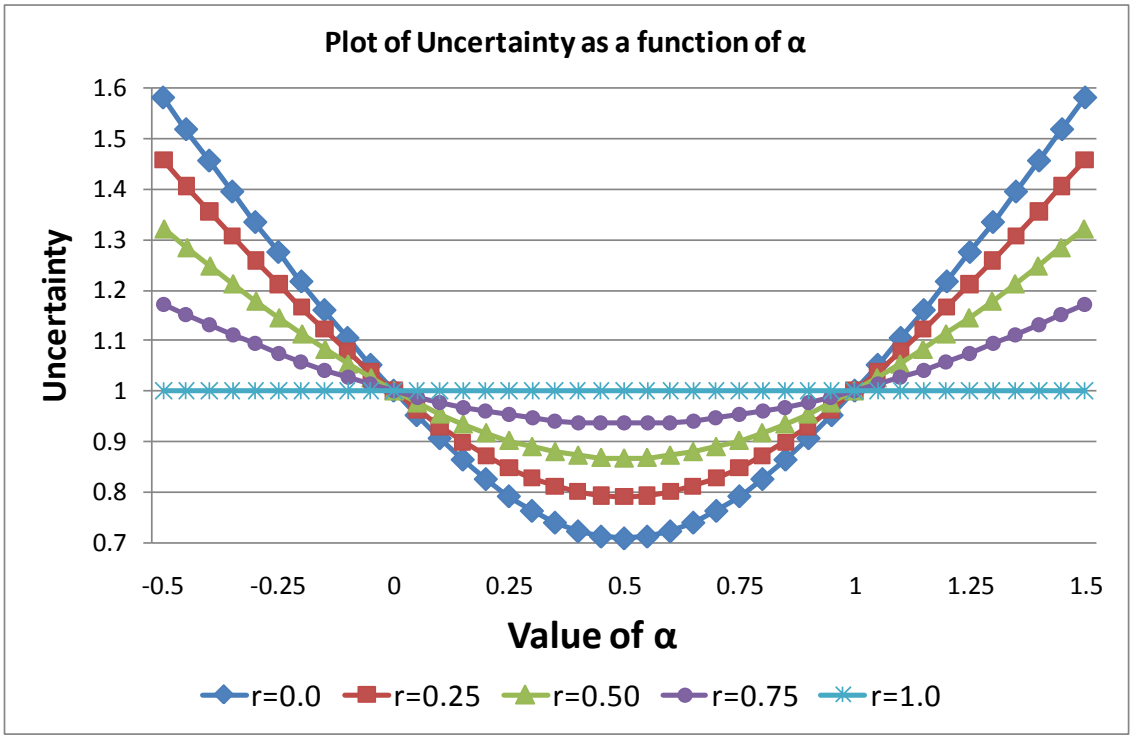

Figure 4-4: Variation of uncertainty due to Abbe offset as a function of α and *r*

As Figure 4-4 shows, the measurement uncertainty for displacement of the POI, shown in Figure 4-3, varies depending on its lateral location, "b"; relative to the measurement axis 1. When measurement axis 1 and 2 are uncorrelated (*r=0*), the displacement measurement uncertainty is a minimum when the POI is midway between the two measurement scales (*α=0.5*). As the correlation coefficient between the two measurement axes approaches unity, the uncertainty for estimating the displacement of the POI remains uniform. However, when the POI is outside of the displacement measurement axes, the uncertainty is always greater than the uncertainty of either

measurement axis; i.e. when α is less than 0 or greater than 1. Ideally all machine operations should take place at the center, "a/2" or α = 0.5, as often as possible, but that isn't always practical. Workpieces can easily span the width of the carriage or more. In these cases, the uncertainty of locating a point on the workpiece will vary when the correlation coefficient between measurements d_1 and d_2 is less than 1.

Assigning a Correlation Coefficient

As mentioned earlier, all the input quantities which are used to calculate the displacement of the POI can be correlated. However, in the present case, only correlation between the two displacement sensors, d_1 and d_2, are considered. Correlation coefficients between two measurement sensors for a given displacement measurement system is not a specification typically supplied by a component manufacturer. They can vary depending on the environment in which the machine operates, and therefore need to be determined experimentally.

When considering the two displacement sensors their uncertainty of displacement measurement can be influenced by many factors. For the laser interferometers used here, we will express their total uncertainty as an uncertainty due to wavelength correction plus a noise component, expressed by the following equation.

$$u_{d_i} = \sqrt{u_{\eta_i}^2 + c_i^2}$$

where: u_{η_i} is the uncertainty due to wavelength correction (4.14)

c_i is the noise present in the displacement sensor

For this instrument, there is only one set of temperature, pressure, and humidity sensors, and therefore the same wavelength correction is applied to both displacement sensors even though their beam paths are separated by a small distance and therefore they actually operate in slightly different environments. Therefore, the uncertainty of the correction due to uncertainties in measuring the inputs to Edlen's equation is common to both sensors and in this respect are perfectly correlated; $r=1$.

However, if one of the beam paths experiences a localized change in air properties not measured by the sensors, that laser will experience a change in wavelength that isn't corrected, hence the two laser interferometers will have some variation, or noise, that has a correlation between 0 and 1. Refering back to equation 4.14, if the magnitude of noise is small compared to the uncertainty of wavelength correction, its influence on the uncerainty of of the displacement measurement will also be small [44]. But, if the noise components are of the same magnitude of the wavelength correction uncertainty, and is uncorrelated, they will cause the uncertainties between the two displacement sensors to be uncorrelated.

For the laser interferometers used in this instrument, what is the expected correlation coefficient between the two measurement axes, and what effect does this have on the uncertainty of the estimated position of the POI using the extended Abbe principle? Three experiments were performed to investigate this phenomenon.

Experimental Setup

These experiments were performed on a machine which was designed and constructed to measure ball bars; the 1-DMM discussed in the previous chapter, shown in Figure 4-5 [6].

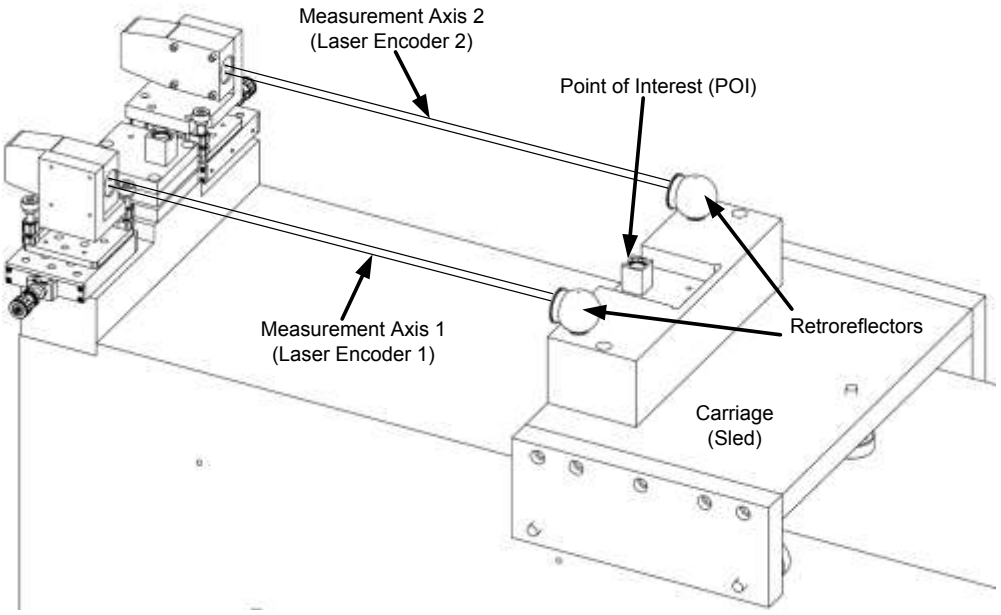

Figure 4-5: Detail of component layout for 1 Dimensional Measuring Machine [6]

These laser interferometers used on the 1-DMM are symmetrically arranged on the machine such that the measurement axes are parallel to the sensitive direction of motion, and co-planar to the axis of a ball bar when it is supported by the kinematic seats. The carriage of this 1-dimensional measuring machine (1-DMM) has a travel length of 3 meters, and the lateral separation between the laser interferometers is 219mm, with the POI nominally located at the midpoint between them.

The experiments performed consist of:

1. measuring the yaw of the carriage as it travels along the guide way,
2. estimating the correlation coefficient between the two measurement axes due to noise, and
3. using a third laser interferometer to measure the displacement of the POI and compare it to the measurement obtained from the other two laser interferometers using the extended Abbe principle.

Yaw measurements were performed quasi-statically, by incrementally moving the carriage along the length of the granite guide way and recording the displacement measured by

each interferometer. Under ideal conditions these two interferometers should measure the same amount of displacement. However since the guide ways that guide the carriage aren't perfectly flat and straight, the carriage will exhibit small error motions, manifested as a yaw displacement of the carriage which causes the two interferometers to measure different displacements. In addition to displacement, the air temperature, humidity, and pressure of the air in which the lasers operate were also recorded. This information was used to estimate the refractive index of the air, and corrections were made to account for changes in the laser wavelength [32]. Figure 4-8 shows the estimated yaw of the carriage as it moves along the guide way.

Estimating the correlation coefficient for the noise component between the two laser interferometers was performed in two separate sub-experiments. Prior to mounting the laser interferometers to the 1-DMM, they were rigidly affixed to a granite surface plate inside a metrology laboratory where the environmental conditions were controlled to 20°C, and 38% relative humidity. In the first of the two sub-experiments, the axial distance between the laser detectors and the retro-reflectors was fixed at 1,100mm while the lateral spacing "*a*" between the lasers was incrementally varied from 38mm to 900mm to test how the correlation coefficient responded to changes in their lateral separation. In addition, a removable shield that could be placed over the beam paths was used to mitigate the air turbulence in the lasers' beam path and to see whether or not it would have an effect on their correlation.

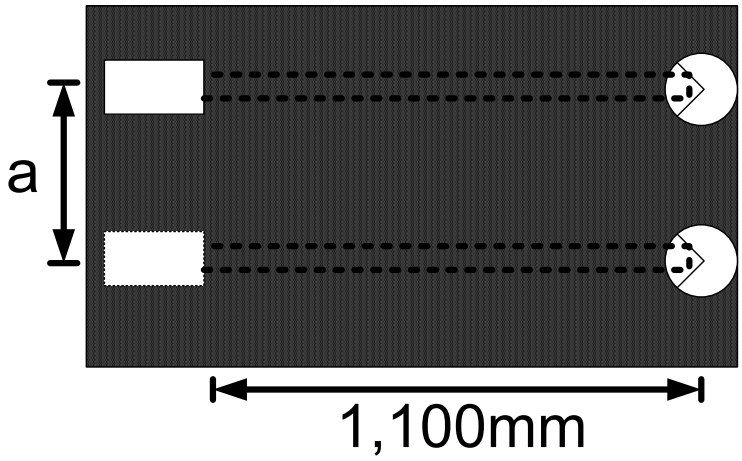

Figure 4-6: Test setup of interferometers on surface plate

In the second sub-experiment, the interferometers were mounted on the 1-DMM, with the laser detectors rigidly fixed to one end of the granite straight edge and the retro-reflectors fixed to the carriage. On the 1-DMM the lateral spacing between the two laser interferometers remained fixed, at approximately 219 mm, while the carriage was quasi statically moved in approximately 100mm increments (Figure 4-5).

In the final experiment, an independent laser interferometer was used to measure the displacement of the POI on the carriage. Normally, the displacement output from the two lasers is used to calculate the position of the POI, using equation 4.4. By placing a third retro-reflector at the POI on the carriage, its displacement can be directly measured by a third interferometer and compared with that estimated by the 1-DMM's measurement scales (Figure 4-7).

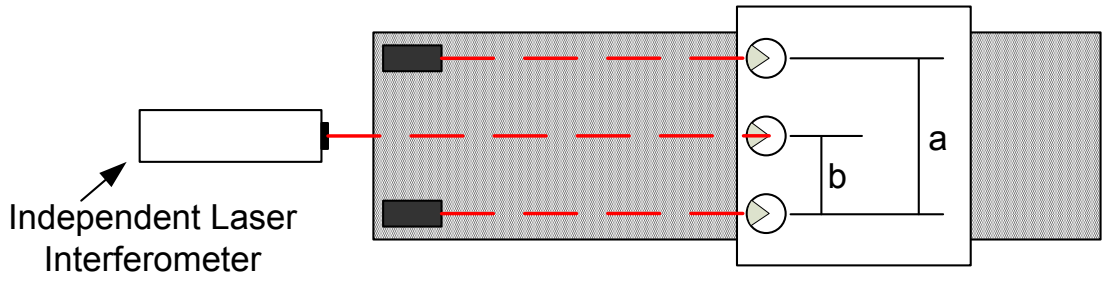

Figure 4-7: 1-DMM's displacement estimate compared using independent laser interferometer

Results

The amount of yaw which the carriage experiences over the entire travel of the 1-DMM was measured to be about 16.8 μrad. This experiment was performed three times, and the carriage's yaw was shown to be repeatable for each position (Figure 4-8)

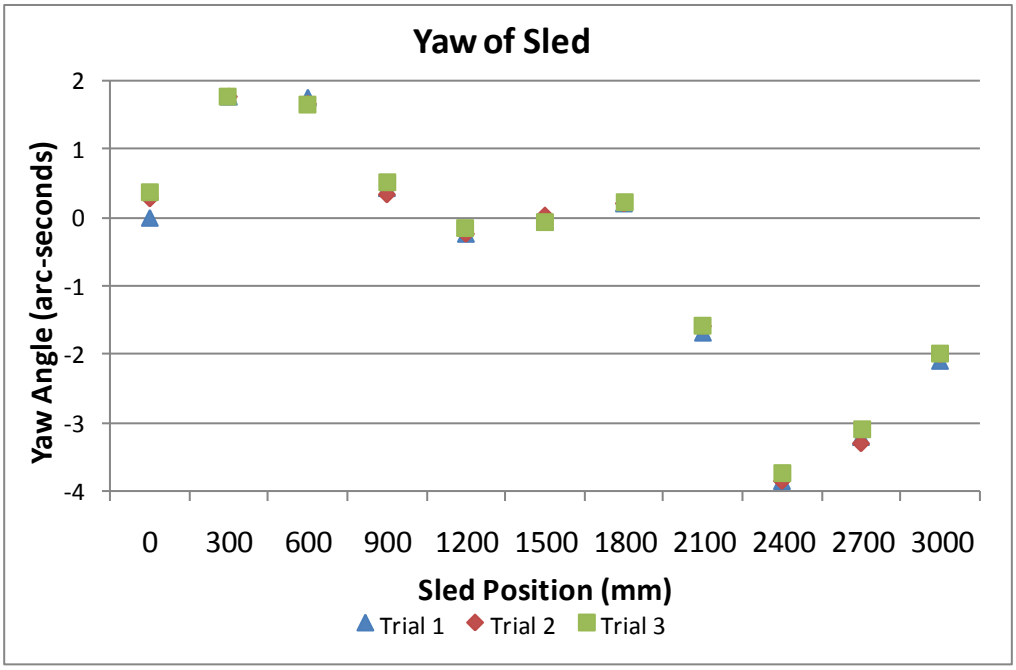

Figure 4-8: Yaw of carriage versus carriage position

Measuring the amount of yaw is important since carriage's yaw affects the sensitivity coefficients outlined in equations 4.7 and 4.8. Depending on the target measurement uncertainty required, the maximum yaw which the carriage experiences needs to be maintained within a certain limit. Prior to the construction of the 1-DMM, tolerances on the surface form characteristics of the granite guide way were taken into consideration in designing the carriage such that the yaw of the carriage was held within acceptable values. The measurements in Figure 4-8 confirm that the form error of the granite guide way meets the tolerance specifications.

In the first set of correlation coefficient measurements, where the only the lateral spacing between the laser interferometers was varied, it was found that the correlation between the two laser units generally decreased as the distance between them increased, but was highly variable. Applying a shroud to shield the laser beam path from air turbulence caused the correlation coefficient to drop further. For each data set, the output from the laser interferometers was recorded at 10 Hz for 20s while they remained in this nominally static position.

Correlation coefficients for noise between the two laser interferometers for each case was calculated using the following equation [45].

$$r = \frac{\sum_i \left(d_{1i} - \overline{d_1}\right)\left(d_{2i} - \overline{d_2}\right)}{\sqrt{\sum_i \left(d_{1i} - \overline{d_1}\right)^2 \sum_i \left(d_{2i} - \overline{d_2}\right)^2}}$$

where: d_{1i} represents each sample from axis 1
d_{2i} represents each sample from axis 2
$\overline{d_1}$ represents average of all samples from axis 1
$\overline{d_2}$ represents average of all samples from axis 2 (4.15)

A sample of the resultant data is displayed in the following figure (Figure 4-9).

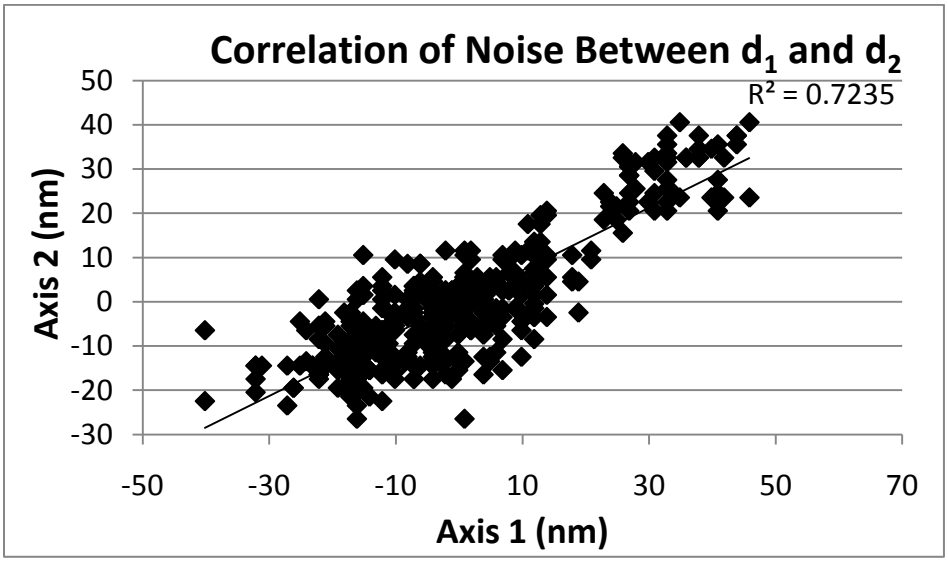

Figure 4-9: Sample correlation data, 38mm spacing unshielded

In this data sample, the correlation coefficient was found to be 0.85. In other cases, when the spacing between the beams was increased, with the beams either shielded or unshielded, the results for correlation coefficient varied greatly, as shown in the following table (Table 4-1)

Table 4-1: Correlation coefficients for noise versus beam spacing, and condition

Lateral Spacing (mm)	Correlation Coefficient	Condition
38	0.908	Shielded
38	0.672	Un-Shielded
200	0.110	Shielded
200	0.651	Un-Shielded
500	0.217	Shielded
500	0.886	Un-Shielded
900	0.507	Shielded
900	0.748	Un-Shielded

In the second set of correlation coefficient measurement experiments for the noise component, where the lateral spacing between the laser interferometers remained constant and the length of the beam path was varied, the results indicated that the correlation coefficient varied between 0.01 to 0.96 (Figure 4-10).

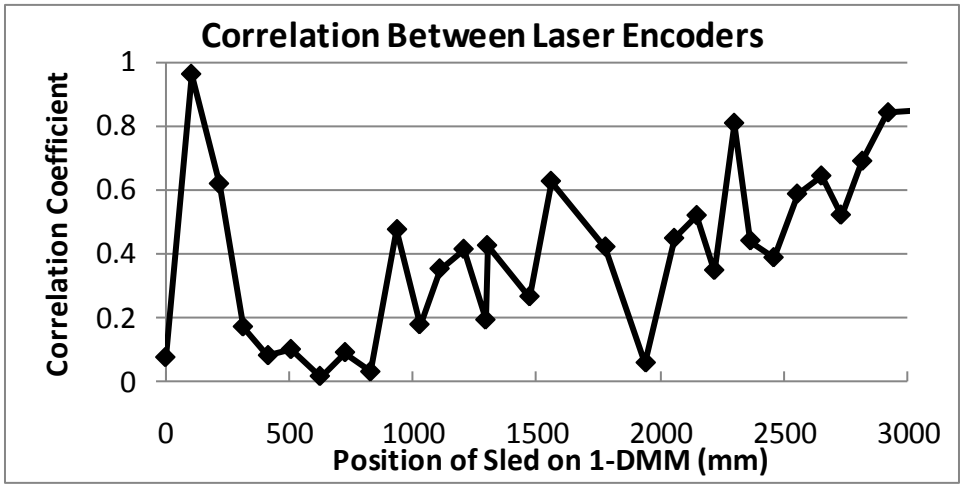

Figure 4-10: Correlation between interferometer Axis 1 & 2 vs. position of 1-DMM's carriage

In the final experiment an independent laser interferometer was used to measure the displacement of the POI on the 1-DMM's carriage, which was then compared to the measurement provided by the pair of laser interferometers mounted on the machine using the extended Abbe

principle. The difference between these two measurements is shown in the following figure (Figure 4-11).

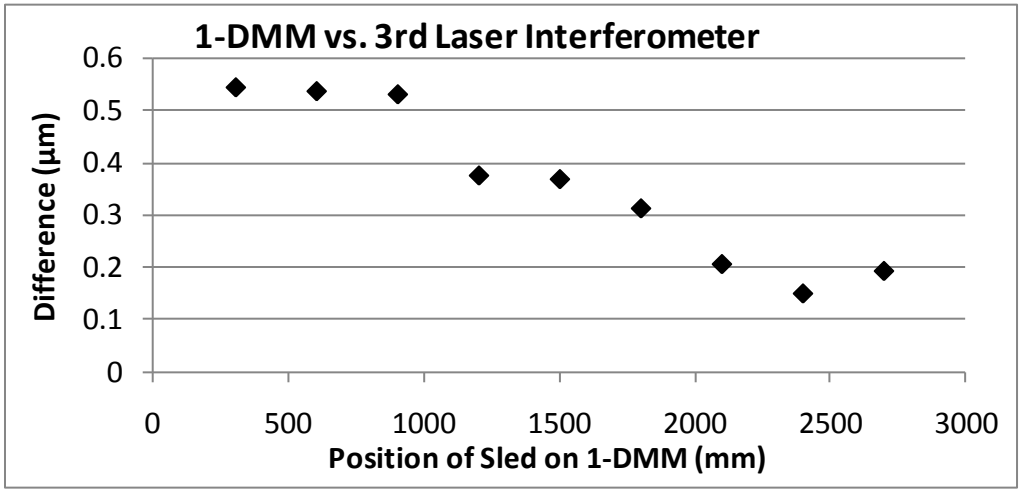

Figure 4-11: Displacement of POI, 1-DMM measurement vs. independent laser interferometer

Discussion

From these experiments we found that correlation coefficients for the noise component between parallel laser interferometers in a fairly well controlled environment ranged from 0.01 to 0.96. Correlations between the two measurement axes are important in the determination of uncertainties introduced in applying the extended Abbe principle. Shielding the laser beam path from air turbulence due to the air handling system was shown to decrease the correlation coefficient. Since the correlation coefficient can't be determined in-situ, a conservative method for estimating uncertainty of the Abbe correction would be to assume that they are not correlated. The magnitude of the noise component for each of the displacement sensors, even though they are uncorrelated at certain times, are about two orders of magnitude smaller than the uncertainty for displacement measurement correction for each sensor due to environmental influences, shown later in Table 4-2.

Yaw of the 1-DMM's carriage is estimated by calculating the difference between the two laser interferometers, and dividing that difference by their lateral separation. In the yaw

measurement experiments using the 1-DMM, the maximum difference measured between the two laser encoders along the 3,000 mm length of travel was approximately 3.6μm. This translates to a maximum yaw of about 16.8 μrad. for the carriage. This amount of yaw is well within the manufacturer's specifications for straightness and flatness of the granite guide way. What is important is that this deviation was detected, allowing a more accurate estimate for the displacement of the POI to be provided as the carriage traverses along the granite straight edge.

Accurate displacement measurement of the POI is a primary function of the 1-DMM. By placing the third laser interferometer co-axially with the path of the POI, inter-comparison between the displacement measured by the dual laser interferometers using the extended Abbe principle and that measured by the independent interferometer was possible. A maximum difference of about 0.55 μm was observed between the two measurements. As the displacement increases, the difference tends to decrease. This may be an indication that the third laser is not perfectly aligned with the two mounted to the 1-DMM; resulting in a cosine error.

Uncertainty in estimating yaw, and displacement of POI

Using the equations outlined earlier, the uncertainty of measuring the displacement of the POI can be calculated as a function of the carriage's position, and the relative yaw angle of the carriage. Using the parameters for our machine and their components, the estimated expanded standard uncertainty (k=2) for position measurement may be estimated; as shown in the following table (Table 4-2).

Table 4-2: Machine and measurement system parameters

Parameter	Value	Description
a	219 (mm)	Separation between measurement axes
b	109.5 (mm)	Location of POI relative to measurement axis 1
d	3,000 mm	Maximum displacement measureable by 1-DMM
U_{d1}	1.744 (µm)	Standard measurement uncertainty of axis 1 (@ 3m)[1]
U_{d2}	1.744 (µm)	Standard measurement uncertainty of axis 2 (@ 3m)[1]
U_a	0.289 (mm)	Standard uncertainty for dimension "a"
U_b	0.289 (mm)	Standard uncertainty for dimension "b"
r	0.4	Correlation Coefficient
Yaw	16.8 µrad.	Maximum yaw experienced by carriage[2]
d_2-d_1	3.6 µm	Maximum difference between interferometers[2]

[1] A function of beam path length
[2] Varies with carriage position

The values for standard uncertainty, outlined in Table 4-2, can be evaluated based on specifications provided by the equipment's manufacturers. However, the value for our correlation coefficient and yaw was assigned based on experimental results presented earlier. From these sets of data, we have observed correlation coefficients "*r*" which vary from 0.01 to 0.96. Under the operating conditions which the 1-DMM will be utilized, we believe that it would be reasonable to assign a value of 0.4 for the correlation coefficient "*r*".

Recall the following equation for evaluating the displacement of the POI:

$$\Delta d = \frac{b\left(d_2 - d_1\right)}{a} \qquad (4.16)$$

Using this equation a Type B uncertainty may be performed to estimate the uncertainty of Abbe offset error correction. Applying the law of propagation of uncertainties to equation 4.16, the following express is obtained for uncertainty of displacement measurement:

$$u_{\Delta d} = \sqrt{\left(\frac{\partial \Delta d}{\partial b}\right)^2 u_b^2 + \left(\frac{\partial \Delta d}{\partial a}\right)^2 u_b^2 + \left(\frac{\partial \Delta d}{\partial d_2}\right)^2 u_{d_2}^2 + \left(\frac{\partial \Delta d}{\partial d_1}\right)^2 u_{d_1}^2} \qquad (4.17)$$

The sensitivity coefficients for the preceding equation are evaluated as follows:

$$\frac{\partial \Delta d}{\partial b} = \frac{d_2 - d_1}{a} \qquad (4.18)$$

$$\frac{\partial \Delta d}{\partial a} = -b\frac{d_2 - d_1}{a^2} \quad (4.19)$$

$$\frac{\partial \Delta d}{\partial d_2} = \frac{b}{a} \quad (4.20)$$

$$\frac{\partial \Delta d}{\partial d_1} = \frac{-b}{a} \quad (4.21)$$

Using the values from Table 4-2, the estimated standard uncertainty for Abbe offset error correction at 3m of displacement is 955nm. When factored into a displacement measurement, the standard uncertainty of measuring 3 meters of displacement on the 1-DMM is 1.456μm.

Using the extended Abbe Principle to track the displacement of a POI, under conditions where the two displacement sensors d_1 and d_2 are uncorrelated ($r<1$), a displacement measurement with a lower uncertainty can be achieved. Referring back to Figure 4-4, if the POI is collinear with a displacement sensor, where (α=0 or 1), the uncertainty of a displacement measurement is equal to the uncertainty of an individual laser interferometer. However, if the POI is located between two laser interferometers ($0<\alpha<1$), a measurement with a lower uncertainty is obtained. The most ideal location for the POI is midway between the laser interferometers, (α=1/2), at this position the uncertainty is minimized.

Concluding Remarks

When utilizing the extended Abbe principle to correct for axis motion errors, the estimation of displacement uncertainty of the POI can vary according to the location of the POI relative to the machine scales. The level of correlation between the two displacement measurement sensors will also affect the uncertainty of the estimated displacement of the POI. Fully correlated measurement scales will result in an uncertainty estimate that is independent of the location of the POI relative to the scales. However uncorrelated measurement axes will result

in a variation of the uncertainty with position of the POI, with minimum uncertainty occurring when the POI is midway between the measurement axes. For multi-axis machines which utilize the extended Abbe principle to improve accuracy, motion of any axis will normally cause a shift in the location of the POI for other axes, resulting in significant variations in positioning uncertainty for those axes. Practical application of the extended Abbe principle on a precision machine found that correlation between two laser interferometer measurement axes was unpredictable, with correlation coefficients found to range between approximately 0.01 and 0.96 when operated in a well controlled environment. Therefore, when the extended Abbe principle is used on multi-axis machines it is likely that the uncertainty of displacement estimation for any axis will be dependent on the positions of the other axes of the machine.

CHAPTER FIVE

INSTRUMENT FOR GAUGEING LARGE RING SHAPED OBJECTS

This chapter discusses the design of a novel self-initializing instrument used to measure the diameter of circular objects. The design of this instrument consists of two arms pinned together on a common pivot. The pivot and the end of each arm each contain a sphere tipped stylus which makes contact at three points along the circumference of the circular part. If the length of each arm and the angle between the arms is known, a closed form solution may be used to calculate the diameter of that part. To initialize the angle encoder of this instrument, a self-initialization method is used. The primary feature of this instrument is the ability to provide an absolute measurement of large circular parts without the needing to be “mastered” on a grand master artifact.

Introduction

Large scale parts circular parts (greater than 400mm) such as ultra large bore bearings, and rocket booster casings often use hand held instruments to inspect their diameters during the manufacturing process. Since it is difficult to move these types of parts around a shop floor due to their size, dimensional inspection instrumentation is typically brought to the location of the part. A traditional instrument that is used to measure these type of parts is an instrument called a bar gauge. This instrument contains two sliding jaws, with a displacement indicating device on one of them to provide feedback on the part’s size (Figure 5-1).

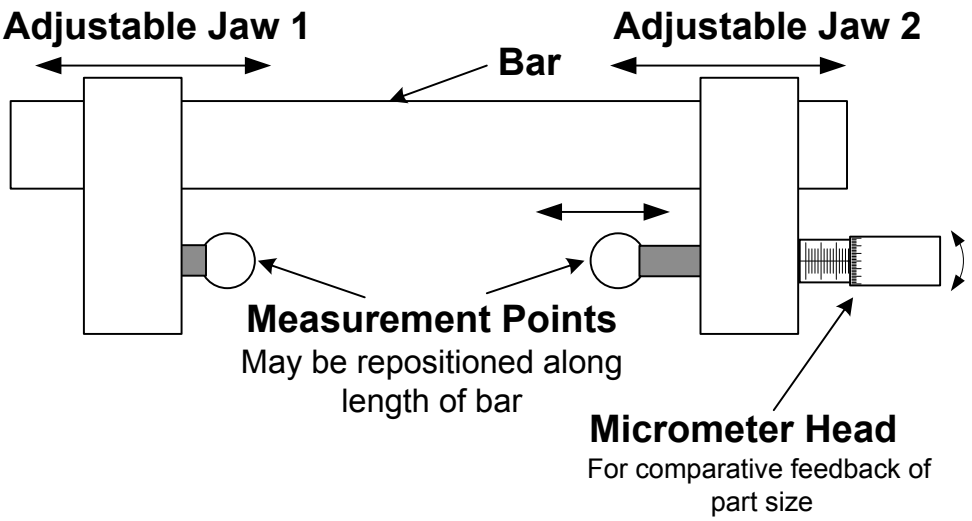

Figure 5-1: Bar gauge with a micrometer head for size feedback

The displacement indicating device can take the form of a micrometer head or dial indicator. Measurement range of these devices is limited, so before the bar gauge can provide an accurate measurement it needs to be initialized on a "*master part*" of a known size. During this phase, the adjustable jaws are adjusted to roughly fit the master part, and final initialization of the bar gauge to the master part is performed by adjusting the micrometer head (Figure 5-1). Because of this, the bar gauge is essentially a comparator instrument, since parts of unknown dimensions are measured relative to a part of known size; a comparison.

There are a few drawbacks to using these types of instruments to inspect bearing dimensions. Reliance on master parts to calibrate bar gauges has been successful for many years. However, these master parts consume a significant amount of floor space in a production facility, space which otherwise could be dedicated to increase manufacturing capacity. This is due to the fact that a master part needs to be maintained for every part goemetry, and cataloged part number. Because of this, a plethora of parts, each with unique geometries, needs to be maintained.

Successful measurements using a bar gauge is dependent on operator skill. With respect to measuring the diameter of large bearing rings, a bar gauge requires the operator to have a well trained tactile feel to detect when the appropriate diameter has been measured. The operator will

typically “sweep” the bar gauge back and forth along the part until the maximum two point diameter is detected. This search for the maximum two point diameter is performed during the calibration stage, and the measurement stage. If the bar gauge is improperly calibrated in the first stage, all subsequent measurements made using the erroneous bar gauge will contain a bias. With all the numerous dimensions on a part, several different instruments are needed to fulfill the measurement tasks. This again, requires more time, man power, and floor space.

In an effort to solve these problems, a new instrument that is capable of measuring, the OD, & ID, is proposed. The following sections describe the concept of this instrument, how it operates, how to self-initialize it, expected measurement uncertainty, and some sample measurement results.

Instrument Design

This new instrument consists of two arms pivoting on a common axis. Its design consists of a mechanism which resembles a proportional caliper, but with an angular encoder monitoring rotational displacement at the rotating joint. The instrument has three co-planar gauging surfaces, which contact the top surface of the part being gauged. Spherically tipped styli protrude an equal distance from each gauging surface. To measure the inside diameter of a part for example, the gauging surfaces of the instrument would be placed onto the top surface of the part, and the three styli would be brought into contact with the inside surface of the ring as shown in Figure 5-2.

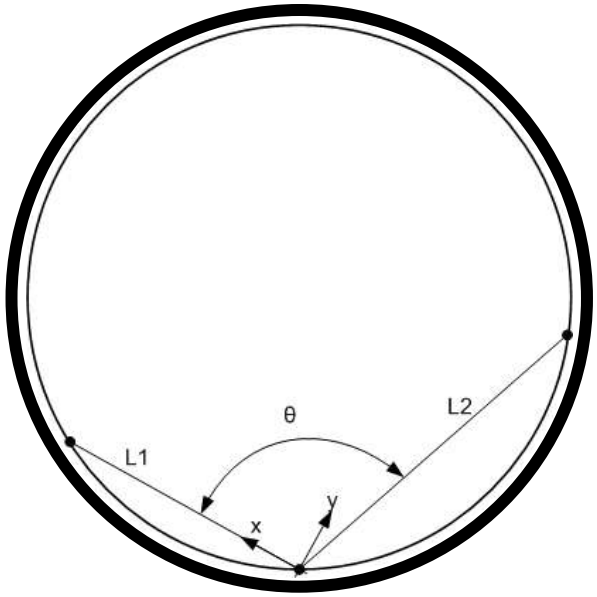

Figure 5-2: Measuring a ring using 3 point contact

By measuring the angle between the arms with the angular encoder, and knowing the arm lengths, L1 and L2, and the radius of the styli, the ID of the bore can be calculated using equation (5.1) [46].

$$D = D_{stylus} + \sqrt{L_1^2 + \frac{L_1^2 \cos^2\theta}{\sin^2\theta} - \frac{2L_1 L_2 \cos\theta}{\sin^2\theta} + \frac{L_2^2}{\sin^2\theta}} \quad (5.1)$$

If the part contains a taper angle, the opposite side of the gauge, has the styli setup with a different stand-off distance from the gauging surface than the first side (Figure 5-3 & Figure 5-4).

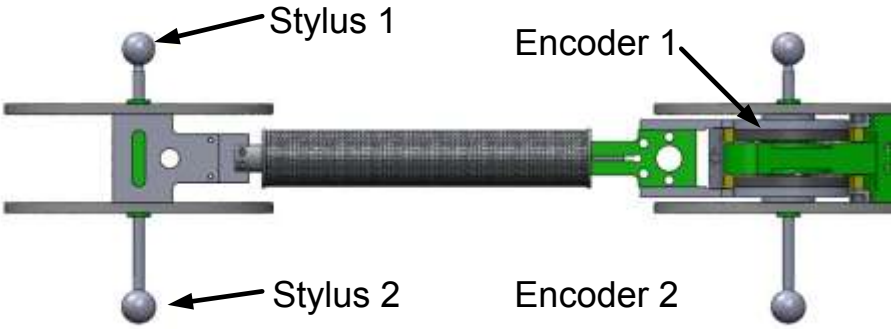

Figure 5-3: Front view of instrument, encoders and styli shown

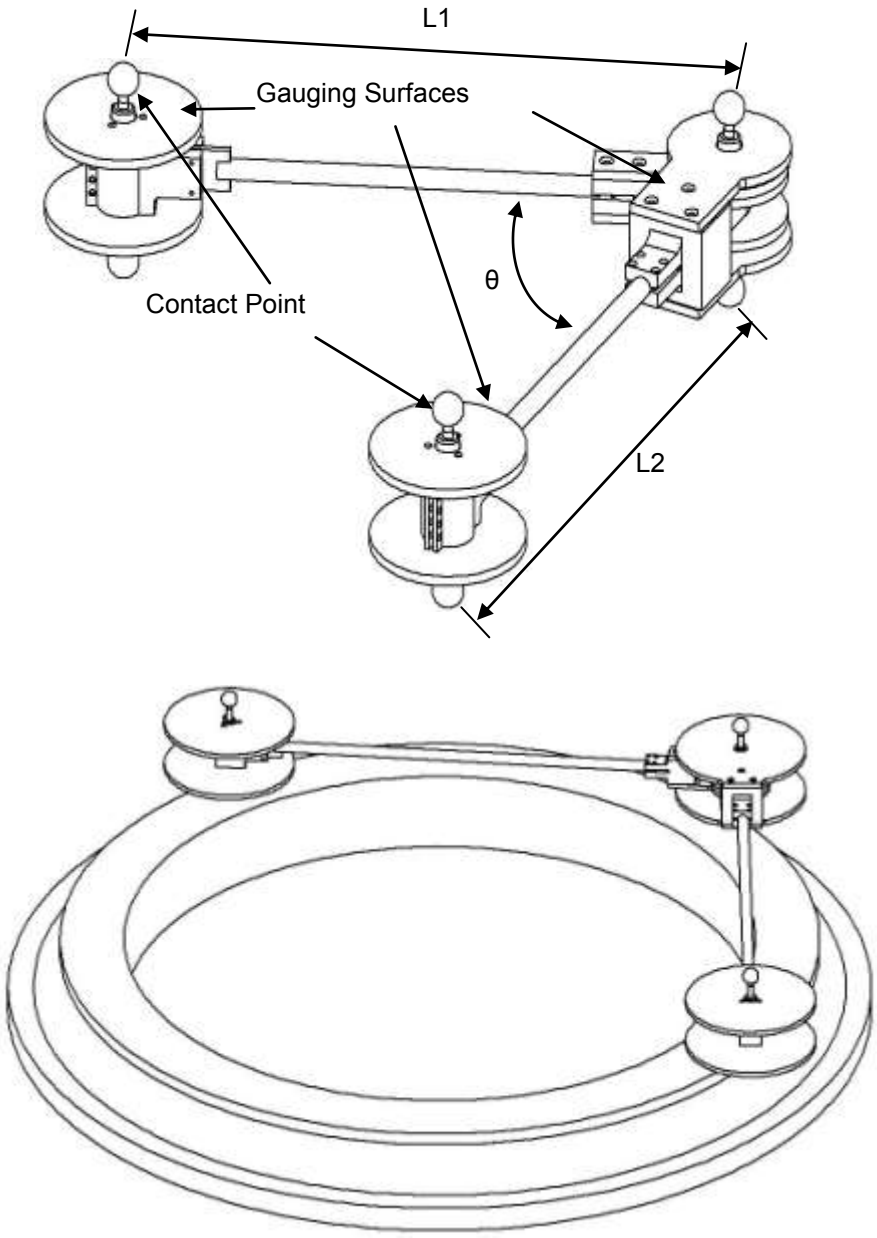

Figure 5-4 *:* Large ring gauge measuring a ring.

Knowing the difference of the stand-off distances between the two sides, and the measured diameter at each height, the taper angle of the tapered ring (Figure 5-5) can be resolved using the following equation (5.2).

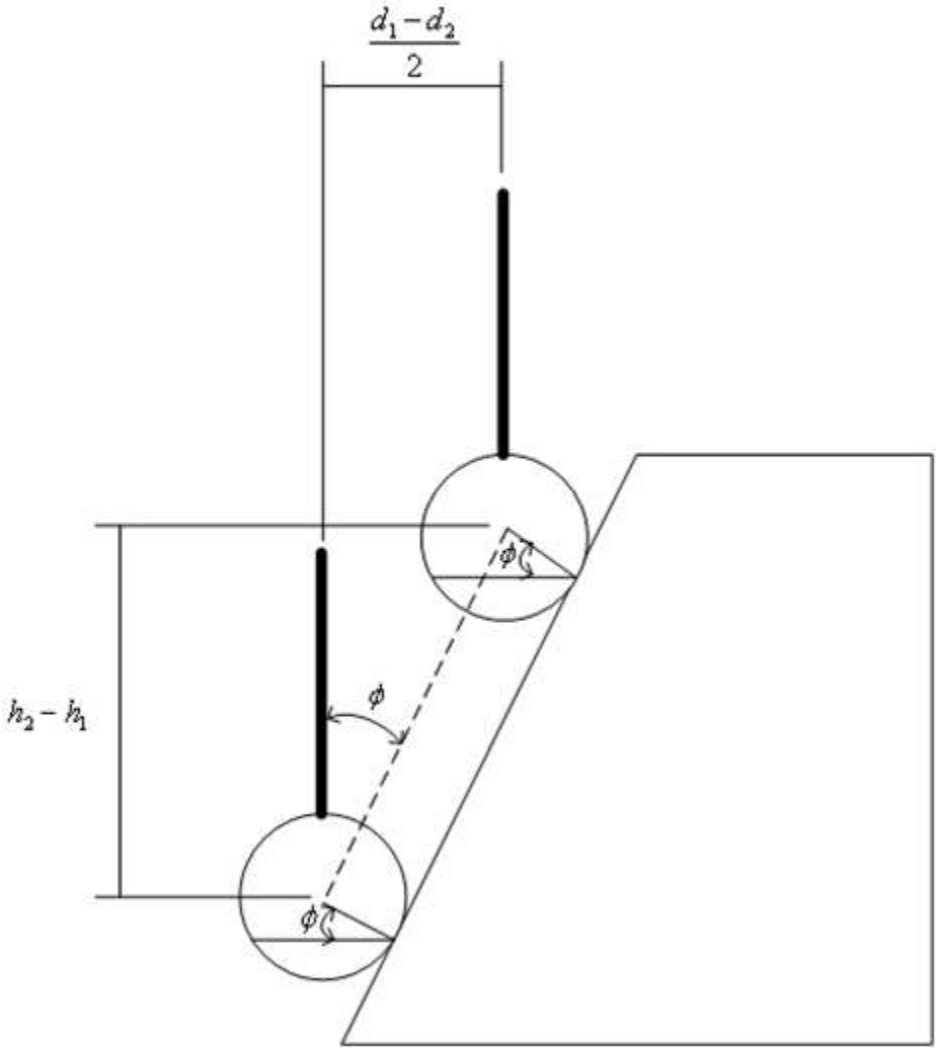

Figure 5-5: Measuring taper of a cone

$$\phi = \tan^{-1}\left(\frac{d_1 - d_2}{2(h_2 - h_1)}\right) \qquad (5.2)$$

Dual angle encoders are used to measure the angular displacement of the arms. They are installed concentric to the axis of rotation, spaced about 44mm apart. Use of dual angular encoders was chosen in hopes of improving the resolution of the instrument, as well as providing an indicator of torsional twist in the arms. We expect any torsional twist in the arms will manifests themselves as a differential reading between the top and bottom.

Setup of the Instrument

Unlike traditional bar gauging methods which transfer measurement from the master part to the part being manufactured, the proposed instrument doesn't require a calibrated fixture to initialize it to provide an absolute angle between the arms of the instrument, as opposed to simply an angular displacement. However certain parts of the instrument require a coordinate measuring machine and gauge blocks to measure, and setup the arms, and styli.

The first step is to select the correct length intermediate rod which will be used to build up each arm. These intermediate rods are used to connect the assemblies which hold the styli to the central pivot, which contain the angle encoders. The ideal arm length, which is measured from the center stylus to the styli attached to the end of each arm, should be at least 60% of the part radius being measured.

Next, install the styli and set the proper stand-off distance from the gauging surfaces. One method is to support the instrument with 1-2-3 blocks on the gauging surfaces, using a flat surface plate as a base. Next insert the styli into the holders, and by using an appropriate gauge block stack, slide it under the styli tip to set the desired stand-off distance, and tighten the locking collar for the styli holder (Figure 5-6).

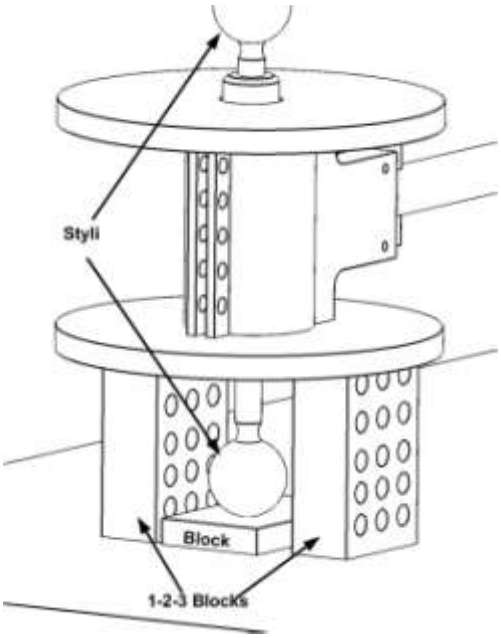

Figure 5-6: Setting the stylus standoff distance using a gage-block stack

Once all of the styli have been installed, the distance from the stylus located at the pivot joint, to the styli located at the ends of the arms is measured. For experiments presented in this report a coordinate measuring machine (CMM) is used. The results of this measurement will be used as lengths L1 and L2. The final stage of the instrument setup involves self-initialization of the digital angular encoder; the following figure displaying the final designed fully assembled (Figure 5-7).

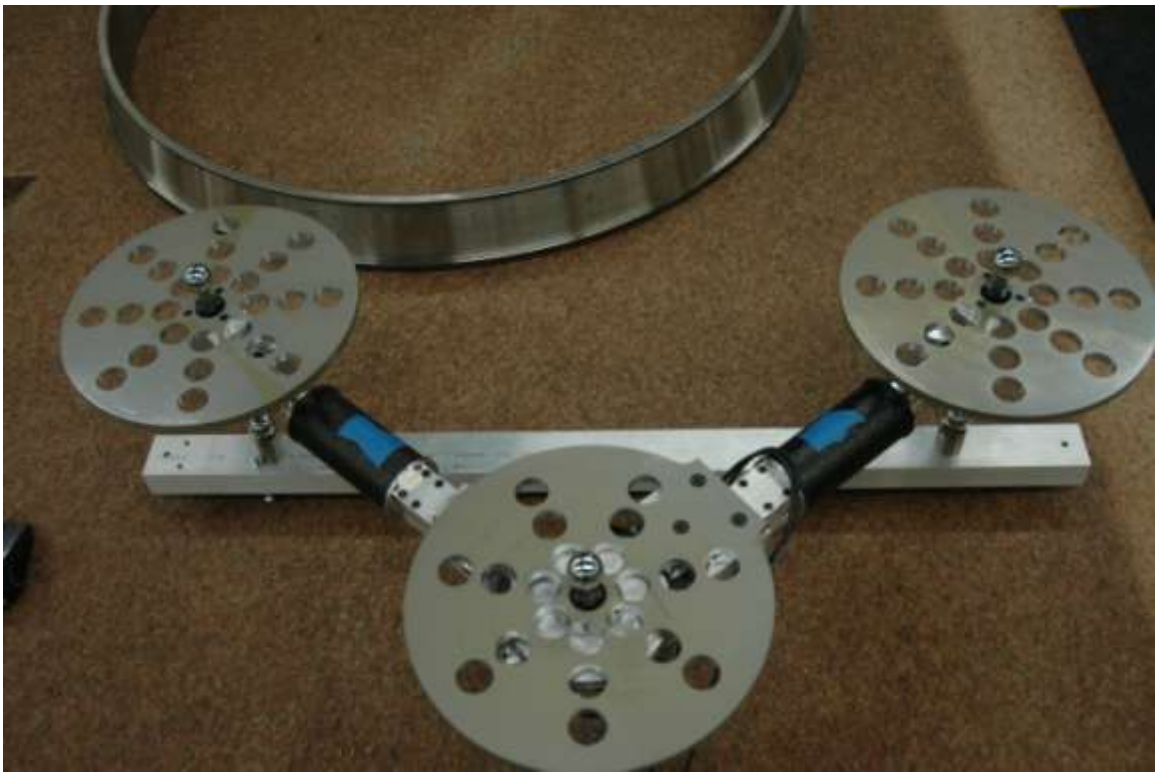

Figure 5-7: Large Ring Gauge fully assembled and resting on initialization fixture.

Initialization of Angular Encoders

This instrument relies on angle encoders as the displacement measurement sensor, in conjunction with other constant inputs to the measurement model (equation 5.1) to resolve a measurement output in the form of a diameter. In order for an encoder to make absolute measurements it needs to be initialized, and with an angular encoder, an angle of a known value needs to be introduced to it. Resolving an absolute angle with this instrument is no different that resolving a length dimension with a comparator type instrument; the total angle is composed of a summation of an initial angle, and a displacement value from it (equation 5.3).

$$\theta = \theta_0 + \Delta\theta$$
$$\text{where: } \theta_0 \text{ is the initial angle} \qquad (5.3)$$
$$\Delta\theta \text{ is the angular displacement}$$

There are two methods which can be used to initialize an angle encoder, use an independently calibrated artifact/fixture, or self-initialization.

One conceivable artifact that may be independently calibrated and introduced to the instrument as a reference value can be a bar/fixture with two quasi-three point kinematic seats (TPKS) affixed to it. These TPKS's can couple with the styli located on the end of each arm. A quasi-TPKS is different from a TPKS that's constructed from three spheres. With a quasi-TPKS the three points of contact are arc sections with burnished surfaces. Conceptually they accomplish the same goal of locating a sphere, but with reduced precision.

By mounting the styli on this fixture, a triangle is formed between the instrument and the artifact. If the length of each arm, and the distance between the two TPKSs is known, an initial angle between the arms may be resolved by the law of cosines (Figure 5-8).

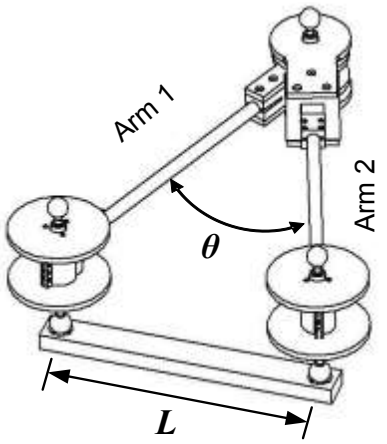

$$L^2 = Arm1^2 + Arm2^2 - 2\left(Arm1\right)\left(Arm2\right)\cos\theta$$

$$\cos^{-1}\left(\frac{L^2 - Arm1^2 - Arm2^2}{2\left(Arm1\right)\left(Arm2\right)}\right) = \theta$$

Figure 5-8: Initializing with an artifact of known length, and using law of cosine to resolve an initial angle (length of arms need to be known)

To estimate the uncertainty of initializing this instrument's angle encoder with an independently calibrated artifact, a Type B uncertainty analysis may be performed.

Uncertainty in Initializing Angle with a Independently Calibrated Fixture

The influencing quantities which affect the uncertainty in evaluating the initialization angle with the law of cosine are:

- The uncertainty the initialization length, L
- The uncertainty in the measured lengths of Arm 1 and Arm 2

Evaluating the equation shown in Figure 5-8 with respect to each influencing quantity, the following sensitivity coefficients are obtained:

$$\frac{\partial \theta}{\partial L} = -\frac{2L}{Arm1 \cdot Arm2\sqrt{4 - \frac{L^2 - Arm1^2 - Arm2^2}{Arm1^2 \cdot Arm2^2}}} \tag{5.4}$$

$$\frac{\partial \theta}{\partial Arm1} = \frac{2\left(\frac{1}{Arm2} + \frac{L^2 - Arm1^2 - Arm2^2}{2 \cdot Arm1^2 \cdot Arm2}\right)}{\sqrt{4 - \frac{L^2 - Arm1^2 - Arm2^2}{Arm1^2 \cdot Arm2^2}}} \tag{5.5}$$

$$\frac{\partial \theta}{\partial Arm2} = \frac{2\left(\frac{1}{Arm2} + \frac{L^2 - Arm1^2 - Arm2^2}{2 \cdot Arm1 \cdot Arm2^2}\right)}{\sqrt{4 - \frac{L^2 - Arm1^2 - Arm2^2}{Arm1^2 \cdot Arm2^2}}} \tag{5.6}$$

The uncertainty of measuring the lengths of the initialization fixture, Arm 1 and Arm 2 could be performed on a CMM which typically measures with a standard uncertainty of 1.73μm. One must not also forget about repeatability of mounting the instrument to the initialization artifact. When the initialization fixture is introduced to the instrument, it couples the tip of their styli to the quasi-TPKS on the fixture. The non-repeatability of a quasi-TPKS and a sphere typically has standard uncertainty of 1.5μm, and there are two attached to the initialization fixture.

To calculate the combined standard uncertainty for initializing the angle encoders with a calibrated artifact, the sensitivity coefficients calculated earlier is multiplied by their respective standard uncertainty; using the following assumptions for the lengths of the arms and initialization artifact (Table 5-1).

Table 5-1: Values for influencing quantities for initializing angle with a calibrated artifact

Influencing Quantity	Value (mm)	Standard Uncertainty (mm)
Arm 1	429	0.00173
Arm 2	429	0.00173
L	650	0.00346

The combined standard uncertainty is calculated as follows:

$$u_\theta = \sqrt{\left(\frac{\partial \theta}{\partial L} u_L\right)^2 + \left(\frac{\partial \theta}{\partial Arm1} u_{Arm1}\right)^2 + \left(\frac{\partial \theta}{\partial Arm2} u_{Arm2}\right)^2} \qquad (5.7)$$

Evaluating this equation with the assumptions in Table 5-1, a standard uncertainty of $13.63X10^{-6}$ radians ($7.81X10^{-4}$ degrees) was estimated.

Uncertainty in Initializing Angle with Self-Initialization

The design of this instrument also allows for a self-initialization method to be used. This can be done by using the instrument's encoder, the fixture mentioned earlier (containing two quasi-TPKS's an unknown distance apart), and two of displacement maneuvers with the instrument on the fixture. This method of self-initialization is similar in concept to that which was introduced with the Laser Ball Bar (LBB) [7, 12].

Using the twin quasi-TPKS fixture mentioned earlier, the instrument is placed into this fixture in two distinct configurations. When the instrument is placed onto the fixture, a triangle is formed, but the internal angle between the two arms is unknown. However, the instrument is able interface with the fixture in two different positions (Figure 5-9).

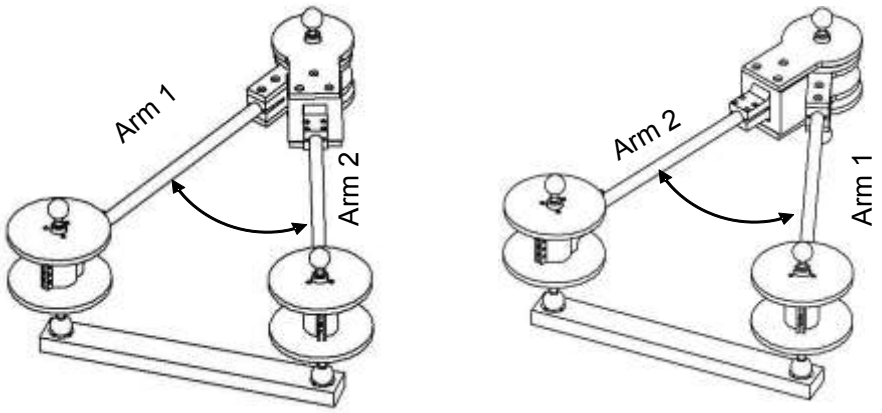

Figure 5-9: Large ring gauge can mount onto calibration fixture in two deterministic positions

By measuring the angular displacement of these arms as they rotate from one position on the fixture to the other, and realizing that a full rotation of the instrument is 2π radians, the unknown internal angle can be calculated. The self-initialization method developed to initialize the angle encoders of this instrument relies on the concept of circle closure. The self-initialization process is outlined in Figure 5-10.

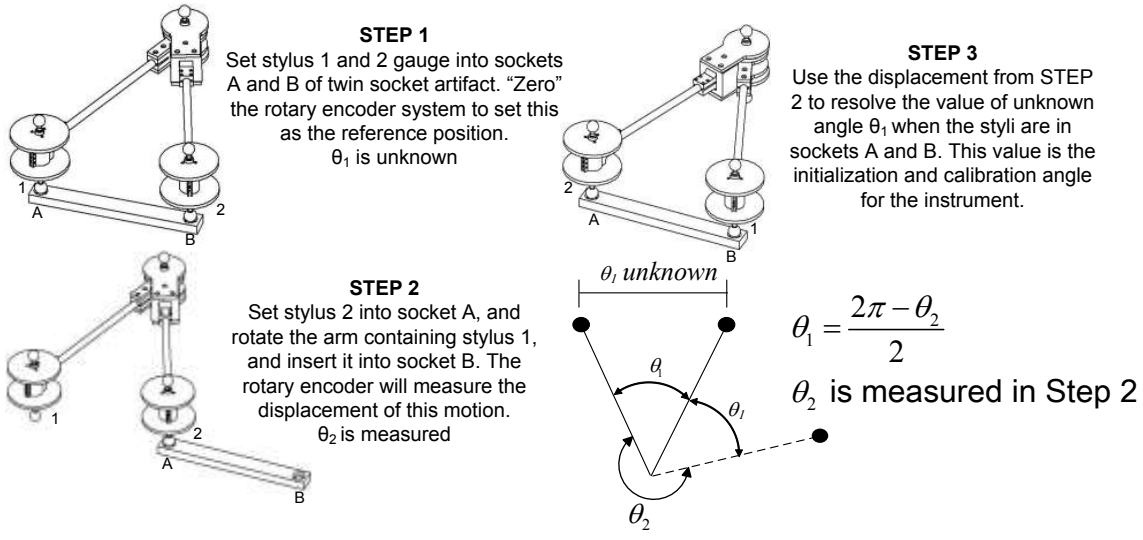

Figure 5-10: Three step initialization and calibration procedure

A benefit of initializing the instrument in this manner is that an independently calibrated fixture is not required. All that is required is that the distance between the two sockets on the fixture be stable during the short time required for the self-initialization procedure. This is beneficial since there is no need to maintain the initialization fixture other than insuring that it is not permanently damaged, or subjected to any significant thermal gradients during the self-initialization phase.

To compare the uncertainty of initializing the angle encoders using self-initialization to initialization with a calibrated artifact, a Type B uncertainty analysis is used again. In this case the measurement model for self-initialization (equation in Figure 5-10) only has one influencing quantity, the angle displaced when the instrument is moved from one configuration of the fixture to the other. In this case the sensitivity coefficient is equal to -1/2.

$$\frac{\partial \theta_1}{\partial \theta_2} = -\frac{1}{2} \qquad (5.8)$$

However angular displacement measurement in this instrument is influenced by two factors, the displacement measurement uncertainty of the angle encoders, and the non-repeatability in mounting to the two quasi-TPKS on the fixture.

The manufacturer of the angular encoder furnished a calibration certificate which indicated that their angular encoder system measures with an error of 1.0 arc second. Assuming that this error is rectangularly distributed, a standard uncertainty from this value is calculated by dividing it by $\sqrt{3}$ which is equals to 2.79 $X10^{-6}$ radians or 1.603$X10^{-4}$ degrees.

The standard uncertainty for non-repeatability of quasi-TPKS is assumed to be 1.5μm each. If each arm is again assumed to be 429mm long, the standard uncertainty for non-repeatability in terms of angle is 7 $X10^{-6}$ radians or 4 $X10^{-4}$ degrees.

To calculate the standard uncertainty for determining the initialization angle, the preceding uncertainties for angular displacement measurement and TPKS non-repeatability are added in quadradure, which is 7.53 $X10^{-6}$ radians (4.32 $X10^{-4}$ degrees).

$$u_{\theta_0} = \sqrt{\left(2.79X10^{-6}\right)^2 + \left(7X10^{-6}\right)^2} = 7.53X10^{-6} rad \qquad (5.9)$$

Concluding Remarks on Angle initialization

Due to the mechanical design of this instrument, it was not possible to create an initialization fixture/artifact to directly introduce an initial angle value to the instrument. The two potential solutions are, to use a calibrated length artifact in conjunction with pre-calibrating the length of each arm of the instrument; or self-initialization, where nothing needs to be calibrated except the angle encoders, which are calibrated by the manufacturer. Under these assumptions, the self-initialization method is expected to have a reduced uncertainty in initializing to an absolute angle. The reason for the discrepancy in uncertainty is due to the number and magnitude of uncertainties in each influencing quantity for the method which relied on an independently calibrated artifact. For this case the assumptions for standard uncertainty for the arm lengths and calibrating the initialization length are reasonable for most commercially available CMM's.

To better understand how this instruments performs when measuring a circular ring 546mm in diameter, a Type B uncertainty analysis is performed for the entire instrument, followed by physical measurements.

Uncertainty Analysis of Circular Measurement

Once the components to embody this design concept were chosen, a Type B uncertainty analysis was performed to evaluate its measurement uncertainty [20]. Most of the components used to construct the prototype of this design concept were custom manufactured. Parts which were purchased off the shelf included the angle encoder system, and the styli holder. To begin the uncertainty analysis for this design concept, the mathematical model for the measurand (equation 5.1) is used to derive the measurement sensitivity coefficients. They are as follows:

- Sensitivity coefficient for the length uncertainty of Arm 1

$$\frac{\partial D}{\partial L_1} = \frac{-L_2 \cos\theta + L_1}{\sqrt{\frac{-2L_1L_2\cos\theta + L_2^2 + L_1^2}{\sin^2\theta}}\sin^2\theta} \quad (5.10)$$

- Sensitivity coefficient for the length uncertainty of Arm 2

$$\frac{\partial D}{\partial L_2} = -\frac{L_1 \cos\theta - L_2}{\sqrt{\frac{-2L_1L_2\cos\theta + L_2^2 + L_1^2}{\sin^2\theta}}\sin^2\theta} \quad (5.11)$$

- Sensitivity coefficient for the uncertainty of angular measurements

$$\frac{\partial D}{\partial \theta} = -\frac{\left(-L_2 \cos\theta + L_2\right)\left(L_1 \cos\theta - L_2\right)}{\sqrt{\frac{-2L_1L_2\cos\theta + L_2^2 + L_1^2}{\sin^2\theta}}\sin^3\theta} \quad (5.12)$$

- Sensitivity coefficient for the uncertainty of styli diameter

$$\frac{\partial D}{\partial D_{stylus}} = 1 \quad (5.13)$$

Next, there are seven sources of measurement error that are anticipated to have a significant impact on the measurement; they are outlined as follows. Uncertainty contributions are computed assuming measurement of a circular part which is 546mm in diameter.

Length of Arms

In the setup process of the instrument, the lengths of each of the measurement arms need to be determined. To perform this task, a CMM is used to measure the distance from the stylus located at the pivot to each of the styli located at the ends of the measurement arms. We assume the CMM has a maximum measurement error of 3.0μm; and assuming a rectangular probability distribution, this gives a standard uncertainty of 1.76 μm for the arm lengths.

Thermal Expansion of Arms

Temperature changes can cause the lengths of the arms to change. From the CMM lab to the shop floor, where the instrument will be used, we assume temperature changes of up to 2°C. The material for each arm will be constructed using carbon fiber and with an assumed nominal coefficient of thermal expansion of $2.5X10^{-6}\frac{1}{^{\circ}c}$ and a length of 429mm, the estimated standard uncertainty due to thermal expansion is 1.24 μm [47].

Radial Run-out of instrument

The functionality of the instrument requires two bearings to allow one arm to rotate relative to the other. Since these bearings are not perfect there will be some radial run-out, which will translate to an error motion. In addition, the ball centers of each of the styli will not be perfectly concentric with the axis of rotation. From the experiment outlined in Table 5-4 (shown later on), one of the arms appears to change in length, most likely due to circular run-out at the pivot axis. The range of arm length variation for this arm is 0.016mm. Assuming that this is the maximum run-out error, and that this error takes on a rectangular distribution, a standard uncertainty of 9.23μm is contributed to the uncertainty estimate.

Form error of Styli Balls

The balls of the each of the styli are not perfect and will deviate slightly from the ideal sphere. For this design grade 3 balls will be used. The estimated standard uncertainty due to spherical deviation for the stylus ball is estimated to be 44.0nm.

Encoder Accuracy

A precision angular encoder is used to record the change in angle between the two arms. The data supplied by the manufacturer of the encoder ring indicates an error of 1.0 arc second which translates to a standard uncertainty of 2.77X10-6 radians.

Initialization of angle encoder

Initialization of the instrument will be dependent on the accuracy and resolution of the encoder, and the repeatability of the interface between the balls and the sockets of the artifact shown in figure 6. Each of the sockets is a quasi-TPKS which provides micron level repeatability. Assuming each socket has a positioning repeatability of 1.5μm, and with each arm nominally 500mm in length we expect an angular uncertainty of 7.53 $X10^{-6}$ radians.

Hertzian Contact Penetration

With the balls of each of the stylus contacting the surface of the part, there will be some elastic deformation at the point of contact. This deformation will cause the angle between the arms to deviate slightly, thus causing a measurement error. Assuming a contact force of 10 N and steel styli of radius 12.7 mm, we estimate a standard angular uncertainty of 8.08X10-7 rad.

Using the values presented in the preceding sub-sections, the expected uncertainties for measuring a 546 mm diameter steel ring are outlined in Table 5-2.

Table 5-2: Estimated measurement uncertainty for measuring a 546mm ring

Uncertainty Analysis	Value	Units
Uncertainty in Length of Arm 1	Std. Uncer.	
Qualification Error (measure point to point on CMM)	1.15E-03	
Thermal Expansion due to Uncer. in temp. change	1.24E-03	
Radial runout of instrument	1.44E-03	
Ball sphericity	4.40E-05	
Combined Uncertainty UL1	**2.23E-03**	mm
Uncertainty in Length of Arm 2	Std. Uncer.	
Qualification Error (measure point to point on CMM)	1.15E-03	
Thermal Expansion due to Uncer. in temp. change	1.24E-03	
Radial runout of instrument	0.00E+00	
Ball sphericity	4.40E-05	
Combined Uncertainty UL2	**1.69E-03**	mm
Uncertainty of Angular Measurement	Std. Uncer.	
Encoder Accuracy	2.77E-06	
Angle change due to Hertzian Contact Penetration	1.88E-06	
Initialization of angle encoder	7.53E-06	
Combined Uncertainty Uθ	**8.24E-06**	Rad
Ball diameter uncertainty	4.40E-05	mm
CombinedStandard Uncertainty (k=1)		
Uncertainty of Diameter Measurement	**4.01E-03**	mm

Experimental Results

To assess the performance of this self-initialized instrument, a series of experiments was performed, they include:

1 Repeatability in mounting to initialization fixture

2 Comparison of absolute angle measured by instrument to CMM

3 Ability of instrument to reproduce a measured value

4 Repeatability in measuring the diameter of a part

All of these experiments were performed in a temperature controlled metrology laboratory with a nominal temperature at 20°C.

Repeatability in mounting to the calibration fixture

The initialization fixture is a key component for initialization of the angular encoders. Since this instrument relies on circle closure to realize an initial angle, the instrument needs to repeatedly interface with the fixture. To test to ability of the instrument to repeatedly mount on to the quasi-TPKS's of the calibration fixture, the instrument is first initialized according to Figure 5-10. Next, the instrument is mounted and dismounted from the calibration fixture, thirty times. While the instrument is mounted on the initialization fixture, the arm length (nominally 429 mm each) and the internal angle between the arm are inputs into equation 5.1, with the output being a diameter measurement. The results are shown in the following table and figure (Table 5-5, Figure 5-11).

Table 5-3: Measurement results from repeat mountings onto calibration fixture

Fixture Mounting Repeatability				
	Top Encoder		Bottom Encoder	
	Diameter (mm)	Angle (deg.)	Diameter (mm)	Angle (deg.)
Average	634.945	160.331	634.950	160.330
MIN	634.939	160.330	634.945	160.329
MAX	634.950	160.3320	634.955	160.331
Range	0.011	0.0016	0.010	0.002
Std. Dev	0.0030	0.0004	0.0029	0.0004

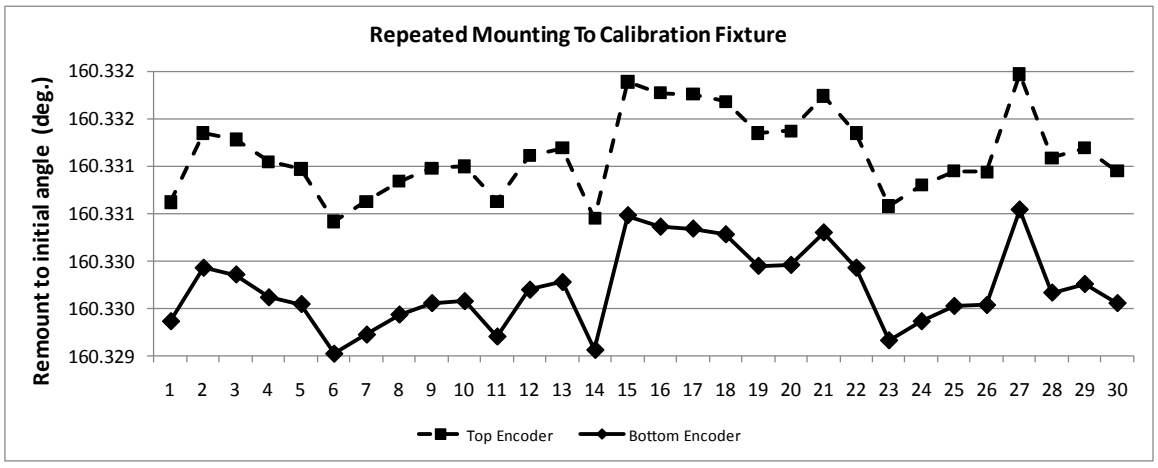

Figure 5-11: Plot of repeatability of multiple mountings on calibration fixture

The numerical results displayed in Table 5-3 show the min, max, average, and standard deviation of the diameter that is measured when the instrument is mounted on to the calibration fixture, along with the variation in angle between the arms of the instrument. From the thirty mount and dismount trials, a standard deviation of 0.003mm was observed for the resultant diameter that was measured when mounted on the calibration fixture, this translates to a standard deviation of 4 $X10^{-4}$ degrees in angular measurement. This is an indication of the non-repeatability of the coupling of the styli on the end of each arm and the TPKS of the initialization fixture.

From Figure 5-11, a noticeable bias between the diameter resolved by the two angular encoders contained within the instrument was observed. It is believed that the torsional compliance of the arms is manifesting themselves into differential readings between the two sensors. When the instrument is placed on the part, twist to the arms is induced when the weight of the instrument bears down on a portion of the instrument that is not through the centerline of the arms, e.g. a torque is applied to the arms (Figure 5-12).

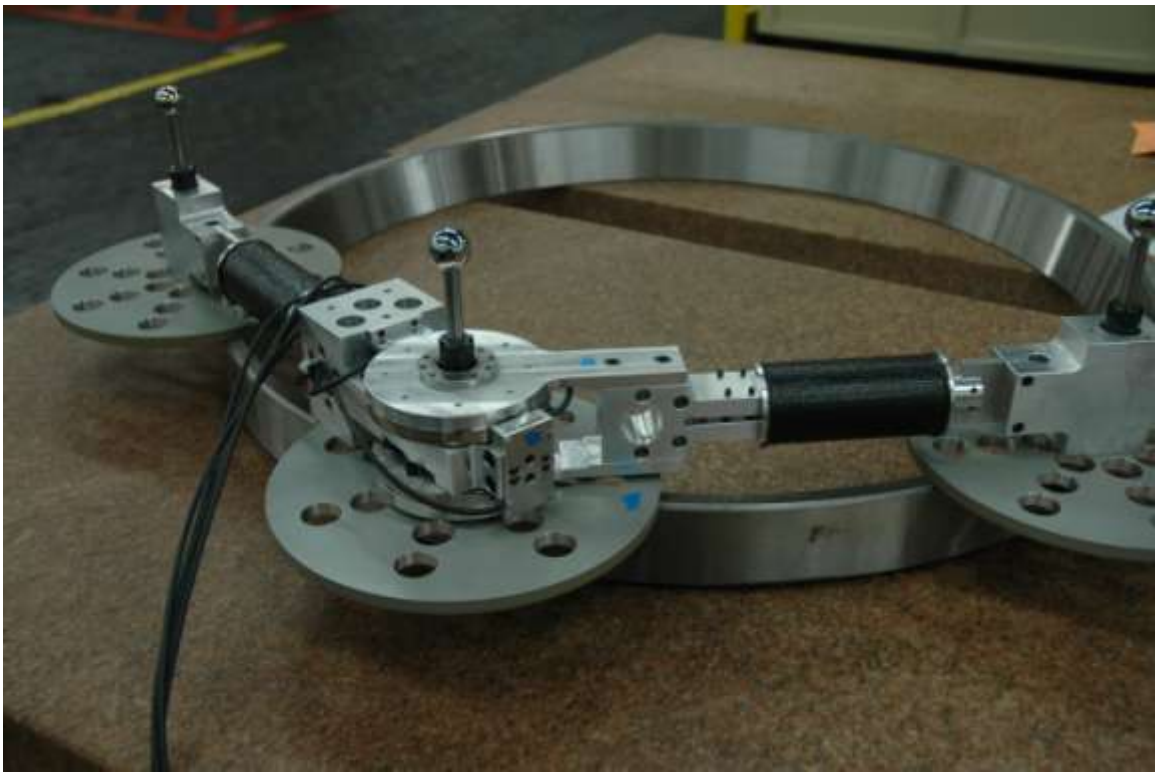

Figure 5-12: Arms of instrument experience torsion due to off axis loading

Angle Encoder to CMM Comparison

Part of obtaining an accurate part measurement with this instrument is to have an accurate measure of the angle between the arms. To obtain a comparison of how well the angular encoders perform in this instrument, the instrument is self-initialized to what is believed to be an absolute angle, and placed onto a CMM. Next, the angle between the arms will be increased in small increments, and a measurement of this angle will be recorded by the instrument's encoders, compared to an angle obtained from CMM measurements of the three sides of the triangle formed by the styli, and using the law of cosines to estimate the included angle. A comparison between the angles measured by the instrument and that of the CMM is shown in the following table (Table 5-4).

Table 5-4: Angle measured by angle encoders compared to CMM

Sample	Arm 1 (mm)	Arm 2 (mm)	Base (mm)	CMM (Degrees)	Encoder	CMM - Instrument
1	429.0440	428.3935	347.9912	47.8888	47.8884	0.0003
2	429.0340	428.4023	410.9281	57.2731	57.2729	0.0002
3	429.0321	428.4003	518.6978	74.4495	74.4482	0.0013
4	429.0279	428.4044	586.1351	86.2501	86.2475	0.0027
5	429.0289	428.4024	680.8177	105.1256	105.1209	0.0047

From this experiment a maximum difference between the angle obtained from CMM measurements and that of the instrument is 0.0047°. This large discrepancy between the angle measured by the instrument and that measured by the CMM is worrisome. If an angular value input to equation 5.1 is changed by this magnitude when measuring a 546mm diameter ring, the estimated diameter will change by 0.020mm. With errors of this magnitude, the precision and accuracy of the instrument is compromised, which limits the capabilities of this instrument.

Self-Initialization and Measurement Reproducibility

The following experiments test the instrument's ability to reproduce a measurement on a ring with a nominal outer diameter of 546.12mm. In the short time that it takes to initialize and manipulate the instrument on the initialization artifact, the lengths between the sockets of the calibration artifact are expected to remain stable. To perform this test, the instrument is initialized using the initialization procedure outlined in Figure 5-10, followed by a measurement of a steel ring. The instrument is then reset, self-initialized again, and another measurement is taken on the steel ring. The diameter measured and angle formed by the two arms is recorded; this initialization and measurement procedure is performed ten times. Results of this experiment are detailed in the following table and figure (Table 5-5, Figure 5-13)

Table 5-5: Measurement results from repeat initializations using initialization fixture; results for 10 initializations and measurements

Angle Initialization Repeatability	Top Diameter	Bottom Diameter
MIN	546.100	546.091
MAX	546.125	546.123
Average	546.109	546.105
Std. Dev.	0.010	0.011

All units in mm

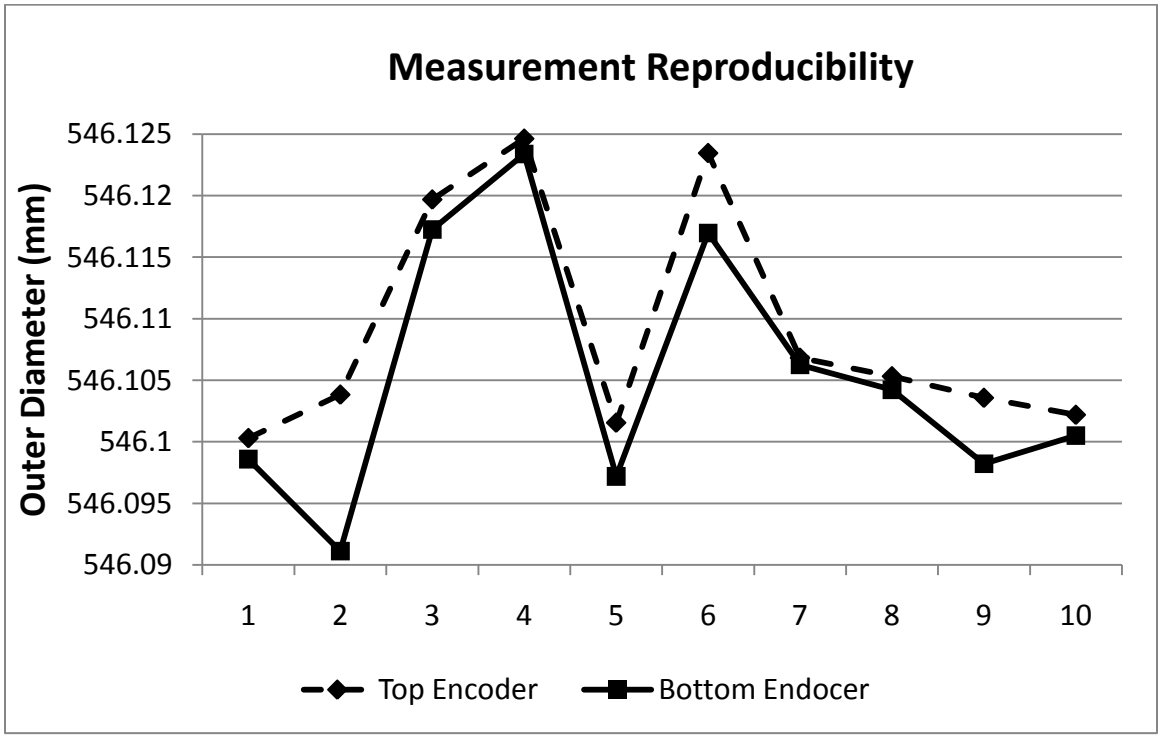

Figure 5-13: Plot of repeatability of multiple initializations using calibration fixture

Measurement repeatability

In a follow up to the previous experiment, the instrument's diameter measuring repeatability was evaluated. This was done by measuring a steel ring with a nominal outer

diameter of 546.12mm. After initializing the instrument once, the ring was measured ten times at the same circumferential location. Results of this experiment are shown in the following table and figure (Table 5-6 & Figure 5-14).

Table 5-6: Repeated measurements of the OD on a 546.12 mm ring

	Ten Repeated Measurements of OD			
	Top Encoder		Bottom Encoder	
	Diameter (mm)	Angle (deg.)	Diameter (mm)	Angle (deg.)
Average	546.1212	82.79567	546.1168	82.79467
MIN	546.114	82.79404	546.1093	82.79295
MAX	546.1293	82.79752	546.1254	82.79662
Range	0.0153	0.00348	0.01609	0.00367
Std. Dev	0.004481	0.001019	0.004628	0.001056

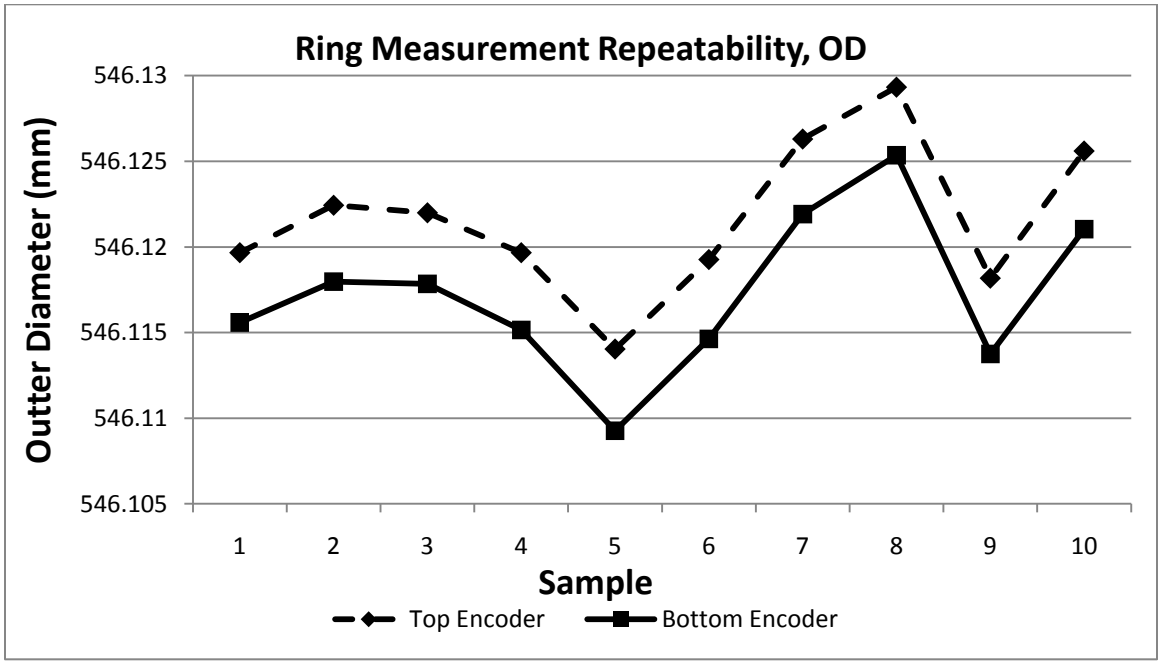

Figure 5-14: Ring measurement repeatability, measuring a ring with a nominal OD of 546.12mm.

Discussion of Results

All of the measurement results presented was from measuring rings with straight walls. Experimental results compare favorably to the Type B uncertainty analysis shown in Table 5-2. Under our best efforts the standard deviation of reproducing a measurement result was no better than 0.01mm. For gauging requirements which require a 15%-25% gauge R&R, the part tolerance that this instrument can measure falls between 0.24 and 0.4 mm. Other than the CMM experiment which measured the included angle between the arms by measuring the relative locations of the styli spheres, there was no readily available method to directly compare the angle measured by the instrument's encoder to a calibrated angular artifact.

Concluding Remarks

This instrument stretched the limits of self-initialization instrument design. With instruments such as the Laser Ball Bar, and the 1-DMM the measurand which the instruments define are similar for both the artifact/fixture, and the objects which they measure. The measurands for these instruments are defined by distances between spheres and three point kinematic couplings. In the case of the of the large ring gauge, the self-initialization procedure uses a sphere and TPKS coupling to establish a length between two TPKS mounted on a bar, which in turn is used to set an initial angle for the instruments angle encoders. However, the objects which the large ring gauge measures have a measurand that is defined by three points of contact along the circumference of a part. These points of contact are not deterministic in nature, but subject to placement on the part, how much contact force is applied, and form error of the part itself. When compared to traditional bar gauging methods, the gauge R&R for a bar-gauge can be up to one order of magnitude lower than the large ring gauge. The principal advantage of a self-initialized instrument is that it does not have to rely on a calibrated artifact to initialize its measurement sensor. However, for this instrument that advantage is compromised by the requirement for a CMM to measure the length of the arms.

CHAPTER SIX

CONCLUDING REMARKS

For dimensional measurement instruments, self-initialization allows for a quick zero adjustment of its displacement measuring scale. For instruments which are unable to realize a null value measurement, an un-calibrated artifact that can interface with the instrument in at least two positions can be used to self-initialize it. However, there are some functional requirements that need to be satisfied in order for it to succeed. This dissertation outlined what those requirements are through a functional decomposition of an instrument (the Laser Ball Bar) which pioneered a self-initialization method for instruments that can't measure a null value.

One of the mechanical implements which allow instruments like the Laser Ball Bar to self-initialize is the sphere, and three point kinematic seat (TPKS) coupling. This type of coupling is able deterministically define a point in space. Using multiple collinear TPKS couplings attached to a stable platform, discrete points in space can be resolved by the instrument. This type of artifact has the capability of capturing a displacement value from an instrument, and transforming it to an absolute dimensional value so that it may be reused by the very same instrument to initialize itself, without relying on measurements of extension.

Determining the metrological traceability and uncertainty of measurement values obtained from self-initialized instruments is critical in determining their measurement capability. The very nature of a self-initialized instrument requires that their traceability be realized through traceable calibrations of their displacement sensors rather than through an independently calibrated artifact. What was unknown before this study was the measurement uncertainty of measured quantities derived with a self-initializing length value, compared to that of an initializing length value from an independently calibrated artifact.

Initially, it was believed that an independently calibrated artifact that provides an initialization length that has a lower measurement uncertainty than what can be achieved through self-initialization, would provide measurements with lower uncertainty, but that is not always the case. In the case of the 1-DMM, the displacement relative to the initialization length needs to be

considered. In situations where the independently calibrated artifact is not measured with a lower uncertainty or unavailable, the self-initialization method is better, as in the case with the Large Ring Gauge, demonstrated through a Type B uncertainty analysis. In the case of the 1-DMM, the Type-B uncertainty analysis predicted that the uncertainty of ball bar measurements made under the self-initialization mode was nearly identical to those made using a ball bar calibrated by the NIST M48 CMM. However, the self-initialization mode displayed a systematic bias when contrasted to the more traditional initialization technique. This bias was likely due to the flexibility of the initialization artifacts. If these systematic biases can be corrected, the 1-DMM would be expected to measure just as well as the NIST M48 CMM.

The independently calibrated artifacts provided for the experiments on the 1-DMM were provided by the National Institutes of Standards and Technology (NIST), the national measurement laboratory for the United Sates, NIST is one of the few organizations in the world that has the capability of realizing the length standard to the lowest available measurement uncertainties. There may be situations where an independently calibrated artifact with suitably low measurement uncertainty is not available to provide an initialization length to the end user. In those types of situations, self-initialization is the only option to set the displacement measuring instrument to a known absolute length. Instruments like the 1-DMM have the capability of measurement repeatability on the same order of magnitude as the NIST M48, but a large systematic bias persists, which needs to be addressed. It is probable that an optimal design of a self-initialization artifact exists for the 1-DMM. The ideal self-initialization artifact, which has yet to be designed, has to balance between minimizing the measurement uncertainty, and elimination of the measurement bias, when compared to the M48 CMM.

Efforts in the design of ultra high precision dimensional measurement instruments are ongoing. In situations where an independently calibrated artifact is not available to initialize the measurement sensor, such as the Large Ring Gauge, a self-initialization method may be the most practical option. Under such conditions, the functional requirements outlined in chapter 2 may serve as a useful guideline to design a self-initializing instrument. During the conceptual

design phase of the Large Ring Gauge, it was realized that a means to initialize the angle encoder of the instrument was required. It wasn't until the embodiment design phase of the instrument was completed that a new self-initialization method was devised. This new technique is a kinematic inversion of the self-initializing method used for the LBB. Recognizing that the instrument used styli which contained spherical tips, it was understood that they can interface with a three point kinematic seat in a repeatable fashion. Because of this, a new variation of a self-initialization technique was born. The availability of low cost precision spherical components, such as those used in the construction of the instruments mentioned in this dissertation, allow self-initialization methods to be possible. Many mechanical components which rely on ultra high precise coupling between two or more objects, where their coupling repeatability is on the order of micrometers or less, are embodied using kinematic couplings which provide exact mechanical constraint.

Aside from investigating the measurement uncertainties of self-initialized instruments, an unexpected outcome of designing the new 1-Dimensional Measuring Machine was fuller understanding of the uncertainty of applying Abbe offset error corrections. By applying what was learned from this discovery, the 1-DMM was redesigned from its original proposed concept to one which has greater potential to measure ball bars with lower uncertainty. Others may find this useful when designing machines which correct for Abbe offset error in-situ.

Future work for this field of study could include the following:

- Investigate the causes of the large relative systematic bias present for self-initialized measurements on the 1-DMM
- Further study the effects of a poorly constructed self-initialization artifacts on the measurement uncertainty of measured values provided by a self-initialized instrument
- Creation of other self-initialization methods to initialize dimensional measurement instruments which traditionally used an externally/independently calibrated initialization artifact.

APPENDICES

CALIBRATION CERTIFICATE FOR A GAUGE BLOCK

The information on a calibration certificate, for a gauge block's indicates its length, its measurement uncertainty, validity conditions, inspection method, material properties, and traceability.

Mitutoyo

Certificate number T07K11871
page 1 of 1

CERTIFICATE OF INSPECTION

Instrument: Gauge Block
Grade: 0 (ASME)
Date of inspection: 15th Nov. 2007

Unit : μ inch

Nominal Length inch	Ident. No.	Central Deviation	Maximum Deviation	Minimum Deviation	Variation
1	07582	+0.8	+2.0	+0.8	1.2

ENVIRONMENT: Air temperature (68 ± 1.8)F [(20 ± 1.0) ℃]
BASIS OF TEST: ASME B89.1.9-2002
MATERIAL: Steel
INSPECTION METHOD: by comparator
COEFFICIENT OF THERMAL EXPANSION: (6.0±0.3)×1E-6/F [(10.8±0.5)×1E-6/K]
EXPANDED UNCERTAINTY (For Central Deviation) (k=2): 4" or less 2.4 μ inch; Up to20" (1.2 + L / 2.3) μ inch (L=Nominal length) L:inch

TRACEABILTY: Traceable to NIST No.821/268634-03
(NIST=National Institute of Standard and Technology)

Date 15th Nov. 2007

M. Kobayashi

M. Kobayashi

F-691(5) MITUTOYO Co. HEADQUARTERS:
Postal code: 213-0012
20-1 Sakado 1-chome, Takatsu-ku, Kawasaki-shi, Japan
Tel: 044(813)8201 Fax: 044(813)8210

Figure 7-1: Calibration certificate for a 1 inch gauge block (Courtesy of Mitutoyo)

For the end user of this artifact to reproduce similar measurement results, the artifact needs to be subjected to the same validity conditions; artifact temperature, measuring technique, measuring force, etc. [48]. Since replicating the same exact validity conditions is not always possible, corrections to the size may be applied to account for slight deviations. However, this

comes at a penalty of increase measurement uncertainty. For example, if the gauge block described in Figure 7-1 was used to initialize a gauge block comparator, its length may need to be corrected for effects due to thermal expansion. This requires measuring its temperature with a thermometer, which itself needs to be calibrated, measures with a known amount of uncertainty, and traceable to the fundamental unit of temperature. Since the length and coefficient of thermal expansion (CTE) is provided for the gauge block, corrected to the defined length is performed by applying the following equation is:

$$L = L_b\left(1 + \alpha\Delta T\right) \tag{7.1}$$

where: L_b is the gauge block's certified length
α is length change due to temperature
ΔT is gauge block's temperature deviation from 20°C

With the information provided by the thermometer and calibration certificate, a Type B uncertainty analysis can be performed.

TYPE B UNCERTAINTY ANALYSIS EXAMPLE

In evaluating the uncertainty for correcting for the length change of a gauge block due to temperature variation from its stated validity condition, a Type B uncertainty analysis may be used. Performing a Type B uncertainty analysis is a systematic process, the steps are:

1 define the measurand

2 identify all influence quantities

3 create a mathematical model of influence quantities

4 compute sensitivity coefficients

5 establish statistical distribution for influence quantities

6 compute standard uncertainty associated with each influence quantity

7 combine uncertainty contributions from all influence quantities

8 select a coverage factor

Defining the Measurand

The term measurand is defined be the VIM [3] as "*the quantity to be measured*". For a gauge block, its length is defined by the distance between two opposing faces. For the gauge block described in the calibration certificate (Figure 7-1) the length of this particular gauge block was measured to be 1.0 inch with an expanded uncertainty (k=2) of 2.4 X 10^{-6} inches at 68°F.

Identify All Influence Quantities

: The possible influence quantities in this case are:

- Gauge block's length
- Gauge block's temperature
- uncertainty of gauge block's coefficient of thermal expansion (CTE).

There may be more influencing quantities, but depending on the target uncertainty defined by the measurement requirements, some of these influence quantities probably may not significantly contribute to the measurement uncertainty.

Model of Influence Quantities

The combined standard uncertainty, u_c, in a evaluation of measurement uncertainty is calculated by applying the law of propagation of uncertainties to a mathematical model $f(x_1, x_2, x_3 \ldots x_i)$ which describes the measured value; that equation is (assuming there are no correlated input quantities) [49]:

$$u_c = \sqrt{\sum_{i=1}^{N} \left(\frac{\partial f}{\partial x_i} \right)^2 u^2 \left(x_i \right)}$$

where: $\frac{\partial f}{\partial x_i}$ is the sensitivity coefficient evaluated at x_i (7.2)

$u\left(x_i \right)$ is the estimated standard uncertainty associated with x_i

The mathematical model of the measurand describes how it changes due to each influencing quantity. To calculate the length of a gauge block at a temperature other than what is stated on the calibration certificate, the following mathematical model may be used:

$$L = L_b \left(1 + \alpha \Delta T \right)$$

where: L_b is the gauge block's length at 68°F

α is length change due to temperature (7.3)

ΔT is gauge block's temperature deviation from 68°F

Compute Sensitivity Coefficients

As the name would suggest, the sensitivity coefficients describe how an uncertainty estimate changes with each input quantity (length, CTE, temperature, etc). For example, if $\frac{\partial L}{\partial \Delta T}$

has a high sensitivity coefficient, any small changes in temperature will have a large effect on the uncertainty in the length measurement. These sensitivity coefficients are calculated by taking the partial derivatives of the mathematical model with respect to each variable in the equation. For equation 7.3 there are three variables, thus the three sensitivity coefficients would be as follows:

$$\frac{\partial L}{\partial L_b} = 1 + \alpha \Delta T; \quad \frac{\partial L}{\partial \alpha} = L_b \Delta T; \quad \frac{\partial L}{\partial \Delta T} = L_b \alpha; \qquad (7.4)$$

Statistical Distribution of Influence Quantities

For each of the influence quantities mentioned, there is an associated error band where the "true value" of the influence quantity lies. For example, the expected error for a temperature measurement is +/-0.5°F of the indicated value. Knowledge of the statistical distribution for this interval is necessary to properly compute the standard uncertainty from each of them, but unfortunately they are sometimes not provided. Since no statistical information is provided for these uncertainties, the Type B approach will be used to determine the standard uncertainty for each of the influencing quantities. Since only the extreme values of these intervals are known, a rectangular probability distribution will be assumed. By using a rectangular distribution, the assumption is that there is a zero percent probability that the true value of the measurement lies outside of the error band. To estimate the standard uncertainty of an error with a rectangular distribution, simply take the half width of the error ("*a*") and divide it by $\sqrt{3}$ [20] .

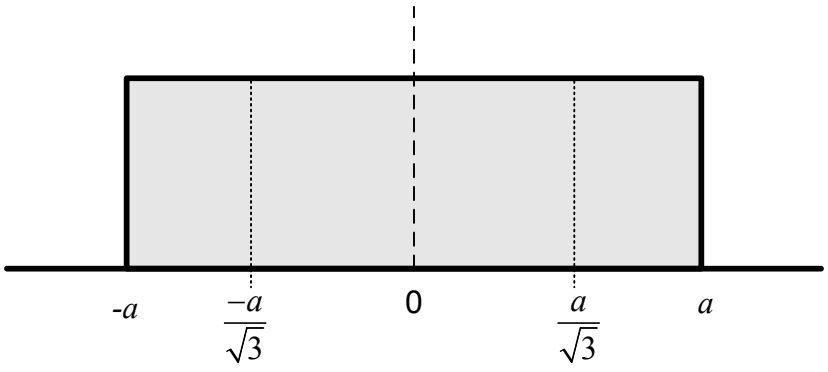

Figure 7-2: Rectangular distribution of error band

Compute Standard Uncertainty
Associated with Each Influence Quantity

Each of the properties mentioned previously (CTE, temperature, etc) are not exactly known, but are known to within an interval, the following values are assumed for this example.

- The standard uncertainty of the gauge blocks length (1.2 X 10^{-6} inches)
- the quoted accuracy of the thermometer measuring the temperature change (+/- 0.5°F)
- the manufacturer's specified error for material CTE (+/- 0.3$X10^{-6}$ 1/°F).

The gauge block manufacturer has stated that the expanded uncertainty (k=2) of the gauge block to be 2.4 X 10^{-6} inches, which also means that the standard uncertainty is 1.2 X 10^{-6} inches over a normal distribution. For the other properties (temperature and CTE), there is no statement provided on their coverage factor of their uncertainties. Because of this we'll assume a rectangular probability distribution for these deviations, the half width of each of these values will need to be divided by $\sqrt{3}$ to obtain the standard uncertainties, which are the following:

$$u_\alpha = \frac{0.3(10^{-6})\frac{1}{°F}}{\sqrt{3}} = 0.346\left(10^{-6}\right) \qquad (7.5)$$

$$u_{\Delta T} = \frac{0.5°F}{\sqrt{3}} = 0.577°C \qquad (7.6)$$

To evaluate the uncertainty of estimating this gauge block's final length due to thermal expansion, the standard uncertainty for each uncertainty contributor needs to be evaluated. These are then added in quadrature (square root of the sum of the squares) to evaluate the total standard combined uncertainty the gauge blocks[16, 20], which is:

$$U_L = \sqrt{\left(\frac{\partial L}{\partial L_b}u_b\right)^2 + \left(\frac{\partial L}{\partial \alpha}u_\alpha\right)^2 + \left(\frac{\partial L}{\partial \Delta T}u_{\Delta T}\right)^2} \qquad (7.7)$$

where: u_b is the uncertainty of gauge block's certified length
u_α is the uncertainty of CTE
$u_{\Delta T}$ is the uncertainty of temperature measurement

Resolving equation 7.7, the estimated combined standard uncertainty the length change of a gauge block which experiences a 2°F rise in temperature is 1.51 micro inches.

Selecting a Coverage Factor

The coverage factor is a multiplier of the combined standard uncertainty that is chosen to increase the confidence interval for our uncertainty estimate. Typically a multiplier of 2 is used to designate a 95% confidence interval for the expanded uncertainty, which assumes a normal distribution for the possible expected values that fall in between that interval; similar to the empirical rule in statistics [45, 49]. In the case of the expanding gauge block, its length after experiencing a temperature increase of 2°F is 1.000012 inches with an expanded uncertainty of 3.02 micro inches. In essence our Type B uncertainty evaluation states that our gauge block, which has undergone a temperature increase of 2°F, has a 95% probability of being between 1.00000898” and 1.00001502.

REFERENCES

1. Swyt, D.A., *New Concepts of Precision Dimensional Measurement for Modern Manufacturing*. 1991, National Institute of Standards and Technology: Gaintersburg, MD.

2. Swyt, D.A., *Length and Dimensional Measurements at NIST.* Journal of Research of the NIST, 2001. **Vol 106**(1): p. 1-23.

3. *International Vocabulary of metrology - Basic and General Concepts and Associated Terms (VIM)*. 2008, Bureau International des Poids et Measures (BIPM).

4. *The New Oxford American Dictionary*, I. Oxford University Press, Editor. 2008, Kreutzfeld Electronic Publishing GmbH
Hamberg, Germany.

5. Doiron, T. and J. Beers, *The Gauge Block Handbook*. 2005, NIST. p. 36.

6. Lee, V., et al., *Design and Testing of a Machine for Calibration of Ball Bars Up to 3 Meters in Length*, in *2010 American Society of Precision Engineers Conference*. 2010: Atlanta, GA.

7. Ziegert, J.C. and C. Mize, D, *The laser ball bar: a new instrument for machine tool metrology.* Precision Engineering, 1994. **Vol. 16**(4): p. 259-267.

8. Ziegert, J., et al., *Design and Testing of a One Dimensional Measuring Machine for Determining the Length of Ball Bars.* Proceedings of the 2001 Annual American Society of Precision Engineers Conference, 2001.

9. Lee, V. and J. Ziegert. *Instrument for Gauging Large Rings, Cups, and Cones*. in *Proceedings of the 2009 American Society of Precision Engineering Annual Conference*. 2009. Monterey, CA: American Society of Precision Engineering.

10. Canning, S.J., J.C. Ziegert, and T.L. Schmitz, *Coordinate Metrology Uncertainty Using Parallel Kinematic Techniques.* International Journal of Machine Tool & Manufacture, 2007. **Vol. 47**: p. 658-665.

11. Culpepper, M.L., *Design of quasi-kinematic couplings.* 2002.

12. Ziegert, J. and C. Mize, D, *5428446: Measurement instrument with interferometer and method*, U.S.P. Ofice, Editor. 1995: United States. p. 11.

13. Doiron, T., *20°C - A Short History of the Standard Reference Temperature for Industrial Dimensional Measurements.* Journal of Research of the NIST, 2007. **Vol. 112**(1): p. Pg. 1-23.

14. *Mutual Recognition of National Measurement Standards and of Calibration and Measurement Certificates Issued by National Metrology Institutes*, BIPM, Editor. 1999, BIPM.

15. Doiron, T., *Gauge Blocks - A Zombie Technology.* Journal of Research of the NIST, 2008. **Vol. 113**(3): p. 175-184.

16. Phillips, S.D., et al., *A Careful Consideration of the Calibration Concept.* Journal of Research of the NIST, 2001. **Vol. 106**(2): p. 371-379.

17. Beers, J., *The NIST Length Scale Interferometer.* Journal of Research of the NIST, 1999. **Vol 103**(3): p. Pgs. 225-252.

18. Bosch, J.A., ed. *Coordinate Measuring Machines and Systems*. 1995, Marcel Dekker, INC: New York, NY.

19. *U.S. Guide to the Expression of Uncertainty in Measurement*. 1997, ANSI/NCSL.

20. *Guide to the Expression of Uncertainty in Measurement*. 2008, International Organization for Standardization.

21. Bell, S., *A Beginner's Guide to Uncertainty of Measurement.* Measurment Good Practice Guide, 2001. **Vol. 11**(2).

22. Estler, T.W., *Concepts and Applications of Measurement Uncertainty*. 2009, ASPE Tutorial.

23. Swyt, D.A., S.D. Philips, and J. Palmateer, *Developments at NIST on Traceability in Dimensional Measurements*, in *Recent developments in traceable dimensional measurements*, SPIE, Editor. 2001, SPIE: Munich, Germany. p. 245-252.

24. Cox, M.G. and P.M. Harris, *Measurement Uncertainty and Traceability.* Measurement Science and Technology, 2006. **Vol. 17**: p. 533-540.

25. *Traceability and Uncertainty*, in *National Physical Laboratory*, N.P. Laboratory, Editor. 2007, National Physical Laboratory: Teddington, Middlesex.

26. Woods, M.J., *Tracibility, Equivalence and Quality Assurance.* Applied Radiation and Isotopes, 1998. **Vol. 49**(9-11): p. 1445-1447.

27. Rea, L.D., *Design, Assembly, and Testing of a Ball Bar Measuring Machine*, in *Dept. of Mechanical and Aerospace Engineering*. 2001, University of Florida: Gainesville, FL. p. 168.

28. Takae, M., *Self-Calibration in One Dimension.* SPIE, 1993. **Vol. 2087**: p. 80-86.

29. Estler, T.W., *Effects of radius change and sphericity errors on center location of a sphere in a 3-ball kinematic seat*. 2007, National Institute of Standards and Technology: Gaithersburg, MD.

30. Gleason, E. *Bal-Tec*. 2010 Sept. 12, 2010]; Available from: precisionballs.com.

31. Potzick, J. *Accuracy and Traceability in Dimensional Measurements*. in *Metrology, inspection and process control for microlithography*. 1998. Santa Clara, CA: SPIE.

32. Estler, T.W., *High-accuracy Displacement Interferometry in Air.* Applied Optics, 1985. **Vol. 24**(6): p. 808-815.

33. Hart, A.J., A.H. Slocum, and P. Willoughby, *Kinematic Coupling Interchangeability.* Precision Engineering, 2004. **Vol. 28**(1): p. 1-15.

34. Bryan, J.B., *The Abbé Principle Revisited: An Updated Interpretation.* Precision Engineering, 1979. **Vol. 1**(3): p. 129-132.

35. Zhang, G.X., *A Study on the Abbé Principle and Abbé Error.* CIRP Annals - Manufacturing Technology, 1989. **Vol. 38**(1): p. 525-528.

36. Koning, R., J. Flugge, and H. Bosse, *A method for the in situ determination of Abbé errors and their correction.* Measurement Science and Technology, 2007. **2**(18): p. 476-481.

37. Stone, J.A. and J.H. Zimmerman. *Refractive Index of Air*. 2001 [cited 2010 September 23, 2010]; Available from: emtoolbox.nist.gov/Wavelength/Documentation.asp.

38. Stoup, J. *A Few Case Studies in Uncertainty Using the NIST M48 CMM*. in *ASPE 2009 Spring Topical Meeting*. 2009. Albuquerque, NM.

39. Stoup, J. *High Accuracy CMM Measurements at NIST*. in *2007 CMM Users Meeting*. 2007. Mexico.

40. *ASME B89.4.1M-1997. Methods for Performance Evaluation of Coordinate Measuring Machines*. 1997, ASME: New York, NY.

41. *ASME B89.4.22-2004: Methods for Performance Evaluation of Articulated Arm Coordinate Measuring Machines*. 2004, American Society of Mechanical Engineers.

42. Slocum, A.H., *Precision Machine Design*. 1992, New Jersey: Prentice-Hall.

43. Kunzmann, H., H. Schwenke, and M. Franke, *Error mapping of CMMs and machine tools by a single tracking interferometer.* CIRP Annals - Manufacturing Technology, 2005. **Vol. 54**(1): p. 475-478.

44. Estler, T.W., *Length measurement uncertainty for Clemson 1D Measuring Machine (1DMM)*, V. Lee, Editor. 2009: Gaithersburg.

45. Ott, R.L. and M. Longnecker, *An Introduction to Statistical Methods and Data Analysis*. 5th Ed. ed. 2001, Pacific Grove, CA: Duxbury.

46. Hopp, T.H., *The Sensitivity of Three-Point Circle Fitting.* 1994(NISTIR 5501).

47. Dootson, M., et al., *Time and temperature dependent effects in the thermal expansion characteristics of carbon fiber reinforced plastics.* Composites, 1980: p. 73-78.

48. Wirandi, J.L., Alexander, *Uncertainty and traceable calibration - how modern measurement concepets improve product quality in process industry.* Measurment, 2006(39): p. 613-630.

49. Taylor, B.N.K., Chris E, *Guidelines for Evaluating and Expressing the Uncertainty of NIST Measurement Results*. 1994, National Institute of Standards and Technology.